

Aus der Medizinischen Klinik und Poliklinik IV  
Klinik der Ludwig-Maximilians-Universität München  
Direktor: Prof. Dr. med. Martin Reincke

**Targeting the residual progression of chronic kidney disease  
with type-2 diabetes beyond the renoprotective effects of  
a metformin-ramipril-empagliflozin combination**

Dissertation  
zum Erwerb des Doktorgrades der Humanbiologie  
an der Medizinischen Fakultät der  
Ludwig-Maximilians-Universität München

vorgelegt von  
  
Manga Motrapu  
  
aus Nimmalagudem, India

2021

Mit Genehmigung der Medizinischen Fakultät  
der Ludwig-Maximilians-Universität München

Berichterstatter                      Prof. Dr. med. Hans-Joachim Anders

Mitberichterstatter                  PD. Dr. Andreas Lechner  
   Prof. Dr. Uwe Heemann  
   PD. Dr. Gerald Bastian Schulz

Dekan                                      Prof. Dr. med. dent. Reinhard Hickel

Tag der mündlichen Prüfung      29.07.2021

## Contents

<b><i>Funding and Publications</i></b> .....	<b>3</b>
<b><i>Zusammenfassung</i></b> .....	<b>4</b>
<b><i>Summary</i></b> .....	<b>7</b>
<b><i>1. Introduction</i></b> .....	<b>10</b>
1.1. Chronic kidney disease .....	10
1.2. Kidney anatomy and function .....	11
1.3. Kidney pathophysiology .....	13
1.3.1. Type 2 diabetes .....	13
1.4. Current therapies .....	19
1.5. Recent findings of the pathogenesis in CKD with diabetes .....	23
1.6. Remaining unmet medical need .....	23
1.7. Podocyte regeneration .....	25
1.8. Glycogen synthase kinase (GSK)- $\beta$ signaling pathway .....	27
<b><i>2. Hypothesis</i></b> .....	<b>30</b>
<b><i>3. Materials and methods</i></b> .....	<b>31</b>
3.1. Materials .....	31
Table 4. Sodium deficient and MRE diet .....	32
Table 5. RNA isolation, cDNA conversion, real-time qPCR .....	33
Table 7. Miscellaneous .....	34
3.2. Methods .....	35
3.2.1. Animals .....	35
3.2.2. Experimental design .....	36
3.3. Collection of urine and blood from mice .....	38
3.4. Urinary albumin to creatinine ratio .....	38
3.5. Glomerular filtration rate (GFR) .....	39
3.6. Immunohistochemistry .....	40
3.6.1. General procedure for staining .....	40
3.6.2. PAS staining (Glomerular size) .....	41
3.6.3. Picro-Sirius Red staining .....	41
3.6.4. WT1 staining (Podocyte number and density) .....	42
3.7. In-vitro studies .....	42
<b><i>4. Statistical analysis</i></b> .....	<b>44</b>
<b><i>5. Results</i></b> .....	<b>45</b>
5.1. Establishing a model of progressive CKD in obesity-related type 2 diabetes .....	45
5.1.1. T2D mice show glomerular hyperfiltration even upon uninephrectomy. ....	45
5.1.2. db/db mice display typical pathophysiological features of progressive CKD .....	46

<b>5.2. Effects of metformin, ramipril, and empagliflozin on kidney function .....</b>	<b>48</b>
5.2.1. Treatment with MRE did not have a substantial impact on GFR .....	48
5.2.2. MRE treatment showed renoprotective effects on T2D-Unx mice .....	49
<b>5.4. Additive nephroprotective effects of metformin, ramipril, empagliflozin, and BIO therapy .....</b>	<b>54</b>
5.4.1. MRE+BIO treatment had a significant effect on $\Delta$ GFR .....	55
5.4.2. MRE+BIO treatment reduced glomerulosclerosis in T2D-Unx mice.....	55
<b>5.5. Nephroprotective effects with BIO alone treatment.....</b>	<b>59</b>
5.5.1. BIO alone treatment had significant protection from GFR decline .....	59
5.5.2. In T2D-Unx mice, BIO alone therapy minimized glomerulosclerosis.....	60
<b>5.6. Effects of BIO on mouse glomeruli in vitro .....</b>	<b>63</b>
<b>6. Discussion .....</b>	<b>65</b>
<b>7 Abbreviations.....</b>	<b>73</b>
<b>References:.....</b>	<b>74</b>
<b>Declaration.....</b>	<b>85</b>
<b>Acknowledgment.....</b>	<b>86</b>

## Funding and Publications

Manga Motrapu was supported by a national overseas scholarship from the Ministry of Social Justice and Empowerment (Government of India).

A part of the work has been published in the *Journal of American Society of Nephrology* (August 2020, DOI: [10.1681/ASN.2019070703](https://doi.org/10.1681/ASN.2019070703)). This work has been presented in the ERA-EDTA 2019 as oral communication and in the American Society of Nephrology (ASN), 2019, and The European Association for the Study of Diabetes (ESAD) 2019, presented as a poster.

Date: .....

Signature: .....

Place: Munich, Germany

(Manga Motrapu)

## Zusammenfassung

Adipositas-assoziiertes Typ-2-Diabetes (T2D) ist eines der größten Gesundheitsprobleme der Welt. Die Morbidität und Mortalität von T2D sind mit Komplikationen wie Herz-Kreislauf-Erkrankungen, chronischer Nierenerkrankung (CKD), diabetischer Retinopathie und diabetischem Fußsyndrom assoziiert. Risikofaktoren für T2D sind ein bewegungsarmer Lebensstil, hyperkalorische Ernährung, Adipositas, Hyperlipidämie und Hyperurikämie. Diabetes führt zu hämodynamischen und metabolischen Stress in der Niere. Der zugrundeliegende Pathomechanismus beruht auf glomerulärer Hyperfiltration und einer Hyperreabsorption. Reaktiv kommt es zu einer Hyperreabsorption löslicher Substanzen im proximalen Tubulus. Dieser „Stress“ stellt eine funktionelle Überlastung der Nierenephrene dar und begünstigt das Auftreten und Fortschreiten von Nierenerkrankungen. Insbesondere Patienten mit einer vorbestehenden, verringerten Nephronenanzahl sind gefährdet. Therapeutisch werden standardmäßig Medikamente zur Senkung des Blutzuckerspiegels (Inhibitoren des Renin-Angiotensin-Aldosteron-Systems (RAAS), Metformin, Inhibitoren des Natrium-Glucose-Transporters-2 (SGLT2) und des Blutdrucks (Erstlinien Therapie mit Inhibitoren des RAAS, sekundäre Therapie mit Statinen sowie Nikotinentwöhnung und salzarme Ernährung) eingesetzt. Oftmals reicht eine Standardtherapie zur Prävention der Progression der Nierenerkrankung und Verbesserung der Prognose nicht aus. Auch unser Verständnis für die zugrundeliegenden Pathomechanismen entwickelt sich weiter. Als Reaktion hierauf muss die Standardtherapie stetig verbessert und angepasst werden. Jüngste Studien legen nahe, dass beispielsweise eine verbesserte Podozytenregeneration (mit Hilfe von Arzneimitteln wie BIO) ein potenzieller therapeutischer Ansatzpunkt zur Milderung von Hyperfiltration und Albuminurie sein könnte.

Die Frühphase der CKD ist durch eine stabile Gesamt-GFR, mesangiale Glomerulosklerose und milde Albuminurie gekennzeichnet. Dies ist mit einem CKD-Stadium G1A1 ( $GFR > 90 \text{ ml/min/1,73 m}^2$  und  $ACR < 3 \text{ mg/mmol}$ ) vergleichbar und wird in den meisten tierexperimentellen Studien nachgeahmt. Im Gegensatz dazu präsentieren sich Patienten mit Diabetes in klinischen Berichten mit einem Rückgang der GFR und Makroproteinurie unter Standardtherapie. Um diesen Sachverhalt im Tiermodell zu überprüfen, wurde zunächst ein Studiendesign für eine progressive Glomerulosklerose etabliert. Hierzu wurden adipöse db/db-Mäuse mit T2D eingesetzt. Der progressive GFR-Verlust konnte durch Uninephrektomie im

Alter von sechs Wochen imitiert werden. Zur Aggravation der glomerulären Hyperfiltration erhielten die Tiere bis zur 20. Woche des Experiments eine salzarme Diät. Im Verlauf entwickelten die Mäuse eine Glomerulosklerose. Die Bewertung der CKD erfolgte mithilfe von Nierenfunktionsparametern wie GFR und Albuminurie. T2D-Unx Mäuse zeigten im Vergleich zu Wildtyp-Kontrollen (WT-Unx) während des gesamten Experiments ein erhöhtes Körpergewicht und einen erhöhten Blutzucker. Hyperfiltration und Albuminurie konnten ebenfalls nur bei T2D-Unx-Mäusen beobachtet werden. Die Auswertung immunhistochemischer Schnittpräparate ergab eine verringerte Podozytendichte und Glomerulosklerose in kortikalen und juxtamedullären Nephronen von T2D-Unx-Mäusen.

Im nächsten Schritt wurde die Standardtherapie zur Behandlung des T2D auf dieses Modell angewendet. Hierzu wurde den Mäusen für vier Wochen Metformin, Ramipril und Empagliflozin (MRE) verabreicht. Die Auswertung der Daten nach der vierwöchigen Therapie ergab, dass Mäuse mit medikamentöser Behandlung eine verringerte Hyperglykämie und Albuminurie im Vergleich zur Kontrollgruppe aufwiesen. In der Sirius-Rot-Färbung war bei MRE-behandelten T2D-Unx-Mäusen eine signifikante Reduktion der Glomerulosklerose, insbesondere in juxtamedullären Nephronen, zu beobachten. Die kortikalen Nephrone der T2D-Unx-Mäusen zeichneten sich zudem durch eine verringerte Hypertrophie und signifikant verbesserte Podozytenregeneration aus. Die Filtrationsspaltweite wurde als Prädiktor für eine ultrastrukturelle Podozytenverletzung mithilfe von STED-Hochauflösungsmikroskopie analysiert. Im Vergleich zu unbehandelten Mäusen erhöhte die MRE-Behandlung die Dichte der Filtrationsschlitze entlang der glomerulären Filtrationsbarriere. Insgesamt konnte also ein nephroprotektiver Effekt durch die vierwöchige MRE-Therapie nachgewiesen werden.

Neben der üblichen Therapie konnte in diesem Modell auch das neuartige Medikament BIO untersucht werden. Hier ist insbesondere BIO zu erwähnen. Es sollte gezeigt werden, dass eine Therapie aus MRE und BIO im etablierten Tiermodell zu einem verbesserten Phänotyp führt. Hierzu wurde die Therapie aus MRE+BIO einer MRE Therapie gegenübergestellt. Interessanterweise zeigte die Kombinationstherapie eine verringerte  $\Delta$ GFR im Vergleich zur alleinigen MRE Therapie. Die Glomerulosklerose war insbesondere in juxtamedullären Nephronen von T2D-Unx-Mäusen (MRE+BIO) signifikant reduziert. Darüber hinaus zeigte die MRE+BIO-Behandlung eine signifikante Verbesserung der glomerulären Hypertrophie sowie Podozytenregeneration in juxtamedullären Nephronen von T2D-Unx-Mäusen. Die MRE+BIO-

Behandlung verbesserte die Filtrationsspaltweite der Podozyten entlang der glomerulären Filtrationsbarriere.

Weiterhin wurden T2D-Unx-Mäuse mit einer BIO Monotherapie Mäusen mit Kombinationstherapie aus MRE+BIO gegenübergestellt. Im Rahmen der Monotherapie konnte eine signifikante Reduktion der GFR beobachtet werden. Ebenfalls wirkte sich die Monotherapie im Vergleich zur Kombinationstherapie nicht negativ auf die sekundären Parameter aus. Zwar reduzierte die BIO-Behandlung signifikant die Glomerulosklerose, hatte jedoch im Vergleich zur MRE+BIO-Behandlung keinen Einfluss auf die Podozytenzahl. Insgesamt kann einer BIO-Supplementierung zu einer MRE Behandlung ein nephroprotektiver Effekt zugeschrieben werden.

Dieser Effekt wurde auch *in vitro* untersucht. Dazu wurden Glomeruli in hoher Reinheit aus Mäusenieren extrahiert. In Anwesenheit hoher Glukose (30 mmol) und BIO wurde die mRNA-Expression des Podozyten-spezifischen Proteins Nephrin untersucht. Als Kontrolle dienten Kulturbedingungen ohne Glukose. Nephrin wurde vor allem von Zellen unter BIO-Exposition vermehrt exprimiert. Insgesamt erwies sich BIO als ein potenter Nephrin-Protein-Induktor in Maus-Glomeruli unter diabetischen und nicht-diabetischen Bedingungen.

Das Ergebnis unserer Experimente zur Weiterentwicklung der Standardtherapie der progressiven CKD unter T2D kombinierte ein Modell aus: progressivem Nephronenverlust, Standard-Komedikation, Berechnung der Gruppengröße, Durchführung einer neuartigen Therapie, vorab festgelegter primärer und sekundärer Endpunkte (orientiert an klinischen Studien), komplexe morphologische Untersuchungen, um mechanistische Erkenntnisse zu gewinnen. Unser neuartiges BIO-Medikament zeigte in diesem experimentellen Design eine signifikante, nephroprotektive Wirkung gegenüber Metformin mit doppelter RAAS / SGLT2-Inhibition. Die Zahl der Podozyten und die morphologischen Veränderungen der Nieren nahmen unter Verbesserung der mutmaßlichen Wirkmechanismen zu. Abschließend legte der Wirkmechanismus der Medikamente eine doppelte RAAS / SGLT2-Hemmung nahe. Hiervon könnten insbesondere T2D Patienten mit einer CKD-Progression profitieren.



## Summary

Obesity-associated type-2 diabetes (T2D) is a leading worldwide medical concern. The morbidity and mortality of T2D links tightly to complications such as cardiovascular disease, chronic kidney disease (CKD), blindness, and foot ulcers. Risk factors for T2D include a sedentary lifestyle, hypercaloric diet, obesity, hyperlipidemia, and hyperuricemia. The diabetes mechanism leading to kidney injury involves glomerular hyperfiltration, and the associated hyperreabsorption of solutes in the proximal tubule is referred to as hemodynamic and metabolic stress for the kidney. This “stress” represents a functional overload to the kidney nephrons, a risk factor for kidney disease onset and progression, especially in patients with low nephron numbers. The current standard medical therapy is limited to the control of hyperglycemia (renin-angiotensin system (RAS) inhibitors, metformin, sodium-glucose transporter-2 (SGLT2) inhibitor) and blood pressure control, preferentially with inhibitors of the RAS as well as adjunct treatments such as statins, smoking cessation, and low-salt diet. However, the mentioned strategies are not sufficient to delay the progression of CKD in most cases. Furthermore, we need to improve potential medication for diabetic patients. Recent studies suggest that enhancing podocyte regeneration (using drugs such as BIO) could be a potential therapeutic strategy to attenuate hyperfiltration and albuminuria.

The initial CKD phase, characterized by stable total glomerular filtration rate (GFR), mesangial glomerulosclerosis, and mild albuminuria similar to CKD stage G1A1 ( $\text{GFR} \geq 90 \text{ ml/min/1.73 m}^2$  and  $\text{ACR} < 3 \text{ mg/mmol}$ ), is mimicked by most animal studies in this domain. Conversely, most clinical reports associate diabetes patients with gradual GFR decline and macroproteinuria under standard-of-care treatment. Furthermore, novel drugs can be studied in an experimental setting of obese db/db mice with T2D with residual progressive GFR loss by induction of uninephrectomy despite antidiabetic therapy and combination therapy RAS/SGLT2 inhibitors.

Therefore, BIO was hypothesized to decrease CKD progression over metformin, ramipril, and empagliflozin (MRE) therapy in uninephrectomized obese db/db mice with T2D (T2D-Unx). A progressive glomerulosclerosis mouse model was developed by induction of uninephrectomy (at six weeks of age) in obese db/db mice with T2D, after uninephrectomy, fed with the low salt diet until week 20 of the experiment to accelerated glomerular hyperfiltration-related CKD progression. CKD was evaluated by kidney function parameters such as GFR and

albuminuria. T2D-Unx showed mice increased body weight and blood glucose throughout the experiment compared with wild type controls (WT-Unx). Furthermore, T2D-Unx mice showed hyperfiltration and albuminuria compared with WT-Unx mice. Immunohistochemical analysis revealed reduced podocyte density and increased glomerulosclerosis in cortical and juxtamedullary nephrons of T2D-Unx mice. These results suggest our model resembles the mouse model with progressive glomerulosclerosis.

After establishing a progressive glomerulosclerosis mouse model, four weeks of diabetic patients treat standard-of-care drugs such as metformin, ramipril, and empagliflozin (MRE). Four weeks of MRE treatment shown hyperglycemia and albuminuria reduction compared with untreated T2D-Unx mice. In Sirius red staining, MRE treated T2D-Unx mice significantly reduced glomerulosclerosis, especially in juxtamedullary nephrons. Furthermore, MRE treated T2D-Unx mice, reducing hypertrophy, and significantly enhanced podocyte regeneration in cortical nephrons. Filtration slit density was analysed as a predictor of ultrastructural podocyte injury by STED super-resolution microscopy on tissue clearing concerning podocyte assessment. Compared with untreated T2D-Unx mice, MRE treatment substantially increased the density of filtration slits along the glomerular filtration barrier.

Therefore, four weeks of MRE therapy was shown nephroprotection in T2D-Unx mice. Further, we included a novel BIO drug to the treatment regimen along with MRE to T2D-Unx mice for four weeks. Interestingly, in the progressive glomerulosclerosis mouse model, four weeks of treatment with MRE+BIO treatment shown significantly reduced  $\Delta$ GFR compared to MRE treated T2D-Unx mice. Complementation of BIO to MRE treatment significantly reduced glomerulosclerosis, especially in juxtamedullary nephrons in T2D-Unx mice. Furthermore, MRE+BIO treatment represented a significant reduction of hypertrophy and enhanced podocyte regeneration in juxtamedullary nephrons in T2D-Unx mice. MRE+BIO treatment substantially improved podocyte filtration slit density along the glomerular filtration barrier correlated to MRE treated T2D-Unx mice.

Finally, BIO alone treated T2D-Unx mice affected the kidney compared with BIO add on treatment with MRE. In T2D-Unx mice, the administration of Bio (without MRE therapy) significantly reduced GFR decline and did not affect secondary outcomes due to MRE therapy's absence. However, BIO treatment could significantly decrease glomerulosclerosis, with no effect on podocyte numbers compared with MRE+BIO treatment. From the above

observation, BIO supplementation, along with MRE therapy, can improve kidney protection during disease conditions. Furthermore, we investigated its direct impact on whole mouse glomerular cells *in vitro*. For that, glomeruli were extracted at high purity from mouse kidneys. In the presence of high glucose (30 Mm), the mRNA expression of the podocyte-specific protein, i.e., nephrin, is highly expressed within glomeruli under the glucose condition control group treated with BIO and quantified. Therefore, BIO is a particular nephrin protein inducer in mouse glomeruli in non-diabetic and diabetic conditions.

The outcome in our experiments to advance drug testing for progressive CKD with T2D combined a model of progressive nephron loss, standard co-medication, group size calculation, randomization to an intervention not approved before disease, pre-specified primary and secondary endpoints similar to those used in clinical trials, complex morphologic estimation to obtain mechanistic insights and detailed safety analysis. Our novel BIO drug demonstrated significant nephroprotective effects over metformin with dual RAS/ SGLT2 inhibition in this experimental setting. Podocyte numbers and kidney morphological changes were increased as the putative mechanism of action was improved. Furthermore, drug targeting in these mechanisms can consider dual RAS/SGLT2 inhibition and be a beneficial add-on medication strategy in patients with gradual CKD progression with diabetes.

## 1. Introduction

### 1.1. Chronic kidney disease

CKD is an unavoidable and gradual decrease of kidney function and leads to kidney failure, termed end-stage kidney disease. CKD define as the kidney undergoes structural changes or functional changes present for three months or longer<sup>1,2</sup>. Kidney abnormalities combine albuminuria (albumin/creatinine ratio >30 mg/g), kidney structural changes, urine abnormalities, electrolyte imbalance due to tubular stress, histopathological changes, and reduction of GFR to <60ml/min/1.73m<sup>2</sup> present for 3 months, with health implications (Fig.1). Furthermore, kidney structural changes such as most to the effect of podocyte catastrophe-associated glomerulosclerosis, e.g., in aging, diabetes, high blood pressure, and glomerulonephritis<sup>4,5</sup>. CKD afflicts 15% of the USA adult population, and its predominance has to rise to 50% over the next two decades<sup>6,7</sup>.

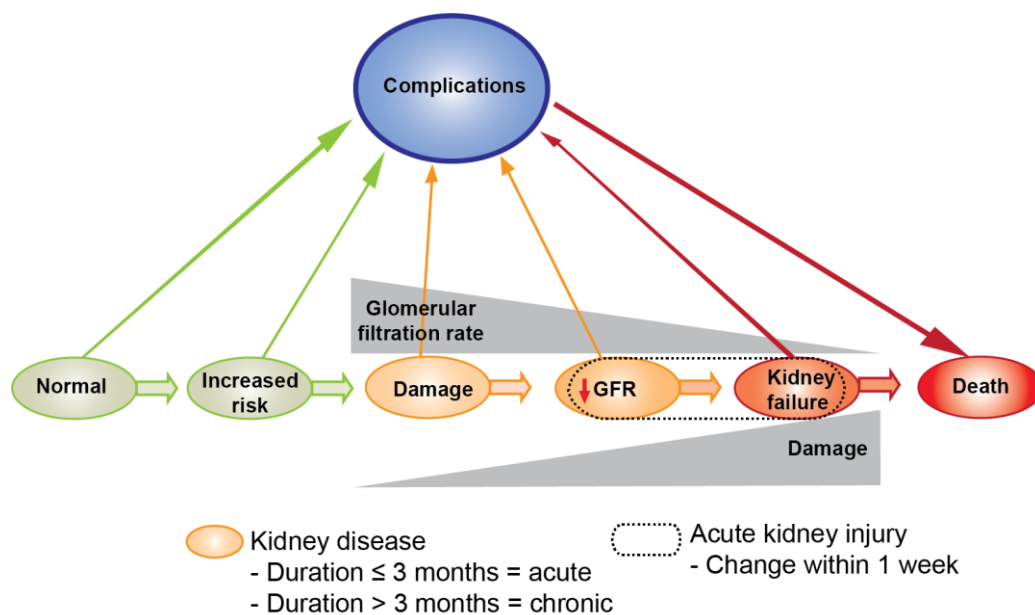


**Figure 1. Theoretical model and allocation of kidney disease.** Components correlated with increased risk of kidney disease (green), phases of disease (orange), and difficulties (death; red). Horizontal arrows show changes between phases (kidney outcomes). From left to right, Solid arrows indicate the progression of kidney disease.

The classification of CKD in five different stages is based on the GFR (Table 1). Moreover, albuminuria and clinical diagnosis involvement in the classification define the disease's severity more accurately and anticipate the prognosis<sup>8,9</sup>. Then, the prevalence of CKD

accounts for almost 15% of the adult US community, and the associated major risk factors are diabetes<sup>10</sup> and heart-related diseases<sup>2,3</sup>.

**Table 1. Developing Global Outcomes (KDIGO) kidney function and disease**

Symptom	abbreviations	Rationale/explanation	Terms to avoid
<b>GFR categories</b>		For use in define GFR level, either presence or absence of kidney disease(ml/min per 1.73 m2)	
Normal to ↑ GFR	G1	GFR >90	
Mildly ↓ GFR	G2	GFR 60-89	
Moderately ↓ GFR	G3a	GFR 45-59	
	G3b	GFR 30-	
Severely ↓ GFR	G4	GFR 15-29	
Kidney failure	G5	GFR <15 (or dialysis)	
Hyperfiltration		The theory of hyperfiltration is accepted but not constantly defined. If this term is used as an exposure-outcome, the GFR threshold must be described (e.g., >120 ml/min per 1.73 m2).	Kidney hyperfiltration
GFR reserve		The theory of GFR reserve is approved as the variation among stimulated and basal GFR	Kidney function reserve
<b>Albuminuria categories</b>		To define albuminuria level, either the presence or absence of kidney disease	
Normal		AER <10 mg/d, ACR <10 mg/g (<1 mg/mmol)	
Mildly ↑ (mild)		AER 10–29 mg/d, ACR 10–29 mg/g (1.0–2.9 mg/mmol)	
Normal to mildly ↑ (normal to mild)	A1	AER <30 mg/d, ACR <30 mg/g (<3 mg/mmol) PER <150 mg/d, PCR <150 mg/g (<15 mg/mmol)	Normoalbuminuria
Moderately ↑ (moderate)	A2	AER 30–300 mg/d, ACR 30–300 mg/g (3–30 mg/mmol) and PER 150–500 mg/d, PCR 150–500 mg/g (15–50 mg/mmol)	Microalbuminuria

Adopted and modified<sup>11</sup>

## 1.2. Kidney anatomy and function

The kidneys are composed of functional units of nephrons<sup>12</sup>. Each nephron has two parts, glomerulus and tubule. A cross-sectional view of the kidney differentiates into two distinct regions: Cortex and Medulla<sup>13</sup> (Fig.2). The kidney cortex comprises the cortical and juxtamedullary glomeruli and proximal tubules, a significant part of distal tubules, whereas the kidney medulla comprises the collecting ducts of the nephron. The glomerulus is vital for the filtration of blood<sup>14</sup>. The glomerulus filters blood and allowing the passage of small molecules such as glucose and electrolytes, i.e., the glomerular ultrafiltrate.

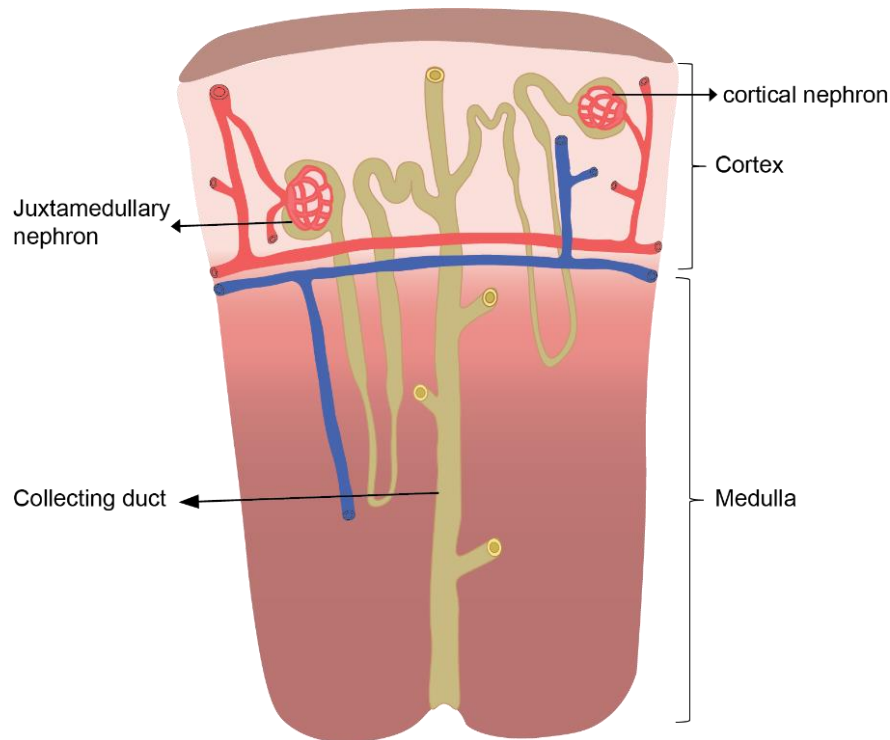


**Figure 2. A cross-sectional view of the kidney.**

The nephron's proximal tubule ensures reabsorption of most of the filtered solutes, including glucose from the glomerular filtrate. The kidney tubule is divided into a proximal and distal tubule connected by the Henle's loop. The distal tubules of many nephrons merge into common collecting ducts. Several kidney tubules and collecting ducts together form a pyramid shape called Bartolini pyramids. The base of each pyramid connects to the kidney pelvis and drains the urine into the ureter.

### **Kidney physiology**

The kidney has a fundamental role in the elimination of metabolic waste products and maintaining homeostasis<sup>15</sup>. Besides filtration, kidneys also secrete molecules that control blood pressure, plasma pH, etc. The kidney's function to produce nearly protein-free urine depends on the mutual contribution of all three components of SD. The glomerulus has highly vascularized blood capillaries, forming the glomerular filtration barrier<sup>16</sup>. Glomerular filtration barrier<sup>16</sup> consists of three pivotal elements: fenestrated endothelium, glomerular basement membrane (GBM), and podocytes (Fig.3). The fenestrated endothelium (70-100 nm) lines the inner area of glomerular capillaries and permits the small molecules to go through the urine<sup>17</sup>. GBM (250-300 nm) is an extracellular matrix composed of structural proteins such as collagen matrix, fibronectin, and heparan sulfate proteoglycans<sup>18</sup>. Podocytes are post-mitotic visceral

epithelial cells<sup>19</sup> that adhere firmly to GBM and offer epithelial coverage to glomerular blood vessels. The slit-pore size between adjacent podocytes is differing from 20 to 60 nm. This three-layered glomerular filtration barrier and particular architecture play a size-specific and charge-dependent molecular sieve, improving the filtration of water, electrolytes, and small solutes. However, limiting the entry of negatively charged macromolecules, such as proteins and polypeptides<sup>20</sup>. Proteins with a molecular weight of 20 kDa will pass through the GBM.

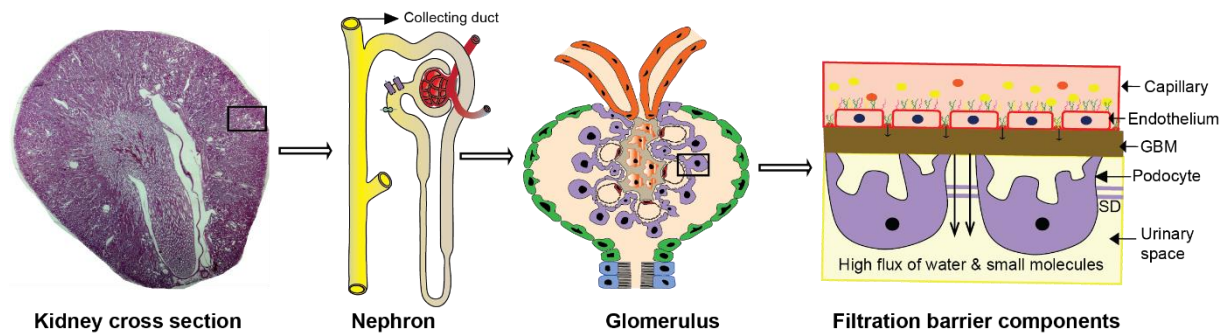


**Figure 3. The kidney structure and the cellular components.** PAS panoramic 1x, nephron structure, and the glomerulus and its cell components.

Furthermore, the smaller proteins are mostly reabsorbed by proximal convoluted tubules, and only a small amount eliminate through the urine. However, due to abnormalities in the nephron, different quantities of plasma proteins, mainly albumin (~65 kDa), are eliminated through the urine. Albuminuria is a well-established marker of filtration barrier dysfunction and indicates kidney injury.

### 1.3. Kidney pathophysiology

#### 1.3.1. Type 2 diabetes

T2D indicates that a class of common metabolic disorders contribute to the essential phenotype of elevated levels of sugars in blood circulation<sup>21,22</sup>. The worldwide diabetic population of patients with diabetes was around 463 million<sup>23</sup>, and more than 59 million affected Europe. The number of diabetic patients was predicted to increase to 51% and even double in North Africa, countries and territories in the Eastern Mediterranean, and South-East Asia by 2045. However, several countries report that the onset of T2D, even in the young population also increasing due to a sedentary lifestyle and obesity<sup>24,25</sup>. According to the reports of high morbidity and mortality rates in 2013, around 5 million people died due to T2D complications. The morbidity of T2D relates to macrovascular complications such as coronary

artery disease, cerebrovascular disease, and microvascular complications such as neuropathy, retinopathy, and nephropathy<sup>10,26,27</sup>.

Diabetes is divided into several types (Fig.4), from which T2D contributes approximately 90% and the rest by type-1 diabetes (T1D). T2D, the pathophysiology, including peripheral insulin resistance, lack of insulin secretion, and an imbalance in glucose resorption<sup>28</sup>. However, T1D represents the absence of insulin due to the destruction of pancreatic- $\beta$  cells and compromised action on target cells<sup>21</sup>. The etiology of T1D and T2D associate with genetic predisposition with environmental factors<sup>29</sup>. In T2D, it has been shown that individual lifestyle contributes massively to the disease's advancement and increase, associated with a high-fat diet and physical inactivity<sup>30</sup>.

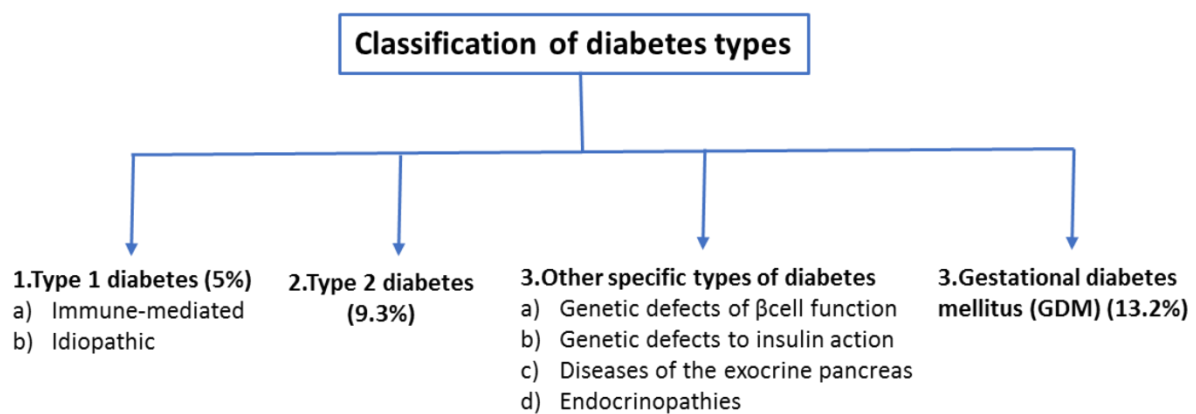


**Figure 4. Allocation of diabetes types.** Adapted and modified<sup>31</sup>

### Pathophysiology of diabetic kidney disease

Diabetic kidney disease (DKD) is the primary chronic problem in diabetic subjects that promote 20-40% of patients with Type 2 DM or Type 1<sup>28</sup>. DKD is a microvascular complexity in diabetes progression characterized by hyperglycemia, constant albuminuria (>300 mg/24 h), declined GFR, and higher blood pressure<sup>32</sup>. The past events of DKD have been extensively studied in T1D because the onset is usually visible. It develops earlier in life, so the period of diabetes is longer as for those with T2D. In general, CKD with diabetes starts with an increase in GFR, gradual albuminuria, and further leads to podocyte injury and, ultimately, leads to kidney failure. Different metabolic changes occur in diabetes, which leads to kidney inflammation and causes fibrosis and kidney hypertrophy<sup>33</sup>. However, the progression of microalbuminuria (>30 mg/day) to macroalbuminuria (>300 mg/day) and decline in GFR, a direct predictor for end-stage kidney disease in DKD<sup>34</sup> (Fig.5). Therefore microalbuminuria is a crucial anticipating



parameter for the progression in the advancement of DKD in diabetic patients<sup>35</sup>. Nevertheless, some other causes such as gender, age, obesity, glycemic regulation, diabetes period, high blood pressure, etc. also contribute to some extent to progressive deterioration of kidney function<sup>36</sup>

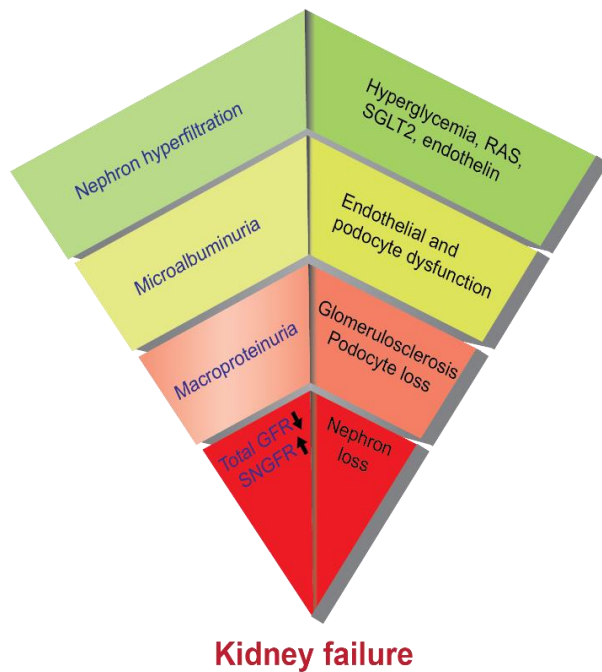


**Figure 5. The natural course of CKD with diabetes diabetic kidney disease.** Predominant clinical and morphological changes in the time of DKD are summarized in this picture. The onset of DKD begins with hyperfiltration and progresses to overt proteinuria. The major structural changes during the progression of DKD are mesangial matrix expansion, GBM thickening, and glomerular sclerosis. DKD was mainly demonstrated with gradual proteinuria, increased SNGFR, and decreased GFR events associated with kidney failure.

### Glomerular hyperfiltration in DKD

The GFR is a primary parameter to check the kidney function, and it shows the plasma flow from the glomerulus into Bowman's space over a particular period<sup>37</sup>. The total GFR represents the sum of all single nephron GFRs (SNGFR) and shown CKD progression and kidney life span<sup>38</sup>. Nephron number is constant at birth, and as mammals cannot replace or regenerate lost nephrons, nephron number declines along with life<sup>39</sup>. In healthy individuals, GFR declines accordingly as no compensatory hypertrophy occurs<sup>40</sup>, indicating that healthy aging requires fewer kidney function<sup>41</sup>, probably due to less uptake of osmolytes and generation of metabolic waste products (Fig.6). A diabetic patient with poorly controlled CKD stage G2 with having a total GFR of 80 ml/min has probably already lost 60% of nephrons as with all nephrons, GFR should be 150 ml/min or more. These remnant nephrons must have an increased SNGFR as a marker of increased workload and are at risk to yield single nephron hyperfiltration and hyperreabsorption<sup>42</sup>.

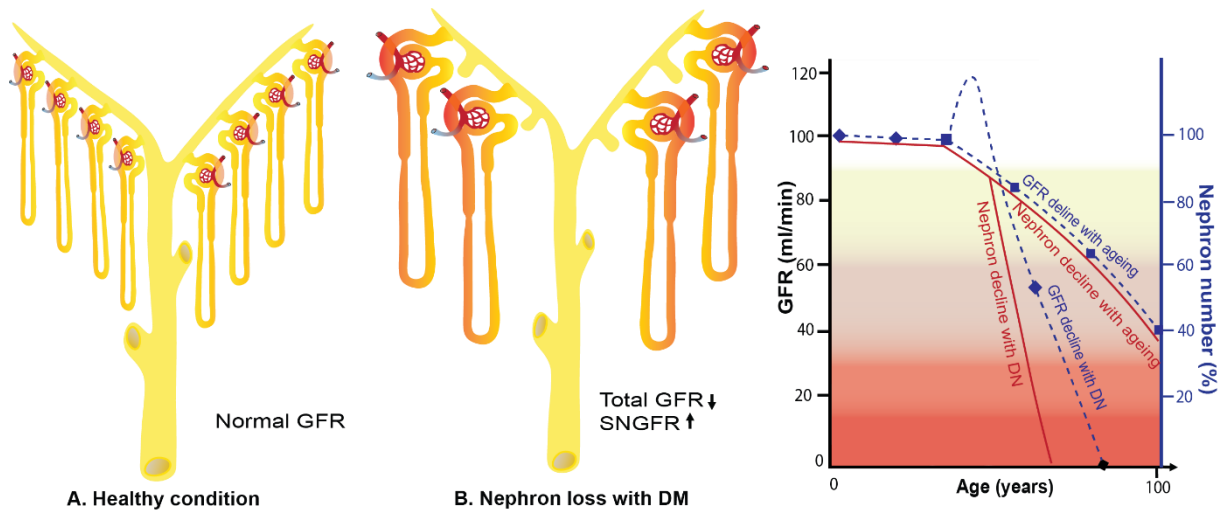


**Figure 6. The kidney lifespan with chronic kidney disease.** In diabetes, hyperglycemia is a central driver of the same mechanisms. Thus single nephron hyperfiltration is a central disease pathomechanism of CKD gradual increase, i.e., shortening kidney lifespan.

The condition is worst in a diabetic patient with poorly controlled CKD stage G3a with having a total GFR of 50 ml/min, with probably only 25% of his nephrons left. Each of them with massively increased SNGFR, massive single nephron hyperfiltration, and hyperreabsorption<sup>42</sup>. Without a robust therapeutic intervention that reduces the workload at the individual nephrons' level, such nephrons loss gets lost quickly, i.e., CKD progression with diabetes<sup>42</sup>. Thus, the increased SNGFR is the central pathomechanisms of advancement in every form of CKD and diabetic nephropathy, a disease where single nephron hyperfiltration is the central pathomechanism<sup>26,27</sup>. While endowment with a large number of nephrons can handle diabetes-related hyperfiltration, conditions of absolute (CKD, aging, or both) or relative low nephron numbers (low nephron endowment, obesity, pregnancy, previous acute kidney injury) may pass the threshold and promote the podocyte loss leads to progressive loss of nephrons<sup>43</sup>. Therefore, reducing single nephron hyperfiltration (and hyperreabsorption) is the main treatment target in diabetic kidney diseases and requires a deeper understanding of the factors determining glomerular filtration in health and diabetes.

### Albumin leakage induces kidney damage

Proteinuria often referred to as albuminuria, is indexed by the amount of albumin is presented in the urine collected in 24 hrs<sup>44</sup>. Under standard physiological conditions, the minimal amount of albumin protein is filtered by the glomeruli again easily reabsorbed into the tubule<sup>45,46</sup>. The increased albuminuria increases kidney injury involves several pathways that finally lead to tubulointerstitial damage<sup>47</sup>. Albuminuria is a primary clinical symptom in DKD.

Albuminuria is ranged from micro to macro to adverse or overt proteinuria. Microalbuminuria, referred to as albumin levels, varied from 30 to 300 mg/24 h urine collected, and macroalbuminuria ranges about  $\geq 300$ mg in 24h urine collected<sup>32,48</sup>. Around 50% of patients with microalbuminuria would proceed to macroalbuminuria in the absence of early intervention, which is correlated with a ten times greater probability of gradual increase to end-stage kidney disease than that about patients along normoalbuminuria<sup>49,50</sup>. However, in patients with T2D, classical cardiovascular risk factors such as the high concentration of albumin present in the urine, high levels of hemoglobin A1C in the blood, hypertension, and hyperglycemia without effect on estimated GFR<sup>51</sup>. In vitro studies showed that high albumin concentrations present in the proximal and distal tubular cells would activate several intracellular signaling pathways such as NF-kB, protein kinase C, etc.<sup>52–54</sup>. In turn, activation of these signaling pathways induces the release of inflammatory response<sup>55</sup>, production of reactive oxygen species<sup>56</sup> followed by endothelin-1<sup>57</sup>, and causes tubulointerstitial fibrosis<sup>58–60</sup>, finally, leading to irreversible kidney injury. However, its partial reversal upon glucose and hypertension control has been shown, suggesting no direct correlation with DKD. On the other hand, macroalbuminuria is considered a standard marker of podocyte loss and an indicator of CKD progression. Often, macroalbuminuria develops into overt proteinuria, a clear sign of establishing ESRD, followed by podocyte detachment from the basement membrane, nephron loss, leading to kidney failure<sup>61</sup>.

			Persistent albuminuria categories			
			A1	A2	A3	
			Normal to mildly increased <30mg/g <3mg/mmol	Moderately increased 30 - 300mg/g 3 - 30mg/mmol	Severely increased >300mg/g >30mg/mmol	
GFR categories (ml/min/1.73m <sup>2</sup> )	G1	Normal or high	>90			
	G2	Mildly decreased	60-89			
	G3a	Mildly to moderately decreased	45-59			
	G3b	Moderately to severely decreased	30-44			
	G4	Severely decreased	15-29			
	G5	Kidney failure	<15			
			Low risk	Moderately increased risk	High risk	Very high risk

**Figure 7. The KDIGO classification of CKD.** Prediction of CKD stages with GFR and albuminuria. The colors display the severities of risk in decreasing order. Adopted and modified<sup>11</sup>

### Podocyte detachment in DKD

Podocytes are highly specialized visceral epithelial cells and structurally and functionally distinct from various cells of the glomerulus<sup>20</sup>. Podocytes are post-mitotic cells and consist of a complex cell body along with expanded foot-processes<sup>62</sup>. These foot-processes further interdigitate with neighboring podocyte's foot processes and form the slit-diaphragm<sup>63</sup>. Several proteins comprised the slit-diaphragm and reported a potential role in maintaining the function as well as the structure of the podocytes<sup>64</sup>. The primary role of the podocyte is (a) to stabilize the glomerular system by opposing the distensions of the GBM, (b) to maintain a large filtration surface across the slit-diaphragm, and also (c) to control the size and charge characteristics features of the glomerular filtration barrier, and (d) also play the central role in the GFR<sup>20</sup>. Podocytes serve as size and charge-selective barrier, counteract intraglomerular pressure, releasing of vascular endothelial growth factor for maintaining the stability of glomerular endothelial cells, and maintenance of GBM<sup>65</sup>.

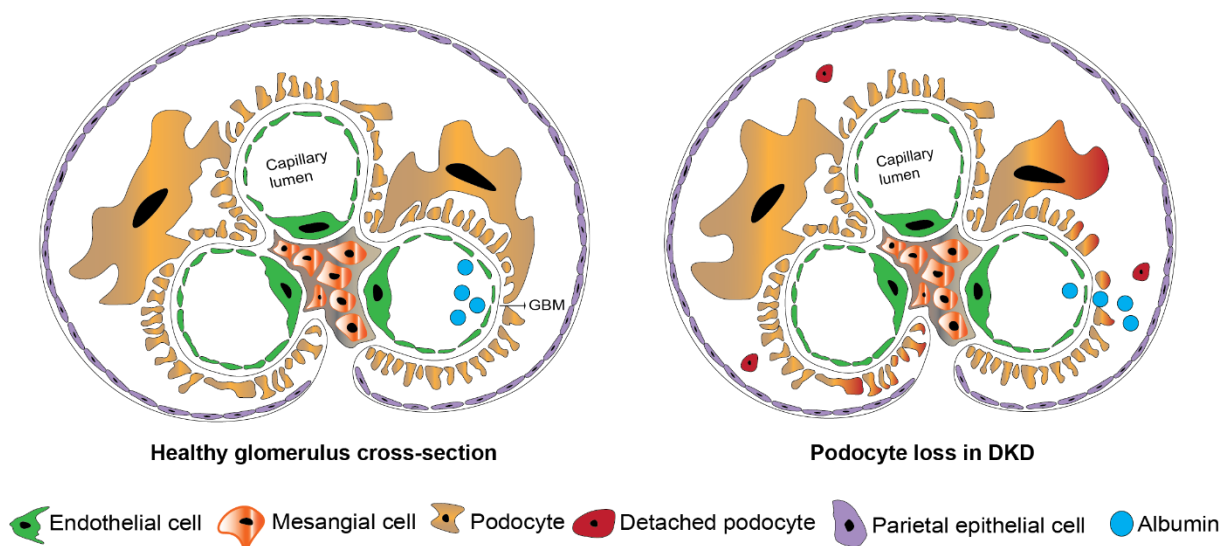


**Figure 8. A cross-section of the glomerulus.** The glomerular capillaries are fixed with endothelial cells (green) joined to the GBM. Podocyte cover the outer part of GBM with large cell bodies and between interdigitating foot processes (yellow). Mesangial cells (orange) and its associate extracellular matrix (gray) connect adjacent capillaries, and the capillary bundle is contained inside the bowman's capsule.

They are involved in the conservation of the capillary wall and capillary loop tension. Podocytes function as an integrated filtration unit; a significant cross-talk between endothelial cells, mesangial cells, and GBM is crucial<sup>66</sup>. Injury to the podocytes leads to lengthening the lamellipodial extensions, and focal adhesion turnover eventually results in retraction, and the movement of foot processes leads to foot processes effacement<sup>63</sup>. Previous studies proposed

that upon injury, podocyte cytoskeleton reorganization is the most common pathway resulting in foot-process effacement.

### **Risk factors of podocyte dysfunction**

Triggers of podocyte injuries are manifold, including impairment metabolism in glucose and lipids, high blood pressure, activation of RAS pathway, inflammation, genetics, toxins, shear stress, etc.<sup>67</sup>. In vitro, high glucose conditions increase podocyte apoptosis via a reactive oxygen species-dependent pathway<sup>20</sup>. In vivo, remnant podocytes expand their size to compensate for lost neighboring podocytes, i.e., podocyte hypertrophy. Several signaling pathways such as ERK1/2, mammalian target of rapamycin, GSK3 and some inflammatory signaling pathways contribute to podocyte injury. The TGF- $\beta$ /Smad signaling pathway is altered in diabetes, further induces epithelial-to-mesenchymal transition, finally leading to the detachment of podocytes from the GBM<sup>68</sup>. The detachment of podocytes from the basement membrane is a major phenotype in diabetic patients with CKD progression because its consequences are hyperfiltration and albuminuria and irreversible nephron loss, ultimately leading to kidney injury. Also, glomerular hyperfiltration-related shear stress increases the detachment of podocytes from the basement membrane<sup>69</sup>. Several cellular pathways affecting podocyte injury in CKD with diabetes include disturbed insulin, Notch, glomerular inflammation, increased proteostasis, autophagy, bypassing cell cycle checkpoints toward mitotic catastrophe, etc.<sup>70–74</sup>.

### **1.4. Current therapies**

Multiple drugs are available to treat CKD with diabetes. Several drugs have been deployed to treat diabetes, but RAS inhibitors showed a promising role in delaying CKD progression with diabetes<sup>75</sup>.

### **The Impact of Renin-Angiotensin System blockade in CKD patients**

The function of the RAS has been extensively studied in the pathophysiology of CKD. In the last decade, many studies have confirmed that the local intrarenal RAS operates separately from the systemic RAS and is stimulated in both experimental and human diabetes<sup>76–77</sup>. However, classically RAS is a simplistic pathway through angiotensin II (Ang II), and angiotensin II type 1 receptor (AT1R). Current observations have demonstrated the complexity of RAS that includes among others, the discovery from angiotensin-converting enzyme 2 (ACE2) in 2000 with its derived Ang II metabolites, along with angiotensin 1-7 (Ang (1-7)) and angiotensin 1-9

(Ang (1-9)), which present an essential function in the advancement and gradual increase of CKD with diabetes<sup>78-79</sup>. The kidney RAS is exclusively different from all other local RAS because the rest of the essential intrarenal Ang II production components are available with the nephron<sup>80</sup>. Ang II formation depends on the angiotensinogen substrates, angiotensin I, and the enzymatic action of renin, angiotensin-converting enzyme, angiotensin-converting enzyme2, and ACE-autonomous enzymatic pathways contains the serine proteases, such as chymase. Ang (1-7), a metabolite of Ang II, can be produced from Ang II via hydrolysis of ACE2 or from the polypeptide Ang I via angiotensin-converting enzyme<sup>81</sup>(Fig. 9). The study of development and complicated interactions among these hormones and their relative receptors has led to enlightening knowledge-related to the pathomechanism of CKD progression.

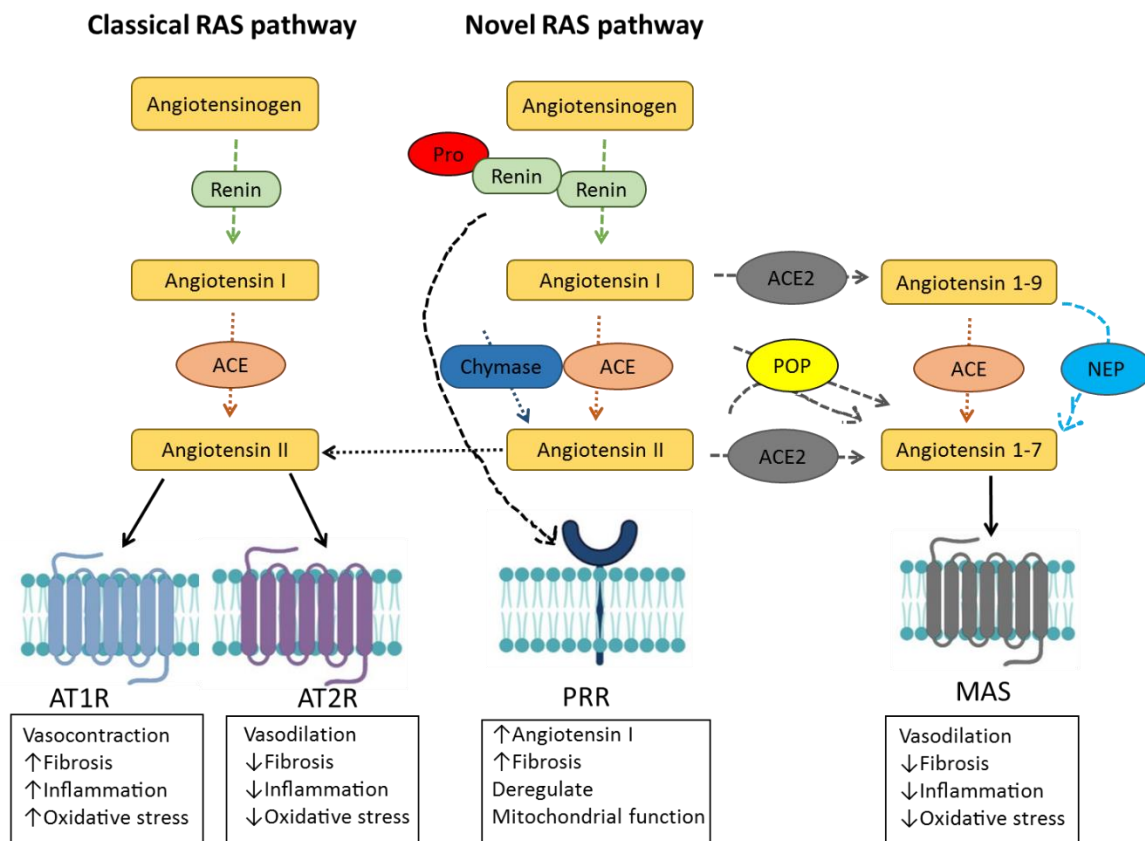


**Figure 9. Classical and novel pathways of the renin-angiotensin-aldosterone system modulated in CKD with diabetes.** RAS - renin-angiotensin-aldosterone system, ACE-angiotensin - converting enzyme, POP – Prolyl oligopeptidase, ACE2-angiotensin-converting enzyme 2, AT1R - angiotensin II type 1 receptor, AT2R - angiotensin II type 2 receptor, PRR - (pro)renin receptor, MAS - Mas receptor.

### Current treatment with RAS inhibitors

The RAS inhibitors enhanced insulin-mediated glucose uptake<sup>82</sup>, reduced inflammatory response, and increased adhesion molecule expression<sup>83</sup>. Ramipril treated group

effectively prevented the progression of diabetes compared with placebo<sup>84</sup>. The RENAAL study strongly supported the use of losartan as part of the standard of care in diabetic patients to lower the risk of progression to ESRD<sup>85</sup>. Telmisartan treated diabetic patients slow down the progression of CKD and high blood pressure compared with placebo. Furthermore, it is an essential therapeutic drug to protect against cardiovascular and kidney complications in CKD with diabetes<sup>86</sup>. However, SGLT2 inhibitors showed a potential effect along with RAS inhibitors on the diabetic population.

### **Sodium-glucose-transporter -2 as a therapeutic target in CKD with diabetes**

Diabetes is unique in involving SGLT2 for deactivating the tubuloglomerular feedback (TGF), thereby installing a persistent glomerular hyperfiltration and hypertension, known to accelerate proteinuria, glomerulosclerosis the progression of CKD<sup>87,88</sup>. Sodium-glucose cotransporter-2 inhibitor (SGLT2i), a negative controller of the SGLT2, is an oral antidiabetic (OAD) that allow a hopeful perspective in the medication of DKD, due to the glycemic control as well as in the remedy of the upset TGF that happens in diabetes (Fig. 10). SGLT2i diminishes glucose reabsorption in the proximal convoluted tubule, advances glycosuria, and decreases hyperglycemia in an insulin-autonomous way by repressing SGLT2. (Dissimilar to other OAD)<sup>89,90</sup>. Simultaneously, in the proximal tubule, glucose is reabsorbed, and then the prevention of sodium cotransport and then the tubular fluid sodium concentration is above in the *macula densa*. SGLT2i reactivates the TGF and reduces the glomerular weight and SNGFR, further decrease hyperfiltration and its unfavorable impacts on CKD with diabetes<sup>87</sup>. Furthermore, the restraint of SGLT2 stop kidney gluconeogenesis and advances weight reduction and lower blood pressure, which offers a slower pace of death from cardiovascular and for any other reason<sup>91</sup>.



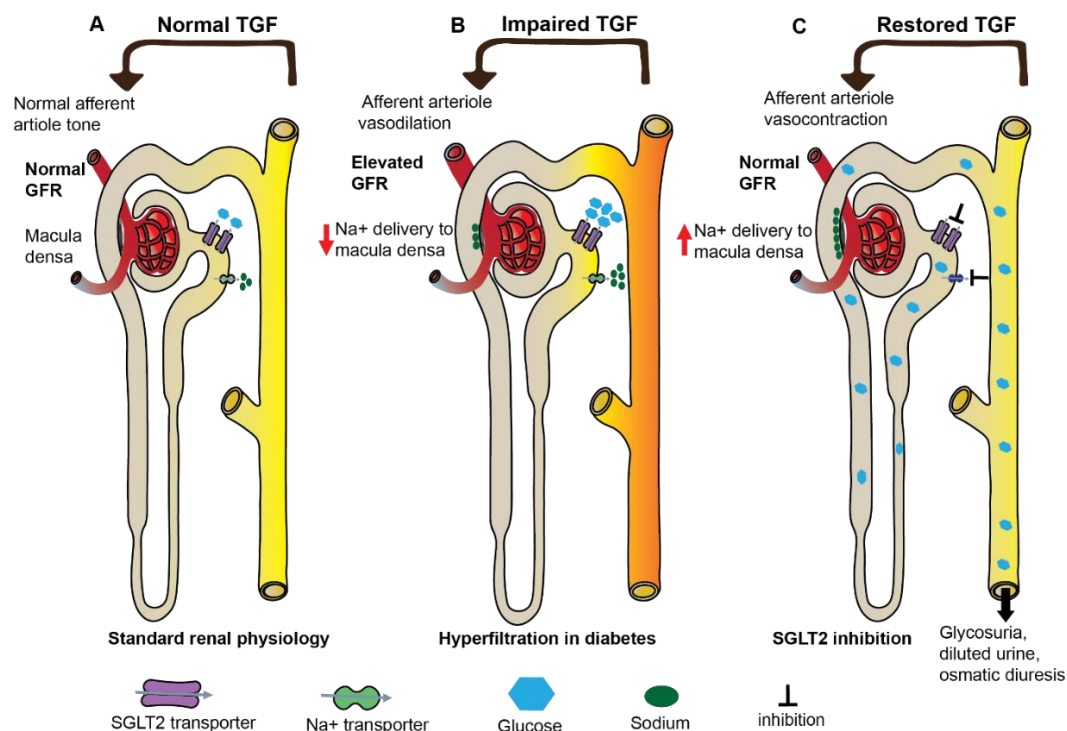


**Figure 10. Postulated tubuloglomerular feedback (TGF) mechanisms:** (A) In normal conditions, by adjusting pre-glomerular arteriole tone, GFR balanced the TGF signaling. (B) In diabetes, improves proximal SGLT2-mediated reabsorption of sodium and glucose reduces this feedback mechanism. Hence, other than the upregulation of GFR, the macula densa is exposed to low levels of sodium concentration. (C) Inhibition of SGLT2 restricts the proximal tubule glucose and sodium reabsorption, leads to increased glucosuria, and subsequently lowers the kidney plasma flow and hyperfiltration.

### Recent breakthrough with SGLT2 inhibitor therapy

SGLT2 inhibitors have been developed as antidiabetic drugs and their potent effects on CV morbidity, heart failure, and CKD progression on diabetic population<sup>92-93-94</sup>. The following three FDA approved drugs, empagliflozin, canagliflozin, dapagliflozin. Empagliflozin was combined with a slower kidney damage progression than in the placebo, even with standard care<sup>90</sup>. Canagliflozin treated diabetic patients reduces the risk of kidney and cardiovascular complications in the placebo group up to 2.62 years<sup>93</sup>. The DAPA-HF randomized patients were the same as those who registered and new HF trials with reduced ejection fraction (HFrEF). Recommended HFrEF therapy was given to these diabetic patients and treated with hypoglycemic drugs.

Consequently, the DAPA-HF trial dapagliflozin was tested in HFrEF patients with and without diabetes<sup>95</sup>. In October 2020, the DAPA-CKD trial first demonstrated that inhibition of the SGLT2 with dapagliflozin attenuates CKD with proteinuria in patients with or without diabetes



at unprecedented results. These results have far-reaching implications for a series of traditional concepts in nephrology. It became evident that CKD with and without diabetes involves predominant SGLT2-driven pathophysiology compared to the other pathogenic pathways currently under consideration in the research domain. Dapagliflozin showed a sustained decline in estimated GFR by up to 50% in CKD patients without diabetes<sup>96</sup>. Several SGLT2 inhibitors have been developed with high selectivity for clinical trials in patients with T2D, such as canagliflozin (Invokana®) dapagliflozin (Farxiga®)<sup>97-98</sup>. These drugs consistently helped T2D patient's glucose levels, along with weight loss and antihypertensive effects<sup>99</sup>. However, limited data on the use of SGLT2 inhibitors are available in T1D patients, and although efficacy is predicted to be identical to T2D, safety concerns remain, e.g., on diabetic ketoacidosis.

### **1.5. Recent findings of the pathogenesis in CKD with diabetes**

SGLT2 inhibition attenuates diabetic and non-diabetic CKD progression with proteinuria at such a vital effect size that it defines a milestone discovery in CKD research<sup>96</sup>. It gives hope to those that fear the morbidity and mortality related to CKD, those that fear the impact of kidney replacement therapy on their lives, especially those who do not have access or cannot afford kidney transplantation. This observation will create advanced motivation for the field of nephrology that has fallen behind in terms of research activity and progress, and that lost attractivity for young doctors. This way, the DAPA-CKD preliminary outcomes imagine another period of eagerness, dynamic changes, and unexpected research opportunities for the upcoming generation of nephrologists and clinical and basic science scientists. The aspirations do not stop with SGLT2 inhibition. The GFR declined with time in dapagliflozin-treated patients of the DAPA-CKD clinical trials. Therefore, there is space for other innovative treatments beyond the dual inhibition of RAAS/SGLT2.

### **1.6. Remaining unmet medical need**

Together, these data identify the hemodynamic changes induced by hyperglycemia as a central pathomechanism in the diabetic population<sup>22</sup>. Genetic factors, comorbidities, metabolic factors, neurohumoral activity, inflammation, and tissue remodeling contribute to the individual risk constellation and overall disease progression. However, hyperglycemia and the related hemodynamic alterations represent the universal abnormality applying to all patients and represent the prime targets for therapeutic intervention.

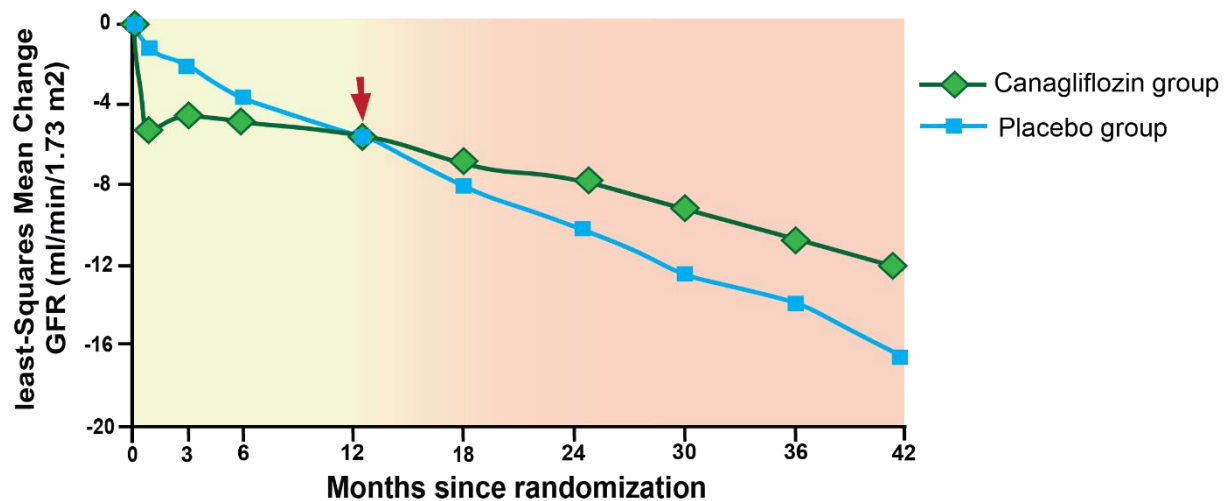


**Figure 11. The estimated GFR change in the treatment group.** The red arrow indicates that after 12 months, GFR decline in both groups.

There is a crucial necessity for novel models of therapy in the CKD population. Currently, pharmacotherapy, dialysis, and transplantation are the only available treatments for CKD and ESRD, limited by efficacy issues, clinical complications, and organ donor availability. Maximal conservative CKD treatments can fully stabilize CKD in non-diabetic subjects but are of limited efficacy. Current standard medical therapy of CKD is limited to hyperglycemia (metformin, SGLT2i) and blood pressure control, preferentially with RAS inhibitors and adjunct treatments such as statins and smoking cessation low-salt diet. Nevertheless, the strategies mentioned above are not sufficient to delay CKD progression in most cases<sup>88</sup>. Because SGLT2 inhibitors have shown their strong effects on CV morbidity, heart failure, and CKD progression on the diabetic population but not for long-term results. For example, canagliflozin maintained stably in the Credence trial GFR up to 12 months after that increased GFR decline, indicating the unmet need to stop CKD progression<sup>93</sup>. Also, mention that the rate of annual GFR decline is still would be physiological -0.7 ml/min/year (Fig.11).

Furthermore, RAS- and SGLT2-driven mechanisms indicate elevated levels of podocyte injury also showed nephroprotection impacts with RAS/SGLT2 dual inhibition but finally confirmed the podocyte injury even in humans<sup>100</sup>. For instance, medications that improve novel podocyte production from local podocyte progenitors may also attenuate glomerulosclerosis, nephron loss, and GFR decline<sup>101</sup>. So, we need to improve our drug targets, and according to recent studies, kidney cell regeneration from local progenitors<sup>102</sup> could be a potential add-on drug option in the CKD with diabetes population.

### 1.7. Podocyte regeneration

Podocytes, once lost, have a low capacity for structural regeneration. Recent studies demonstrated that mesangial and endothelial cells could proliferate and compensate for the loss of adjacent cells upon injury or apoptosis. However, this phenomenon is challenging for podocytes<sup>103</sup> because they are structurally highly differentiated and interconnected, post-mitotic, and hence they cannot proliferate<sup>104</sup>. Injured podocytes detach from the GBM frequently followed by focal sclerosis as a wound healing process<sup>105</sup>. Recent studies suggest that adult human glomeruli harbor resident progenitor cell (stem cell) populations along the urinary pole of the Bowman's capsule<sup>102</sup>. These cells' recognition is based on the expression of cluster of differentiation 24 (CD24) and prominin-1 (CD133)<sup>106-107,108</sup>. These cells have regeneration properties and can differentiate into either tubule cells or podocytes in *in-vitro* as well as *in-vivo*<sup>105-109</sup>. Such progenitors represent <2% of the kidney cells in mature kidneys<sup>106,110</sup> and behave as precursors of all kidney epithelial cells of the cortical nephron<sup>111</sup>.

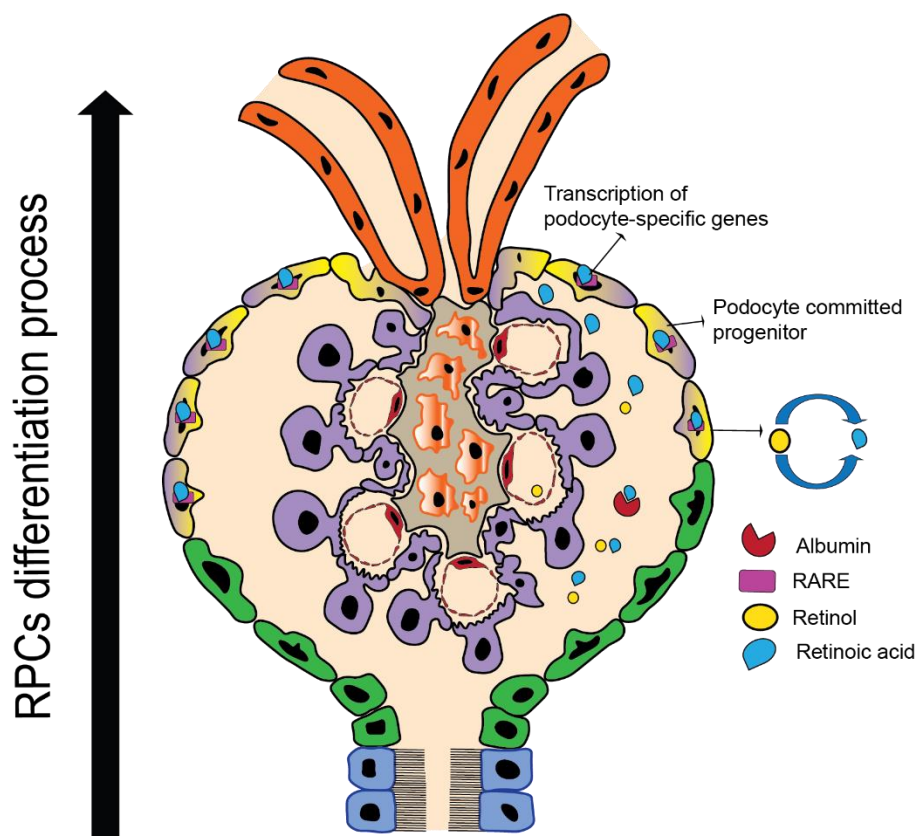


**Figure 12. Schematic representation of RPCs differentiation into podocyte lineage during mild proteinuria.** A glomerulus with low protein leakage, retinoid promotes RPC differentiation into podocytes. However, glomerulus presented with high protein leakage RA is sequestration with the albumin and abrogate the podocyte regeneration.

Nevertheless, in glomerular injury, parietal epithelial cells with stemness are not enough due to the difference between the degree of injury and proliferative response<sup>102,112</sup>. Also, collapsing glomerulopathy is represented with a proliferative response by podocyte progenitor cells<sup>105,113,114</sup>. This indicates the lack of terminal differentiation after clonal progenitor expansion to reestablish lost podocytes<sup>105,115,116</sup>. Glomerular progenitors show diverse regenerative possibilities through certain damage arranges and adjusted by the encompassing environment<sup>117-118</sup>. A recent study has shown the environmental components that liberated the RPC-recovery and albumin amount in the urinary proteinuria<sup>119</sup>. This observation showed that albumin compromised the RPC ability towards podocyte differentiation. Albumin protein has an affinity for retinoic acid sequestration. During GBM injury, the retinol goes into the Bowman's space and convert into retinoic acid by the podocyte retinaldehyde dehydrogenases (Aldh1) compound. This aggregation of retinoic acid in BS induces RPCs differentiation into podocytes. Retinoic acid enhances PECs differentiation towards podocyte lineage by the retinoic acid reaction element has presented in fig.12<sup>119</sup>.

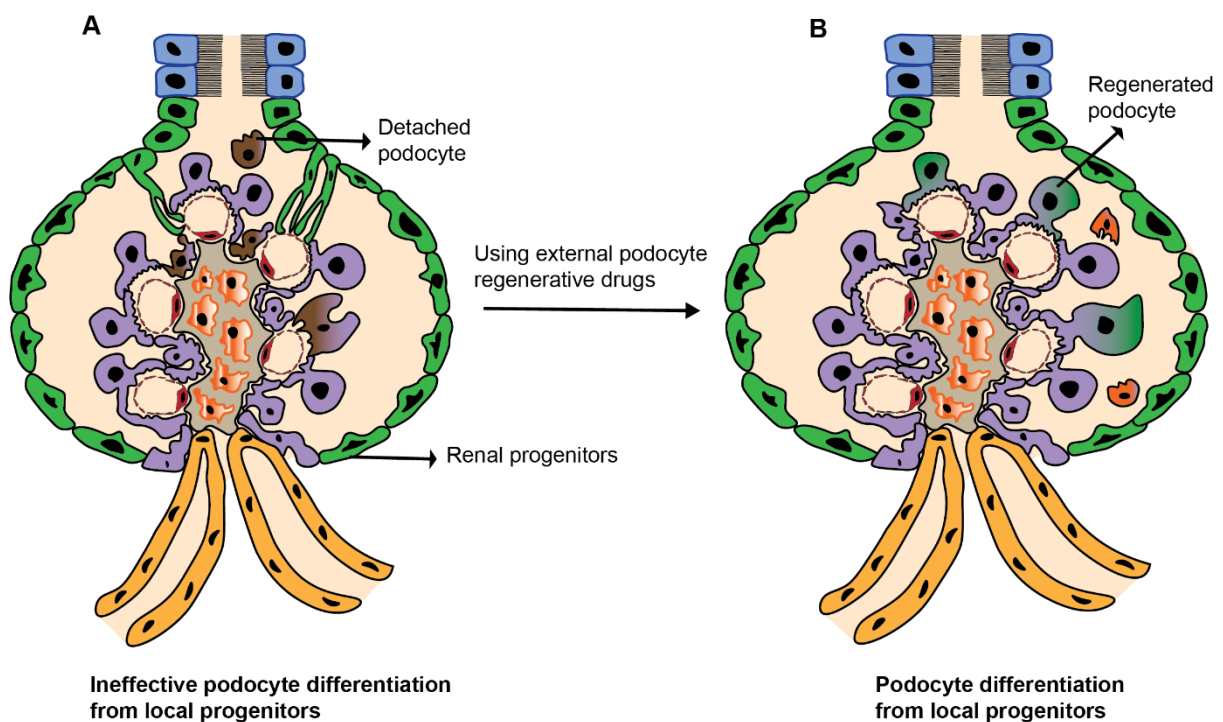


**Figure 13. Podocyte regeneration by pharmacologically enhanced from local progenitors**

Albumin is with a retinoic acid in the circulatory system, explains low albumin protein levels in the Bowman's space binds all retinoic acid, and decreases RPC differentiation factor, activated and multiplying RPC weakness podocyte<sup>119</sup>. Therefore, the excessive accumulation

of PECs in the Bowman's capsule and Bowman's space formed to crescent formations leads to the FSGS disease<sup>105,119,120</sup> (fig.13A).

Multiple studies have shown that drugs protect podocytes *in vitro* and *in vivo* models with podocyte damage. Previous studies were shown (2'Z,39E)-6-bromoindirubin-39-oxime (BIO), a compound that showed a variety of the above-mentioned molecular pathways<sup>121</sup>, to increase podocyte regeneration *in vitro* and *de novo* development of podocyte terminal differentiation *in vivo*<sup>122–124</sup>. It has shown that adriamycin nephropathy mice protect from albuminuria, increased podocyte number, and reduced progressive glomerulosclerosis by inhibiting glycogen synthase kinase (GSK3) signaling pathway with BIO<sup>102</sup>. Therefore, BIO (GSK3 inhibitor) would be a potential therapeutic target for reducing CKD progression.

### **1.8. Glycogen synthase kinase (GSK)- $\beta$ signaling pathway**

GSK3 $\beta$ , a well-persevered and signifying serine/threonine-protein kinase, plays a crucial function in regulating the cytoskeleton arrangement and cellular mobility<sup>125,126</sup>. There are numerous substrates mediated pleiotropic effects. This adaptability may come with the various complex systems that control the activities of GSK3, give that it phosphorylates substrates just at the ideal period, and inconsiderate subcellular components, generally framed by complexes of protein. Accordingly, post-translational modifications, substrate formation, protein complexes, cellular trafficking, and all provide the perfect regulation of GSK3<sup>127</sup>. Certainly, inhibition of the GSK3 $\beta$  pathway support to reduction of cell motility in multiple cell types, including glioma cells<sup>128</sup>, vascular smooth muscle cells<sup>129</sup>, gastric cancer cells<sup>130</sup>, and kidney tubular epithelial cells<sup>131</sup>. In the kidney, the GSK3 $\beta$  pathway has lately been implicated in acute kidney injury and kidney repair<sup>132</sup>. Even though GSK3 has presented exceptional developmental flexibility, each novel substrate of GSK3 that develops in any novel mechanism organized GSK3 function supports novel essential activity that could be affected by diseases. The GSK3 autonomous-activating procedure improves its further initiation, especially in other complications and novel therapeutic interventions.

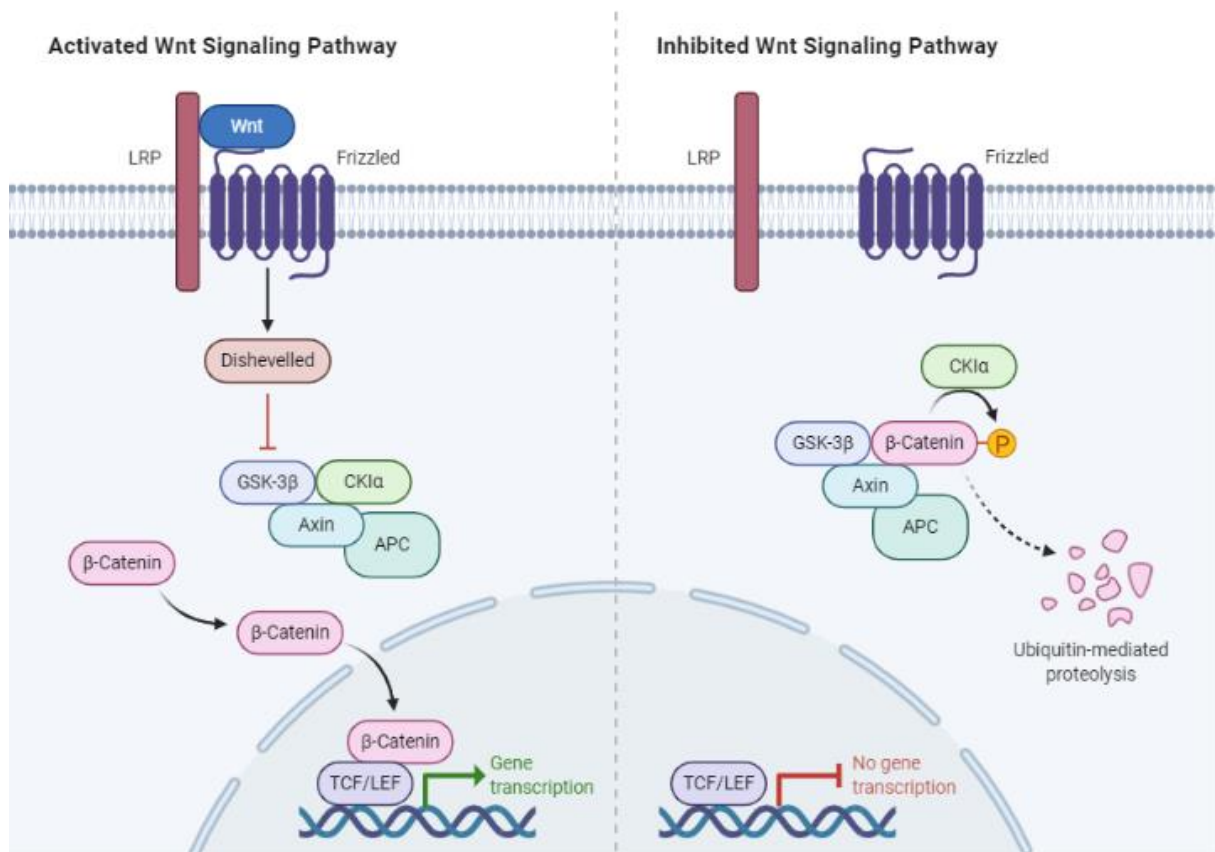


**Figure 14. GSK3β signaling pathway.**

### **Glycogen synthase kinase-3β is a novel drug target in diabetic kidney disease**

As per the human protein atlas, GSK-3β expression at mRNA and protein levels are poor in the human kidney<sup>124</sup>. However, for a more comprehensive study specifically, specific cell type expression and the diabetes impact on specific cell types of Gsk3β mRNA levels were tried appropriate to the current single-cell RNA sequencing for kidney cells from both diabetes non-diabetic mice<sup>101</sup>. Gsk3β mRNA levels were accessible in all glomerular cells (Fig.15). Moreover, there was no significant difference between the diabetic and control mice of the gene expression on GSK-3β based on the single-cell results<sup>101</sup>. Several GSK-3 inhibitors of small molecules have been developed and evaluate the therapeutic effects in different pathological models. Recent reports have demonstrated that the Inhibition of the GSK-3 signaling pathways the real-life essential drug target for severe CKD conditions with diabetes<sup>133,134</sup>. Also, MFG-E8 (GSK-3 inhibitor) was revealed as a novel therapeutic target and shown protection from CKD by down-regulation of MFG-E8, along with the GSK-3β signaling pathway<sup>135</sup>.

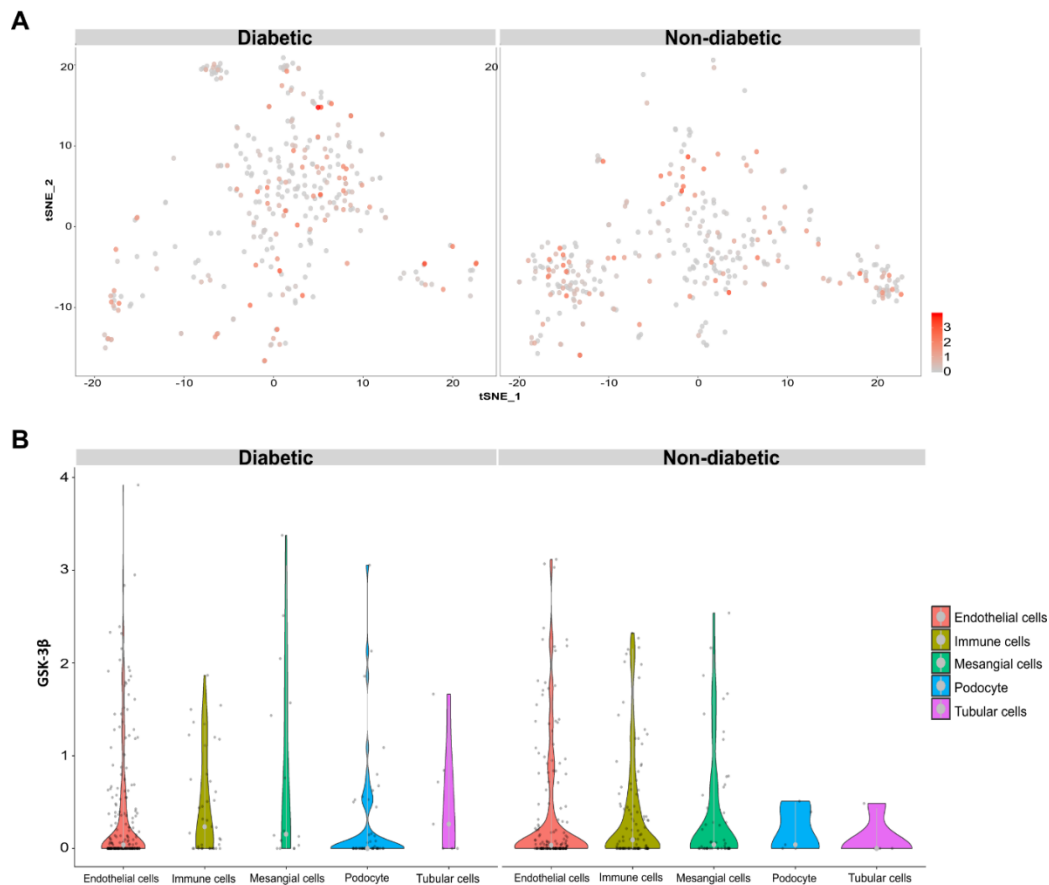


**Figure 15. *Gsk3β* single-cell RNA expression in glomerular cells in both diabetic and non-diabetic mice.** (B) tSNE analysis of *Gsk3β* expression in glomerular cells in diabetic (left) and control (right) mice. (C) The Violin plot shows the normalized expression for *Gsk3β* (in log-scale) across cell types for diabetic (left) and control (right) mice. (Adopted from Fu J. et al.)

GSK-3 inhibitors are the potential targets for diabetes by the increase of insulin sensitivity to maintain glucose homeostasis<sup>134</sup>. Furthermore, GSK-3 inhibition is potentially reduced the diabetic-associated islets inflammation in rats<sup>136</sup>. Subsequently, inhibition of GSK-3β might be an essential novel therapeutic target to delay disease progression beyond MRE treatment in CKD with diabetes.

## 2. Hypothesis

Chronic kidney disease is considered a leading global health problem<sup>6,137</sup>. Treatment with dual inhibition of RAS/ SGLT2 reduces CKD's progression rate and increases the regression of glomerulosclerosis<sup>138–145</sup>. For patients with advanced CKD, addressing podocyte dysfunction and their injury may be an attractive approach to dual inhibition RAS/SGLT2. Recent findings from Lasagani et al. reported that GSK3 $\beta$  signaling pathway inhibition by BIO (a GSK3 $\beta$  inhibitor) in adriamycin-induced nephropathy mice with increased podocyte numbers and decreased glomerulosclerosis and protected from albuminuria<sup>102</sup>. However, diabetes involves many other pathological pathway activations; therefore, an identical therapeutic effect is speculative. There is no systematic research in a model that precisely mimics the clinical scenario residual progression of DKD above standard therapy.

Therefore, based on the previous observations and questions, which is still to be addressed, we have made the following hypothesis:

**Glycogen synthase kinase inhibition with BIO induces renoprotective effects beyond standard-of-care therapy includes metformin, ramipril, and empagliflozin (MRE) in mice with type-2 diabetes.**

Objectives are as follow:

1. To set up a pre-clinical animal model with the following characteristics:
  - a. Obese mice to develop T2D.
  - b. Induction of nephron loss
2. Accelerated CKD progression and followed by with or without the standard-of-care therapy, i.e., MRE and +/- BIO.



### 3. Materials and methods

#### 3.1. Materials

**Table 2. Animal studies**

<b>Animal material</b>	<b>Company</b>
<b>Animal anesthesia</b>	
Isoflurane CP	CP-Pharma, Burgdorf, Germany
Medetomidine	Sanofi-Aventis GmbH, Paris, France
Midazolam	Ratiopharm GmbH, Ulm, Germany
Fentanyl	Zoetis GmbH, Germany
Atipamezol	CP-Pharma, Burgdorf, Germany
Flumazenil	Hexal AG, Munich, Germany
Buprenorphine	Bayer Vital GmbH, Leverkusen, Germany
<b>Animal surgery</b>	
BD Microlance™ Stainless Steel Needles	Becton Dickinson, NJ, USA
BD Plastipak™ Syringes	Becton Dickinson, NJ, USA
Sterile gauze balls (Mulltupfer)	Verbandmittel Danz, Germany
Sterile swab	Verbandmittel Danz, Germany
ETHIBOND EXCEL Polyester Suture 5-0	Ethicon, Germany
Vicryl™ 5-0 absorbable suture	Ethicon, Germany
Bepanthen Eye and Nose Ointment	Bayer, Germany
Surgical scissors and forceps	Integra LifeSciences, France
Brinsea Octagon 20 Eco Incubator Auto	Brinsea, UK
Infrared 100W Heat Emitting Bulb	Philips, Germany
Operation table	Medax, Germany
<b>Animal sample preservation</b>	
Histology embedding cassettes	NeoLab, Germany
Formalin 4 %	Merck, Darmstadt, Germany
EDTA	Carl Roth, Germany
<b>GFR measurement</b>	
NIC-Kidney device	Mannheim Pharma and Diagnostics, Germany
Double-sided adhesive patch	Lohmann GmbH and Co. KG, Germany
FITC-sinistrin	Mannheim Pharma and Diagnostics, Germany
Rechargeable miniaturized battery	Mannheim Pharma and Diagnostics, Germany
Sterile compress	Verbandmittel Danz, Germany
Medical adhesive tape	BSN Medical GmbH, Germany
Razor blades	Gillette, USA
<b>Urine and blood measurement</b>	
Mouse Albumin ELISA Quantitation Set	Bethyl Laboratories, USA
Creatinine FS	Daisy's, Germany
Urea FS	Daisy's, Germany

96wellMicroWell™ MaxiSorp™plate	Thermo Fisher, MA, USA
Nunc™ MicroWell™ 96-Well Microplates	Thermo Fisher, MA, USA
Bovine serum albumin fraction v	Roche Diagnostics, Mannheim, Germany
Tris	Carl Roth, Karlsruhe, Germany
Sodium chloride	Merck, Germany
Tween 20	Sigma-Aldrich, Germany
Sodium carbonate	Merck, Germany
Sodium bicarbonate	Merck, Germany
TMB Substrate Reagent Set	BD Biosciences, NJ, USE
Sulfuric acid	Sigma-Aldrich, München, Germany
pH meter	WTW GmbH, Weilheim, Deutschland
Tecan GENios™ Microplate Reader	Tecan, Germany

**Table 3. Standard mice diet**

<b>Ingredient</b>	<b>Quantity</b>
Crude protein	22.00%
Crude fat	4.50%
Crude fiber	3.90%
Raw ash	6.70%
Calcium	1.00%
Phosphorus	0.70%
Vitamin A	25000 U/kg
Vitamin D3	1500 U/kg
Vitamin E	125 mg/kg
Iron (II) sulfate monohydrate	100mg/kg
Zinc sulfate monohydrate	50mg/kg
Manganese (II) sulfate monohydrate	30mg/kg
Copper (II) sulfate pentahydrate	5 mg/kg
Calcium iodate Anhydrate	2.0 mg/kg

**Table 4. Sodium deficient and MRE diet**

<b>Ingredients</b>	<b>Quantity</b>	<b>Sodium deficient diet</b>	<b>MRE diet</b>
Crude protein	21.00%	+	+
Crude fat	5.10%	+	+
Crude fiber	5.00%	+	+
Raw ash	4.90%	+	+
Starch	28.90%	+	+
Sugar	11.50%	+	+
Nitrogen free extracts	60.00%	+	+
Calcium	0.92%	+	+

Vitamin A	15,000 U/kg	+	+
Vitamin D3	1500 U/kg	+	+
Vitamin E	150 mg/kg	+	+
Vitamin K	20 mg/kg	+	+
Thiamine (B1)	26 mg/kg	+	+
Copper	14 mg/kg	+	+
Sodium	<0.03%	-	-
Metformin	1500 mg/kg	-	+
Ramipril	6 mg/kg	-	+
Empagliflozin (12.5%)	480 mg/kg	-	+

**Table 5. RNA isolation, cDNA conversion, real-time qPCR**

Reagents	company
<b>RNA isolation</b>	
2-Mercaptoethanol	Sigma-Aldrich, München, Germany
DNase and RNase free water	Thermo Fisher, MA, USA
96% Ethanol	Merck, Darmstadt, Germany
RNase AWAY® spray	Sigma-Aldrich, München, Germany
RNAlater™ Stabilization Solution	Thermo Fisher, MA, USA
PureLink™ Mini RNA Kit	Ambion, Germany
RNase-Free DNase Set	Qiagen, Germany
Homogenizer Ultra-Turrax® T25	IKA GmbH, Germany
<b>DNA conversion</b>	
NanoDrop™ Spectrophotometer	Biotechnologie, Erlangen, Germany
5x First Strand-Puffer	Invitrogen, Karlsruhe, Germany
Acrylamide	Ambion, Darmstadt, Germany
Dithiothreitol	Invitrogen, Karlsruhe, Germany
dNTP Set	GE Healthcare, München, Germany
Hexanucleotid-Mix	Roche Diagnostics, Mannheim, Germany
RNAasin	Promega, Mannheim, Germany
SuperScript II Reverse Transcriptase	Invitrogen, Karlsruhe, Germany
Thermomixer 5436	Eppendorf, Hamburg, Germany
<b>Real-time qPCR</b>	
SYBR green I	Sigma-Aldrich, München, Germany
PCR Optimizer	Biomol, Hamburg, German
MgCl2 25Mm	Thermo Fisher, MA, USA
Bovine Serum Albumin PCR grade	Thermo Fisher, MA, USA
PCR-Primer	Metabion, Martinsried, Germany
Taq-Polymerase	New England BioLabs, Ipswich, USA
10X Taq Buffer	New England BioLabs, Ipswich, USA

Lightcycler 480 PCR with 96 wells	Sarstedt, Germany
Optical lid strip for 96-well plates	Sarstedt, Germany
LightCycler 480 Multiwell-Plate 96	Roche Diagnostics, Germany
LightCycler 480 Instrument	Roche Diagnostics, Germany

**Table 6. Histology**

<b>Antibodies and reagents</b>	<b>Company</b>
<b>Antibodies used in histology</b>	
Anti-mouse Wilms Tumor (WT)-1	Cell signaling, MA, USA
Anti-mouse Wilms Tumor (WT)-1	Santa Cruz Biotechnology, CA, USA
HRP linked Anti-Goat secondary Ab	Dianova, Hamburg, Germany
HRP linked Anti-Rabbit secondary Ab	Cell signaling, Danvers, MA
<b>Reagents used in histology</b>	
DAB substrate chromogen system	DakoCytomation, Glostrup, Denmark
Avidin-Biotin Complex Kits	Vector Laboratories, USA
Antigen unmasking solution	Vector Laboratories, USA
Avidin	Vector Laboratories, USA
Biotin	Vector Laboratories, USA
DAB Peroxidase Substrate Kit	Vector Laboratories, USA
Nuclear Fast Red solution	Sigma-Aldrich, Munich, Germany
Ammonium persulfate (APS)	Bio-Rad, CA, USA
Disodium tetraborate	Merck, Darmstadt, Germany
Antifade Mounting Medium with DAPI	Vector Laboratories, CA, USA
Picro-Sirius red solution	Sigma-Aldrich, Munich, Germany
Eosin	Merck, Germany
Fixation solution	Acquascience, Uckfield, UK
Formaldehyde	Merck, Germany
Hydrogen peroxide	Merck, Germany
Methanol	Merck, Germany
Paraffin	Merck, Germany
Periodic acid	Carl Roth, Germany
Schiff Reagent	Sigma-Aldrich, Munich, Germany
Nitric acid	Merck, Darmstadt, Germany
Silver nitrate	Carl Roth, Germany
Thiosemicarbazide	Sigma-Aldrich, Munich, Germany
Xylene	Merck, Germany

**Table 7. Miscellaneous**

<b>Miscellaneous</b>	<b>Company</b>
Falcon, 15/50 ml	Greiner Bio-One International GmbH, Germany
Reaction tubes, 1.5/2.0 ml	Paul Boettger GmbH Co. KG, Germany

PCR Safe lock tubes, 1.5/2.0 ml	Eppendorf, Germany C
ryovial, 2.0 ml	Alpha Laboratories, UK
Refill pipette tips	Greiner Bio-One International GmbH, Germany
Serological Pipette	Greiner Bio-One International GmbH, Germany
PBS	PAN-Biotech
Tissue culture dish, 100 mm	TPP, Trasadingen, Switzerland
Analytic Balance	BP 110 S Sartorius, Göttingen, Germany
Mettler PJ 3000 Mettler-Toledo	Greifensee, Switzerland
Heraeus, Minifuge T	VWR International, Darmstadt, Germany
Heraeus, Biofuge primo	Kendro Laboratory Products GmbH, Germany
Heraeus, Sepatech Biofuge A	Heraeus Sepatech, Germany
Leica DC 300F	Leica Microsystems, UK
Olympus BX50	Olympus Microscopy, Germany
Microtome HM 340E	Microm, Heidelberg, Germany
Thermomixer 5436	Eppendorf, Hamburg, Germany
Vortex-Genie 2™	Bender Holbein AG, Zürich, Switzerland
Water bath HI 1210	Leica Microsystems, Bensheim, Germany
Easypet® pipette controller	Eppendorf, Germany
Pipetman® pipette	Gilson, Middleton, WI, USA
Research Pro electronic pipettor	Eppendorf, Germany
Multi-channel pipettor, 30-300 µl	Eppendorf, Germany

---

## 3.2. Methods

### 3.2.1. Animals

At the age of five-week male BKS.Cg-m<sup>+/+</sup>*Lepr*<sup>db</sup>/BomTac mice were purchased from the Taconic (Ry, Denmark). All mice were homozygous for the Leptin receptor gene spontaneous mutation; therefore, it induces obesity and becomes T2D (*Lepr*<sup>-/-</sup>). We were used as the experimental (T2D) group, and specific age-matched non-diabetic mice (*Lepr*<sup>+/+</sup>) were used as the control group (WT). The universal marking identified animals on the tail. Each cage had individual cage cards to display details such as the animal number, the study number, the initiation dates, and the experimenter. The regional government authorities based on the EU directive for the Protection of Animals only used for Scientific Purposes (2010/63/EU) approved this experimental protocol.

### Animal surgery model - uninephrectomy

Uninephrectomy performed under general anesthesia. During the surgery, the body temperature was maintained constant at 36–37 °C by keeping the mouse on a heating pad. Firstly, shaved the fur with a razor blade then sterilized it with alcohol. After that, using curved scissors opened the skin layer and, later, the muscle layer without interfacing these two layers.

A knot was made using a non-absorbable suture near the hilus region to stop blood flow towards the kidney. By using curved scissors, separated the kidney by cutting the kidney artery above the knot. After separation of the mouse's kidney by using an absorbable Suture closed both muscular and skin layers. Then injected 200  $\mu$ L of buprenorphine and antagonist subcutaneously in different sites of mouse skin. After surgery, 0.5 ml of saline (NaCl 0.9%) supplemented all mice to maintain internal fluid balance. The two consecutive days from the surgery mice under post-surgery care.

### 3.2.2. Experimental design

The experimental animal study design is illustrated in detail in figure 15. All mice undergo uninephrectomy at six weeks<sup>146–149</sup> (T2D-uNX, n = 43; WT-Unx, n=23) to reduce the number of nephrons associated with aging and injury-related nephron numbers in clinical patients. After two weeks of surgery (T0), all mice fed with a low-sodium diet (sodium  $\leq$  0.03%) during the study as an effort to increase hyperfiltration in the glomerulus further accelerates the progression of CKD as stated in Fig.16<sup>150</sup>. At 20 weeks of age (T12 of the study), some T2D-Unx mice have sacrificed at week six as a baseline (T-2 of the study) for histological analysis (n = 6).

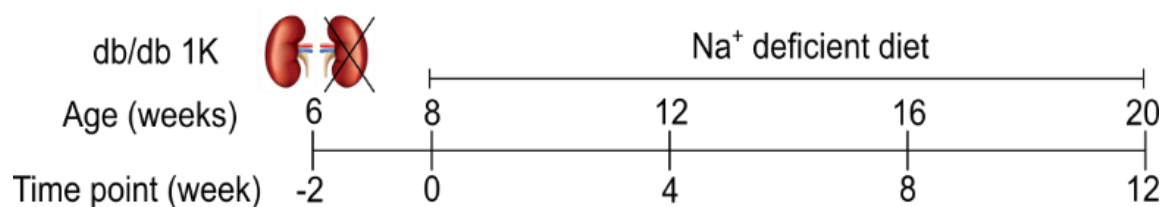


**Figure 16. Standardization of progressive glomerulosclerosis in male T2D-Unx mice.**

MRE therapy contains metformin (1500 mg/kg), ramipril 6 mg/kg, and empagliflozin (480 mg/kg) of 12.5% (=60 ppm). BIO (2  $\mu$ mol/kg) was injected subcutaneously to the mice five days/week. Additionally, another group of mice has randomly treated with MRE, as well as BIO add-on therapy (Fig.17). At this point, T2D-Unx and WT-Unx mice were randomized to either no-treatment, treatment with MRE, and treatment with BIO (calculation of the number of animals per group were detailed in Table 8).

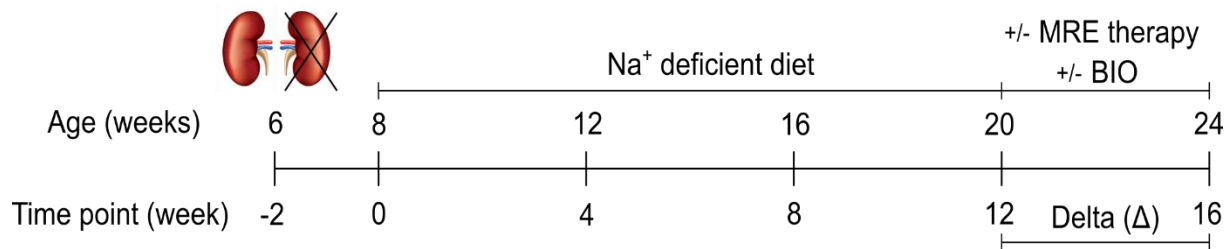


**Figure 17. The experiment design to study the impact of combined MRE+ BIO therapy.**

The rest of the T2D-Unx group animals were continued for further experiments ( $n = 37$ ). Group size calculation was based on the GFR as a primary endpoint and quantitative assumptions from our previous studies<sup>148,151,152</sup>.

**Table 8. Animals are included for the analysis at the end of the experiment**

	T2D-Unx	T2D-Unx + MRE	T2D-Unx + BIO	T2D-Unx + MRE + BIO	WT-Unx	WT-Unx + MRE	WT-Unx + MRE + BIO
Body weight (g)	6	11	10	10	10	11	10
Blood glucose (mg/dl)	6	11	10	10	10	11	10
GFR ( $\mu$ l/min)	6	11	10	10	10	11	10
UACR ( $\mu$ g/mg)	6	9	10	9	10	11	10
Glomerular area (AU) [Superficial nephrons]	5	7	10	7	-	-	-
Glomerular area (AU) [Juxtamedullary nephrons]	5	7	10	7	-	-	-
Podocyte number(AU) [Superficial nephrons]	5	7	10	7	-	-	-
Podocyte number (AU) [Juxtamedullary nephrons]	5	7	10	7	-	-	-
Podocyte density (%) [Superficial nephrons]	5	7	10	7	-	-	-
Podocyte density (%) [Juxtamedullary nephrons]	5	7	10	7	-	-	-
Sirius red positive area (AU) [Superficial nephrons]	4	6	8	7	-	-	-
Sirius red positive area (AU) [Juxtamedullary nephrons]	4	6	8	7	-	-	-
Tubular area (AU)	4	7	7	11	-	-	-
Open capillaries	4	7	10	8	-	-	-

Abbreviations: GFR, glomerular filtration rate; UACR, urinary albumin creatinine ratio; AU, arbitrary units.

Before mice sacrifice by cervical dislocation, urine and plasma samples were collected at week 24. Then mice kidneys were isolated for the next analysis. The isolated kidneys were separated into three parts: one part that was instantly frozen in liquid nitrogen, later preserved at -80 °C to estimate protein and cryosections. For RNA isolation, the second portion was transferred to 500 µl of RNA later solution and preserved at -20 °C, and the last portion of the mouse kidney was transferred to in 4% formalin minimum 24 hours for tissue fixation before paraffin embedding for assessment of histology.

### **3.3. Collection of urine and blood from mice**

Mice urine samples were obtained every two weeks throughout the study with the certified procedure, and urine was immediately preserved at -20 °C until additional analysis. Blood was collected every two weeks throughout the study by facial vein bleeding technique covered by isoflurane anesthesia. Blood samples were collected into tubes with ten µl EDTA (0.5M), centrifuged at 7168 g for 5 minutes, and then isolated plasma preserved at -20 °C until further assessment. Blood glucose was measured every two weeks throughout the study by using the ACCU-CHEK device.

### **3.4. Urinary albumin to creatinine ratio**

#### **Urinary albumin**

Mice albumin concentration in the urine was estimated with an albumin Elisa kit recommended by the manufacturer's protocol (Bethyl laboratories). The urine samples were briefly diluted (1:1000), and the primary antibody was added into the respective wells of a NUNC 96 well maxisorb plate and whole night incubation at 4 °C. The next morning, with wash buffer, the plate was washed thrice and incubated with blocking buffer (TRIS-NaCl 1times + BSA 1%) for one hour to reduce the nonspecific binding. Next, the ELISA plate was washed thrice with wash buffer, and a secondary antibody with HRP conjugated (1:100000) was added, and the plate was incubated in the dark at room temperature (RT) for 1hr. After secondary antibody incubation, the plate was washed thrice with wash buffer and incubated for 5-10 minutes in the dark at RT. TMB reagent (by mixing two identical parts from two substrate reagents) was added and incubated in the dark until the appearance color, followed by a 50 µl stop solution. The absorbance was measured at 450 nm within 10 minutes after stopping the reaction. The albumin concentration in each sample was determined using the



regression line equation produce by plotting observed absorbance of individual standards versus their known concentrations.

### **Urinary creatinine**

The plasma and urine creatinine concentration levels were estimated as described manufacturer's protocol (DiaSys Diagnostic system, GmbH, Germany). Briefly, urine was diluted 1:10 ratio in distilled water, and also standard preparations were done. According to the protocol, the working reagent contains four parts of R1 reagent, one part of R2. Then 10  $\mu$ l of diluted samples and standards were placed into the 96-well plate. Later added 200 $\mu$ l of working reagent into the plate and waited for 1 minute, and then absorbance was measured at 492nm with an ELISA plate reader. Furthermore, absorbance was measured after 60 seconds and 120 seconds of different incubations at time intervals. Urine creatinine concentration was measured as creatinine (mg/dl) =  $\Delta A$  sample /  $\Delta A$  standard \* standard concentration (mg/dl).

### **3.5. Glomerular filtration rate (GFR)**

All mice were anesthetized with isoflurane to mount a NIC-device onto the shaved neck using a double-sided adhesive patch. The NIC-device has light-emitting diodes and a photodiode that connects to a battery<sup>65</sup>. The background signal of the skin was recorded for 5 min before the i.v. Injection of 150 mg/kg FITC-sinistrin. The animal was conscious and unrestrained in a single cage, and the recording of signal duration is approximate 90 minutes. After detachment of the NIC-device, the data were analyzed with MPD Lab software. The GFR ( $\mu$ l/min) was measured from the decrease of fluorescence intensity in the blood circulation over time using a three-compartment model and body weight, and an empirical conversion factor<sup>153</sup>.

For the CKD progression assessment, delta GFR was measured as the percentage of difference from week 20 to week 24 of the treatment period. Moreover, the difference in GFR between week 20 to week 24 was showed as an increase (> 10%), stable (+/- 10%), or decreased (< 10%). The number of mice in each group were measured and shown as a percentage.



**Figure 18.** fixation of the transdermal GFR monitor to the mouse. Photos of fur removal and NIC-device and battery placed the NIC-device on the mouse's skin. After that securing the NIC-device by wrapping around with the adhesive tape.

### 3.6. Immunohistochemistry

#### 3.6.1. General procedure for staining

For immunohistological studies, I immediately fixed each kidney's middle part in 4 % formalin for 24 h. Kidneys were fixed with Leica tissue processors and embedded in paraffin blocks. The kidney paraffin blocks were cut to 2  $\mu$ m followed by de-paraffinization, sections were kept in xylene for 5 min and repeated the same step three times. The re-hydration was performed by 3 min x 3 in 100 % ethanol, 3 min twice in 95 % ethanol, and 70 % ethanol for three minutes. In the end, washing the sections with PBS for 5 min and repeat two times. Then, endogenous peroxidase was blocked in H<sub>2</sub>O<sub>2</sub>, and methanol mixture contains 20 ml of 30 % H<sub>2</sub>O<sub>2</sub> in 180 ml of methanol for 20 min in the dark and then washed in PBS for 5 min and two times. Endogenous biotin was blocked with one drop of Avidin for 15 min, then Biotin for another 15 min. All sections were washed with PBS for 5 min and two times after the incubation. The sections were prepared for further immunostaining. Different primary antibodies were incubated overnight at 4°C in a wet chamber. After washing with PBS (2x 5 min), sections were incubated with biotinylated secondary antibodies for 30 min at RT, followed by a PBS (2x 5 min) wash. Sections were incubated with substrate solution for 30 min at RT in a humid chamber followed by PBS wash for 5 min. Rinsing sections in Tris buffer for 5 min before

staining with DAB, the following is counterstaining with methyl green. To removing excess stain and xylene, sections were washed with 96 % ethanol, then dried and mounted with VectaMount.

The primary antibodies used in studies were mentioned above in table 9. For each immunostaining, a negative control was performed by incubation with the respective isotype antibody instead of the primary antibody.

### 3.6.2. PAS staining (Glomerular size)

Two-micrometer sections were stained with the periodic acid-Schiff (PAS) reagent to measure glomerular size. Briefly, each kidney randomly was chosen 40x images were captured containing superficial or juxtamedullary glomeruli. Table 11 defines The total number of images taken per section for each time point. Two observers conducted a blinded quantification of the glomerular tuft area performed for each glomeruli using Image J (1.51u) software.

**Table 9. Staining procedures**

Staining	Primary solution	Incubation time	Secondary solution	Incubation time
PAS staining	Periodic acid	5 min	Hematoxylin solution	2 min
	Schiff solution	20 min		
WT1 staining	WT-1	60 min	Goat a-rabbit. biot	30 min
Sirius red staining	Picro-Sirius red solution	60 min		

### 3.6.3. Picro-Sirius Red staining

#### Glomerulosclerosis

Picro-Sirius Red (Collagen; Sigma-Aldrich, US, 0.1%) stain was used in 40x images to quantify diffused glomerulosclerosis, both superficial and juxtamedullary glomeruli (Table 11). All the images were subsequently posterized with GIMP (2.8.22) tools to isolate Picro-Sirius Red stains' positive color for collagen deposition. The percentage of glomerulosclerosis in each glomerulus was measured by two blind observers in the modified images using Image J.

#### Tubular size

The number of tubules per section in 20x images, we used the Picro-Sirius Red stain. All histological structures were removed from the image, other than proximal tubules. Using GIMP (2.8.22) software to separate the yellow color, represented the tubular area, the image

was posterized, and the Picro-Sirius Red color staining for collagen positive was eliminated. The number of tubules per section was measured and divided by the tubular area to count the average tubular size. Quantification was performed in a double-blinded fashion using Image J software.

#### 3.6.4. WT1 staining (Podocyte number and density)

Two-micrometer sections were stained with Wilms tumor 1 (WT-1) (Santa Cruz, Santa Cruz, CA; 1:200) to count the podocytes. Images of superficial and juxtamedullary glomeruli were taken at 40x magnification (Table 11). Moreover, WT-1 positive cells were separately quantified in the glomeruli. Podocyte density is expressed as a percentage by the number of podocytes per respective glomerular tuft area. Two observers conducted the quantification using Image J software in a blinded manner.

### 3.7. In-vitro studies

#### Cell culture and experimentation

Glomeruli are isolated from high purity mouse kidneys. The isolated glomeruli were resuspended in 2 ml of RPMI 1640 medium (Sigma-Aldrich, Darmstadt, Germany) with 15mM HEPES, 1.7  $\mu$ M Insulin (Sigma- Aldrich, Darmstadt, Germany), 1% PS. The experiment processes were performed on ice except for the collagenase digestion at 37 °C. For *in vitro* study, about 5000 glomeruli isolated from healthy control mice and were incubated in 2 mL RPMI 1640 medium (Sigma-Aldrich, Darmstadt, Germany) with 15mM HEPES, 1.7  $\mu$ M Insulin (Sigma- Aldrich, Darmstadt, Germany) and 1% PS and stimulated for 24 hours with or without 30 mM glucose, 10  $\mu$ M BIO and/or 100ng/ml LPS. These treated glomeruli were used for subsequent further analysis.

#### RNA isolation and RT-PCR

Total RNA was isolated with the help of an RNA isolation kit from Ambion. Briefly, after treatment, cells were washed with ice-cold PBS and collected in 1.5 ml of RNAase free tube by centrifugation at 103541 rpm for 6min. However, RNA isolation from kidney samples was performed in lysis buffer (600  $\mu$ l) and homogenized at 4 °C for 30 seconds. Next, samples were placed onto the RNeasy mini-columns with 2 ml collection tubes and spin for 15 seconds at 103541 rpm at RT. Next column washing was done by wash buffer 1 and 2 by spinning for 15 sec at 103541 rpm, and this step was repeated one more time. Finally, the final filtrate was collected in a 1.5 ml sterile recovery tube and resuspended in 40  $\mu$ l of RNase-free water. The

isolated RNA purity measured with Nanodrop at the optical density ratio at 260 nm and 280 nm and the sample quality of 1.8 or higher was advisable. Synthesis of cDNA was performed according to the standard protocol. A total of 1 µg of RNA was used for cDNA synthesis. Briefly, RNA was incubated in reverse transcriptase buffer supplemented with dNTPs, Hexanucleotide, linear acrylamide, Superscript, or ddH<sub>2</sub>O as a control. Next, the reaction mixture was placed in a thermal cycler at 42°C for 1 h. For real-time polymerase-chain-reaction, cDNA was diluted by 1:10 dilution. SYBR green master mix and the recommended standard protocol was used for performing the RTPCR.

### Oligonucleotide primers used for RT-PCR

The following primers were used in this study.

**Table 10. Primers sequences**

Gene target	Sequences
Ccnd1	5'-TCATCAAGTGTGACCCGGACTG-3' (forward) 5'-TGTCCACATCTCGCACGTC-3' (reverse)
Nephrin	5'-CTGGGGGACAGTGGATTGAC-3' (forward) 5'-GGTCTGTGTCTTCAGGAGCC-3' (reverse)
αSma	5'-TCCTTCGTGACTACTGCCGAG-3' (forward) 5'-ATAGGTGGTTTCGTGGATGCC-3' (reverse)
Il-6	5'-TAGTCCTTCCTACCCCAATTCC-3' (forward) 5'-TTGGTCCTTAGCCACTCCTTC-3' (reverse)

## 4. Statistical analysis

All data are shown by means with standard deviation (SD) or as boxplot statistics. Data were quantified for normal distribution before statistical analysis by testing the data distribution against the predicted normal distribution with a quantile-quantile (Q-Q) plot and verifying the Shapiro-Wilk test. For multiple comparisons, checks of normally distributed data for statistically significant differences were used by ANOVA and post-hoc Tukey's correction. Non-normally distributed results are consistent with multiple Wilcoxon signed-rank testing comparisons or else Kruskal Wallis testing with post-hoc Dunn's test correction (Table 12). Survival was plotted as Kaplan-Meier curve, and using log-rank tests, comparisons between groups were evaluated. The value of  $p < 0.05$  was considered to indicate statistical significance. The R version (3.5.3) was used to run all statistical tests and analysis.

## 5. Results

### 5.1. Establishing a model of progressive CKD in obesity-related type 2 diabetes

#### 5.1.1. T2D mice show glomerular hyperfiltration even upon uninephrectomy.

To establish a progressive CKD model in T2D-Unx mice, and fed with a low sodium diet from 8 to 20 weeks. T2D-Unx mice were average weight at the baseline later developed the obesity contrasted with uninephrectomized non-diabetic control mice (WT-Unx) (Fig.19A). T2D-Unx mice shown hyperglycemia and increased hyperfiltration throughout the experiment compared to WT-Unx mice (Fig.19B-C).

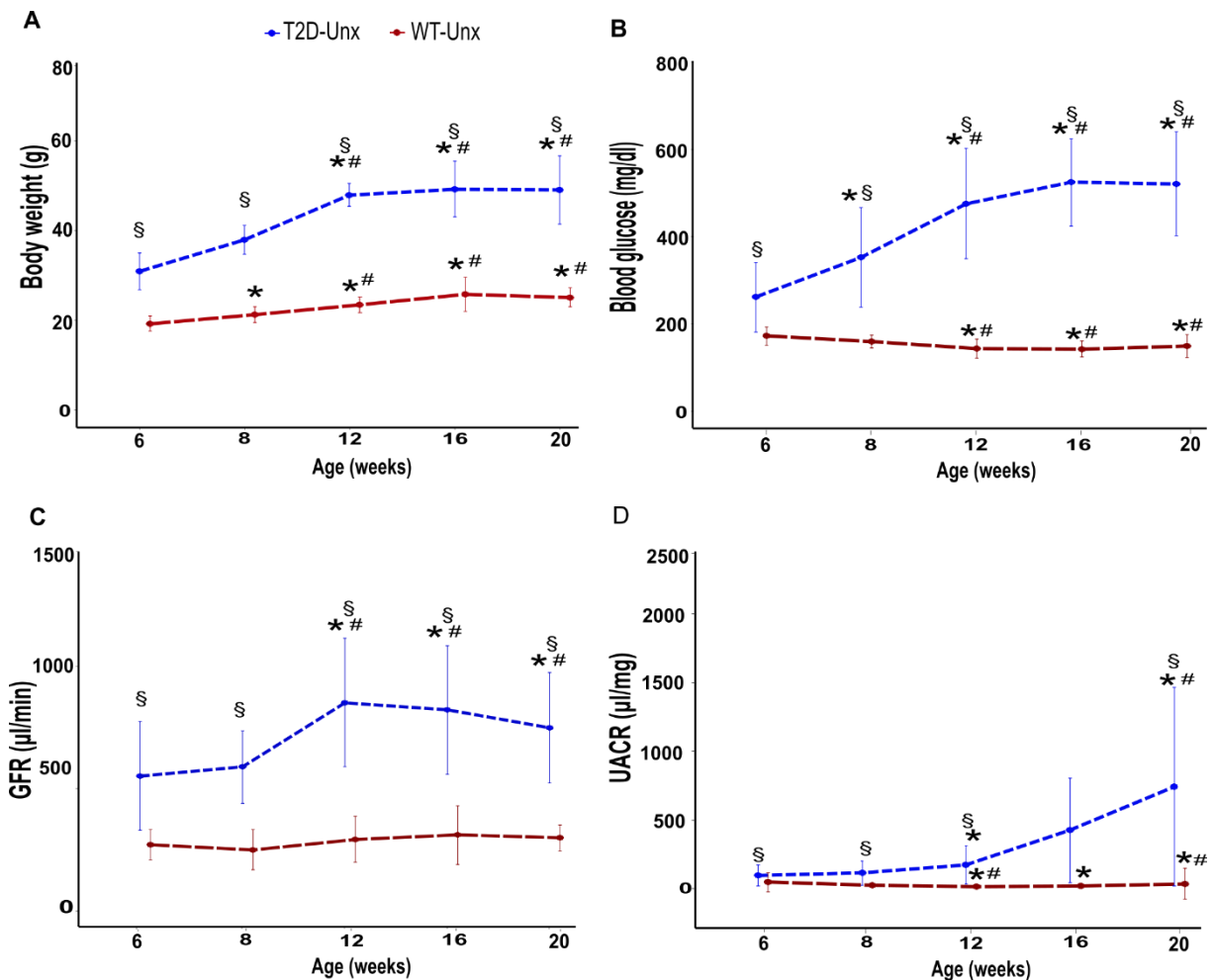


**Figure 19. Establishment of a model of hyperfiltration with T2D-Unx in male mice.** (A) Bodyweight progression. (B) The evolution of blood glucose. (C) GFR evolution, all data expressed as mean  $\pm$  SD (T2D-Unx (n=34) and WT-Unx (n=23)). (D) Progression of UACR, expressed as mean  $\pm$  SD (T2D-Unx (n=26) and WT-Unx (n=18)). \*p-value  $\leq$  0.05 versus week 6; #p-value  $\leq$  0.05 versus week 8; \$p-value  $\leq$  0.05 versus WT-Unx. Statistics were summarized in Table 12.

Urinary albumin to creatinine ratio (UACR) continuously increased right after surgery (Fig. 19D). Consequently, hyperfiltration increases in the remaining nephrons and consistently maintained higher than in WT-Unx controls at week 20.

Mortality in T2D-Unx mice was not observed right after surgery, so no infection was detected after the surgery. However, about 30% of T2D-Unx mice died before week 20, which could be due to internal infections or other unknown causes and severity compared to 10% in WT 1K mice (Fig.20A).

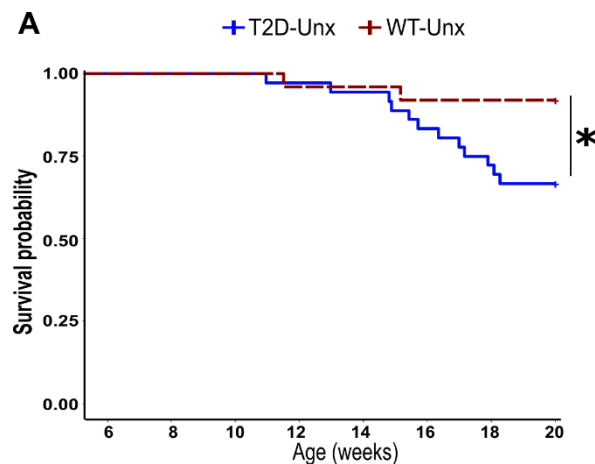


**Figure 20. Survival analysis.** Survival analysis for T2D and WT mice upon uninephrectomy surgery (6 weeks of age) and until 20 weeks of age. \*p-value  $\leq 0.05$ . Statistical analyses were summarized in Table 12.

#### 5.1.2. db/db mice display typical pathophysiological features of progressive CKD

To study the secondary outcome in T2D-Unx mice, analyzed histological parameters separately in superficial and juxtamedullary nephrons at week 6 and week 20. Compared to baseline, Sirius red positive area increased in the glomerulus mesangial matrix at week 20, which indicated progressive glomerulosclerosis in both types of nephrons (Fig.21A). In PAS-stained sections, increased glomerular structural changes indicated a single nephron's hyperfiltration at week 20 (Fig.21B).



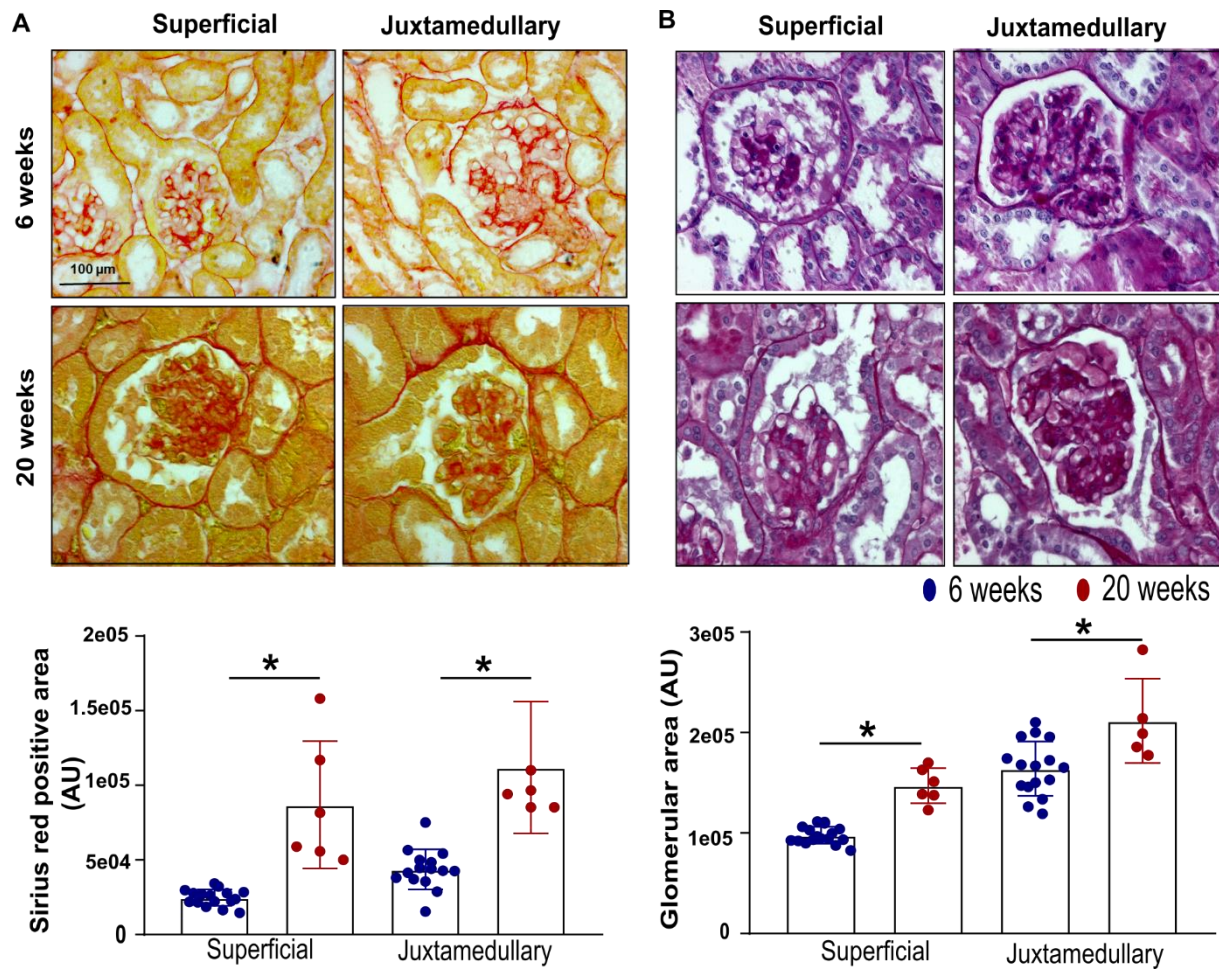


**Figure 21. Setting up a progressive glomerulosclerosis model in T2D-Unx mice.** (A) In T2D-Unx mice, estimated as Sirius red positive area (AU) as a Glomerulosclerosis. (B) In T2D-Unx mice, calculated as the glomerular tuft area (AU) in PAS sections as a Glomerular area assessment. Both types of nephrons were analyzed separately, and the average number of glomeruli quantification was summarized in Table.12. Statistics were summarized in Table 12.

In WT1-stained sections, podocyte number and podocyte density reduced significantly in superficial and juxtamedullary nephrons at week 20 (Fig.22A-A2). Thus, T2D-Unx mice show common structural and functional characteristics of progressive CKD in obesity-related T2D.

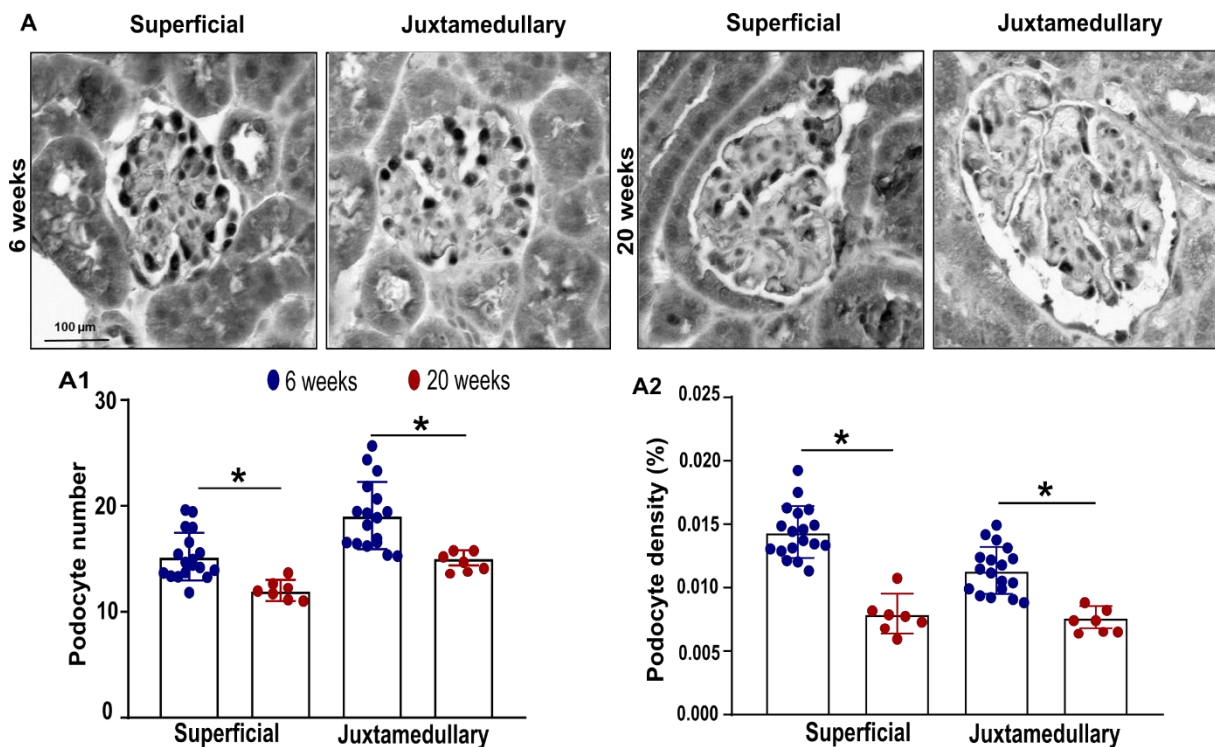


**Figure 22. Set up a progressive glomerulosclerosis model in T2D-Unx mice.** (A) The podocyte density was calculated as the number of podocytes by the glomerular tuft area in WT-1 staining sections from T2D-Unx mice as a Podocyte number assessment. Both types of nephrons were analyzed separately, and statistics were summarized in Table 12.

## 5.2. Effects of metformin, ramipril, and empagliflozin on kidney function

To test the nephroprotective effect of metformin, ramipril, and empagliflozin (MRE) treatment on T2D-Unx, and WT-Unx mice were randomly treated with MRE (T2D /WT + MRE) or no treatment (T2D/WT) from age 20 to 24 weeks.

### 5.2.1. Treatment with MRE did not have a substantial impact on GFR

To study the primary outcome, GFR was measured on T2D-Unx and WT-Unx mice starting with the condition of diabetes-related hyperfiltration at week 24 (Fig.23A). There was a decrease in GFR from week 20 to week 24 ( $\Delta$ GFR), more than half of the untreated T2D-Unx mice. In comparison, the GFR was retained by about 14%, and the GFR increased by 29% (Fig.23B1). Four weeks of MRE therapy has little effect on both  $\Delta$ GFR and also GFR in absolute numbers in T2D-Unx or WT-Unx mice (Fig.23).

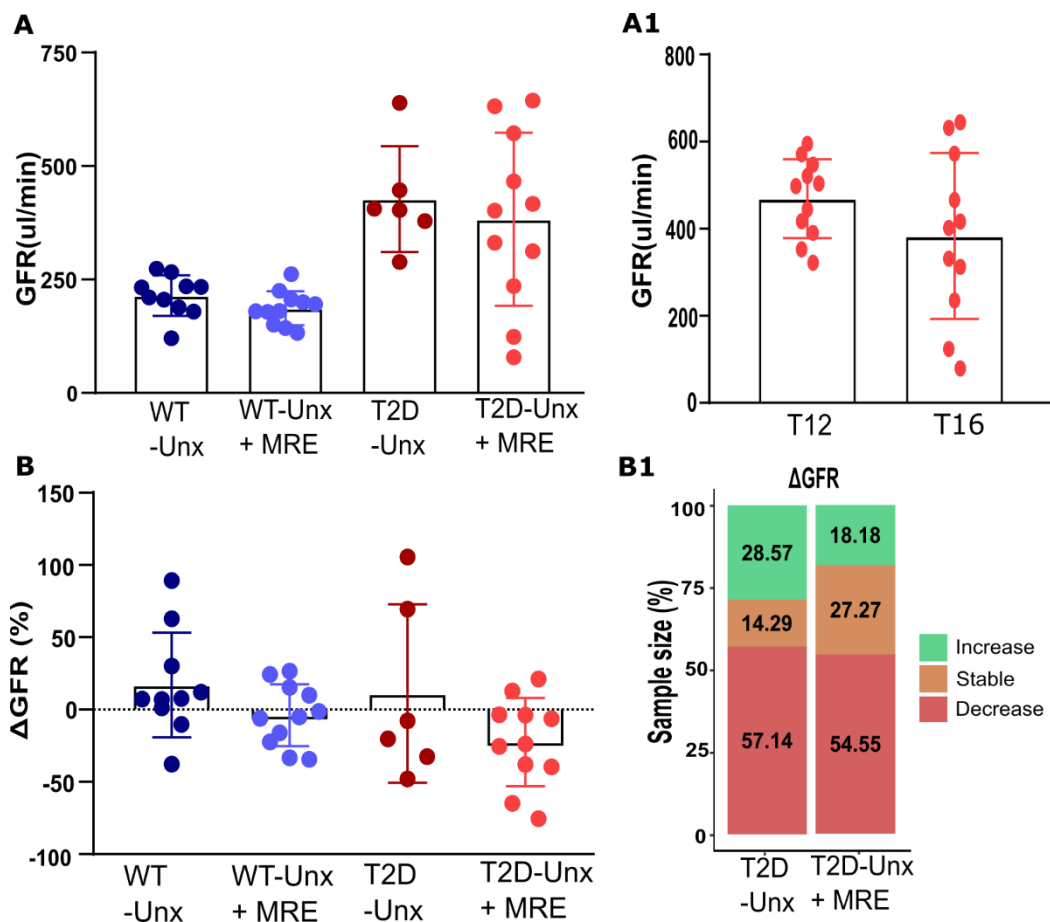


**Figure 23. Impact of MRE therapy on primary outcome.** (A) GFR at the endpoint. (A1)  $\Delta$ GFR. (A) The mice from each group percentage were shown in the stacked bar graph. \*p-value  $\leq 0.05$ . Abbreviations: GFR, glomerular filtration rate. Statistics were summarized in Table 12.

### 5.2.2. MRE treatment showed renoprotective effects on T2D-Unx mice

Four weeks of MRE treatment had no impact on the profound obesity of T2D-Unx or WT-Unx mice (Fig.24A-A2). In contrast, T2D-Unx mice showed blood glucose levels about 4-times higher compared with WT-Unx mice in untreated groups. T2D-Unx mice showed blood glucose levels at levels about 2-times higher compared with WT-Unx mice in MRE treatment groups. In T2D-Unx mice, MRE combination treatment (especially two anti-diabetic drugs, i.e., metformin and empagliflozin) was significantly reduced blood glucose (Fig.24B-B2). In WT-Unx mice, there was no such effect. MRE treatment reduced albuminuria in around 33% of T2D-Unx mice, whereas untreated T2D-Unx mice elevated albuminuria levels within the experiment period (Fig.24C2). Thus, MRE therapy potentially decreased albuminuria (Fig.24C).

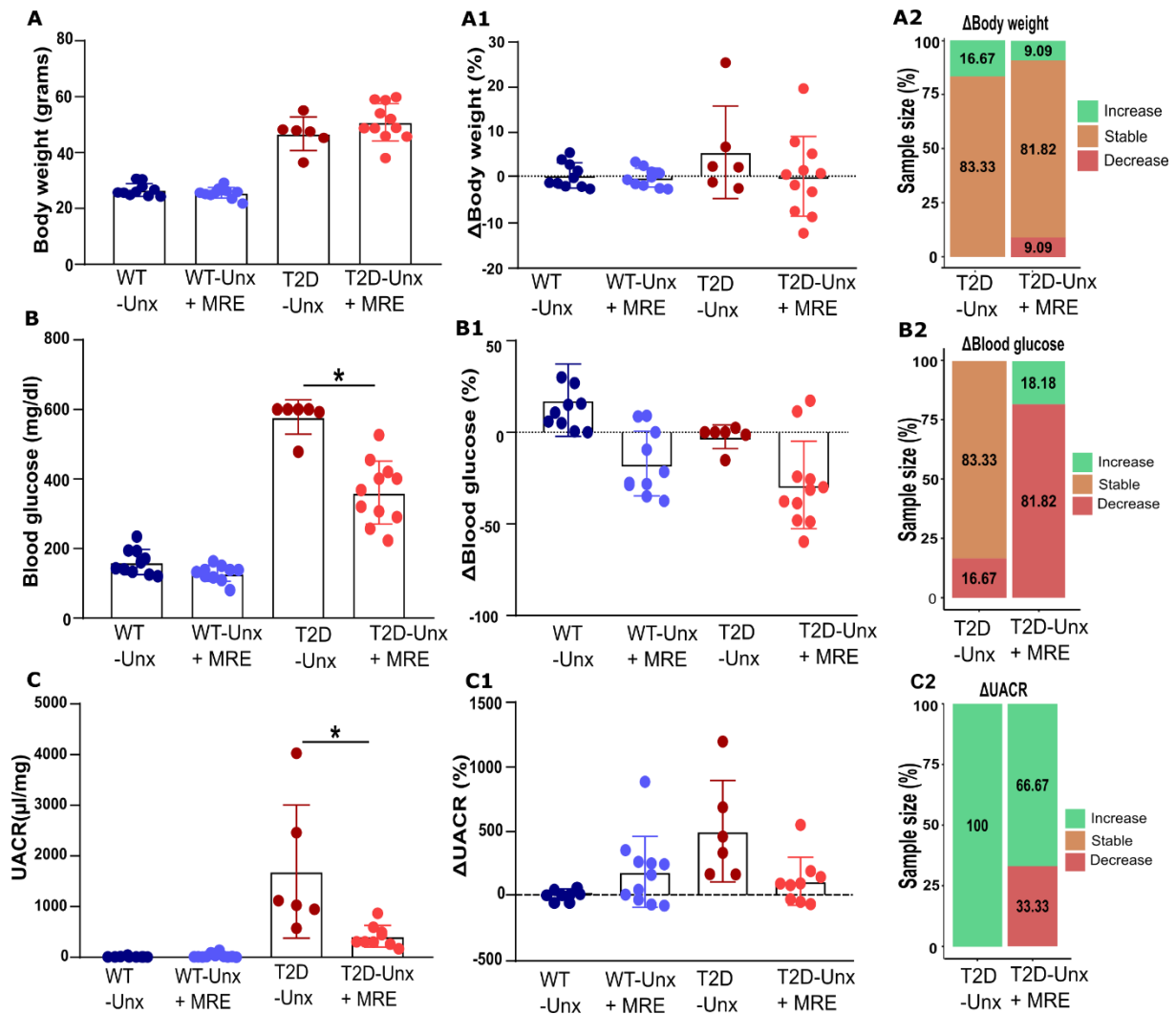


**Figure 24. Effect of MRE therapy on secondary outcomes.** (A) Bodyweight at the endpoint (A1) Δbodyweight. (A2) The mice from each group percentage were indicated in the stacked bar graph. (B) Blood glucose at the endpoint (B1) Δblood glucose. (B2) The mice from each group percentage were indicated in the stacked bar graph. (C) UACR at the endpoint (C1) ΔUACR. (C2) The mice from each group percentage were given in the stacked bar graph. \*p-value ≤ 0.05, # p-value ≤ 0.05 versus the WT-Unx group. Abbreviations: UACR, urinary albumin-creatinine ratio. Statistics were summarized in Table 14.

MRE therapy in T2D-Unx mice potentially decreased diffuse glomerulosclerosis in superficial and juxtamedullary nephrons, respectively (Fig.25A1). MRE with four weeks of treatment did not substantially affect the glomeruli and tubules' size, while a non-significant shift towards smaller-sized tubules was noted. (Fig.25B1).



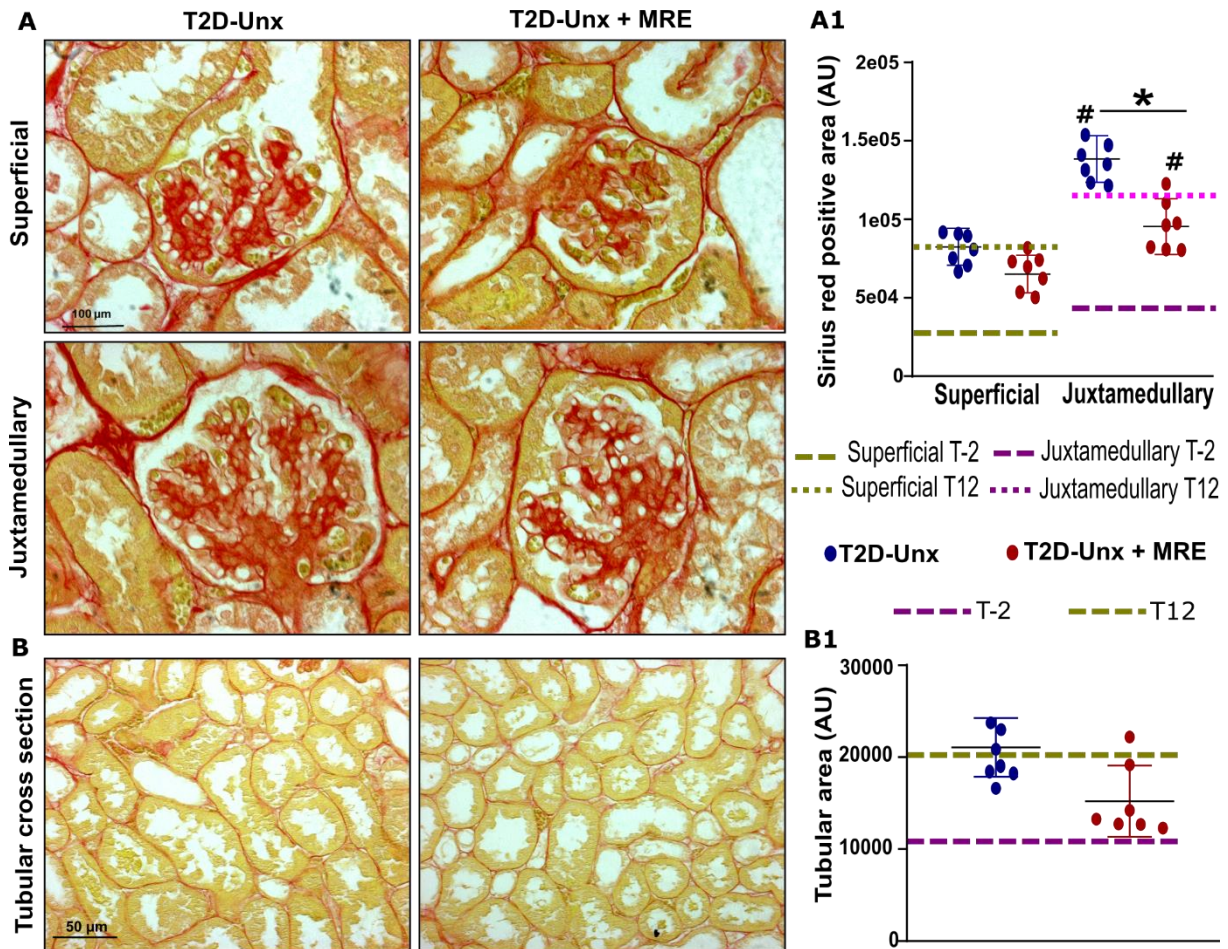


**Figure 25. Impact of MRE treatment on histological outcomes.** (A) Glomerulosclerosis, assessed as Sirius red positive area (AU) under x40 magnification. (B) Tubular size is evaluated in the Sirius red-stained sections with x20 magnification. \*p-value  $\leq 0.05$ , # p-value  $\leq 0.05$  versus superficial nephrons. Additionally, both types of nephrons were assessed separately, and statistics were summarized in Table 14.

PAS-stained sections measured the glomerular area separately in both superficial and Juxtamedullary nephrons in T2D-Unx mice, and the structural changes were enhanced compared with the MRE treatment group (Fig.26A-A2). With regards to glomerulosclerosis, there was substantial protection in the MRE treatment group, especially in juxtamedullary nephrons (Fig.26A1), without altering the sizes of glomeruli or tubules (Fig.26A1-A2) as well as a higher number of open capillaries leading to improved GFR (Fig.26A2).

Therefore, podocyte numbers and podocyte density in both superficial and juxtamedullary nephrons in T2D-Unx mice are potentially improved by MRE treatment (Figure 26B-B2). On the other hand, juxtamedullary nephrons remained with fewer podocytes upon MRE therapy (Fig.26B1). Still, podocyte densities remained well below those young T2D mice before

uninephrectomy (a week 6) in both superficial and juxtamedullary nephrons (Fig.22A). When quantifying podocyte loss/recovery, and occasionally recorded in untreated T2D-Unx mice WT-1+ podocytes detachment from the glomerular tuft of both cortical and juxtamedullary nephrons (red arrows), a phenomenon was reduced in T2D-Unx +MRE group (fig.26B2).

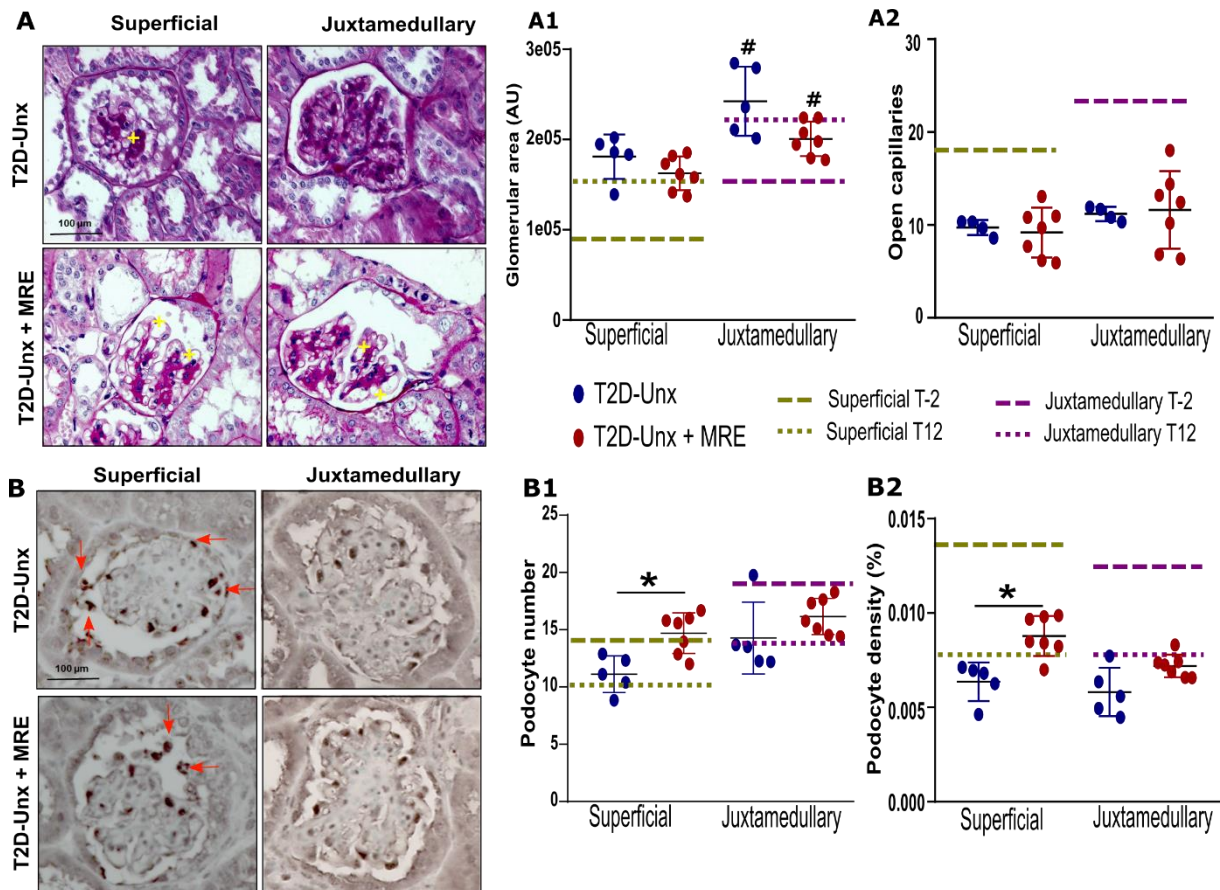


**Figure 26. Impact of MRE treatment on histological parameters.** (A) In T2D-Unx mice, PAS staining sections (A1) Quantified the glomerular tuft area (AU) expressed as a glomerular area assessment (A2). Open capillaries (denoted by yellow marks) were analyzed in superficial and juxtamedullary nephrons. (B2) Podocyte number, estimated in WT-1 sections. (B3) The detachment of podocytes was analyzed for all groups in both types of nephrons. Red arrows indicate detached podocytes. Both nephrons were measured separately, and statistics were summarized in Table 12. \*p-value ≤ 0.05, # p-value ≤ 0.05 versus superficial nephrons.

**Table 11. The number of glomeruli assessed per section of histological analysis for both types of nephrons.**

		T-2		T12		T16	
		Superficial nephrons	Juxta medullary nephrons	Superficial nephrons	Juxta medullary nephrons	Superficial nephrons	Juxta medullary nephrons
Glomerular area (AU)	T2D-Unx					20.29 ± 0.88	19.57 ± 1.50
	T2D-Unx + MRE	21.19 ± 4.02	14.00 ± 5.93	20.33 ± 2.98	6.83 ± 3.80	20.57 ± 0.73	18.29 ± 4.16
	T2D-Unx + BIO					20.00 ± 0.00	13.14 ± 2.17
	T2D-Unx + MRE + BIO					20.00 ± 0.00	13.33 ± 2.49
Sirius red positive area (AU)	T2D-Unx					19.17 ± 1.46	14.00 ± 3.00
	T2D-Unx + MRE	20.10 ± 4.02	9.58 ± 6.28	18.00 ± 3.61	5.67 ± 2.36	19.00 ± 1.07	12.29 ± 2.49
	T2D-Unx + BIO					19.90 ± 0.30	15.80 ± 2.71
	T2D-Unx + MRE + BIO					21.50 ± 1.50	9.00 ± 1.58
Podocyte number / Podocyte density (%)	T2D-Unx					20.14 ± 0.35	19.86 ± 0.35
	T2D-Unx + MRE	21.29 ± 3.39	14.32 ± 4.71	19.33 ± 6.82	6.67 ± 4.82	20.00 ± 0.00	17.14 ± 3.44
	T2D-Unx + BIO					20.00 ± 0.00	13.14 ± 5.36
	T2D-Unx + MRE + BIO					20.00 ± 0.00	14.33 ± 2.36

Data expressed as mean ± SD.

Regarding ultrastructural podocyte injury, nephrin protein stained as filtration slit density was determined using STED super-resolution microscopy upon tissue clearing. MRE therapy potentially increased filtration slit density correlated with un-treated T2D-Unx mice along the glomerular filtration barrier, but not up to the standard of WT-Unx mice (Fig.27D). The impact of MRE therapy on CKD with diabetes-related podocyte injury and foot process effacement in podocytes adjacent to the gaps was also evident from all three groups of mice from 3D reconstruction data from confocal microscopy (Fig.27B).



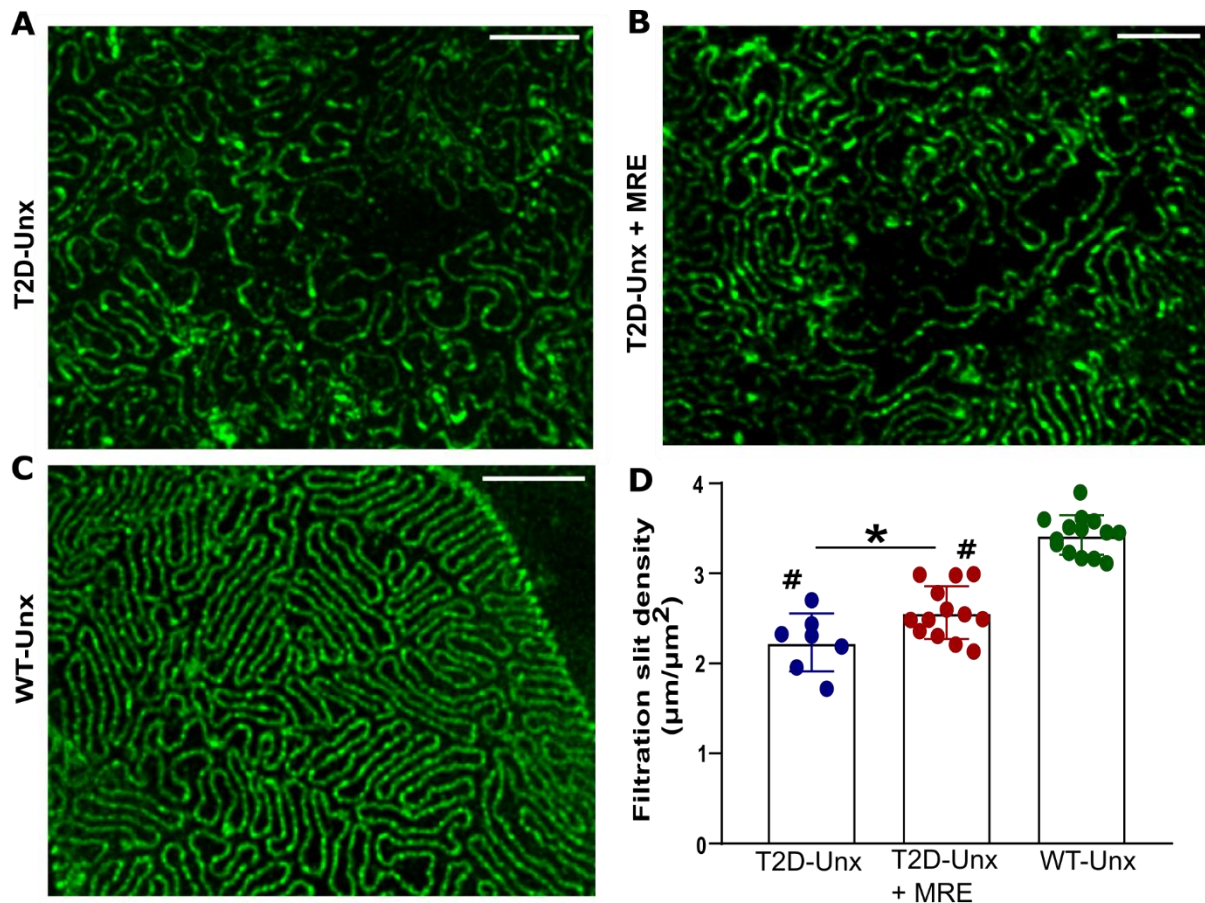


**Figure 27. Impact of MRE therapy on histological outcomes at the endpoint.** (D) Filtration slit density. The analysis was carried for five randomly picked glomeruli per mouse. Scale bars = 2μm with x100 magnification. \*p-value ≤ 0.05 versus superficial glomeruli. #p-value ≤ 0.05 versus WT-Unx. Statistics were summarized in Table 12. *The collaborators from the University of Florence produced this data.*

Until the study completion, all WT-Unx animals survived, while two mice dropped out ahead of time in the T2D-Unx and T2D-Unx + MRE groups. The proportionate survival of both T2D groups does not raise MRE-related safety concerns, compatible with these drugs' human experience. Therefore, four weeks of MRE therapy did not (yet) improved GFR even though developed various other nephroprotective effects on CKD with diabetic mice compatible with respective clinical trials.

#### 5.4. Additive nephroprotective effects of metformin, ramipril, empagliflozin, and BIO therapy

Later, in T2D-Unx and WT-Unx mice, I verified BIO's therapeutic impacts added to MRE combination therapy.



#### 5.4.1. MRE+BIO treatment had a significant effect on $\Delta$ GFR

To assess the primary outcome, I checked the GFR on these T2D-Unx and WT-Unx mice (Fig.28A). The combination therapy treated mice showed a 30% decrease in GFR, compared to more than 50% in the MRE alone treated mice group (Fig.28A2). The 4-weeks therapy period with BIO add-on therapy significantly reduced  $\Delta$ GFR (Fig.28A1). It indicates a protective impact on progressive GFR decline compared to treatment with metformin, ramipril, and empagliflozin alone.

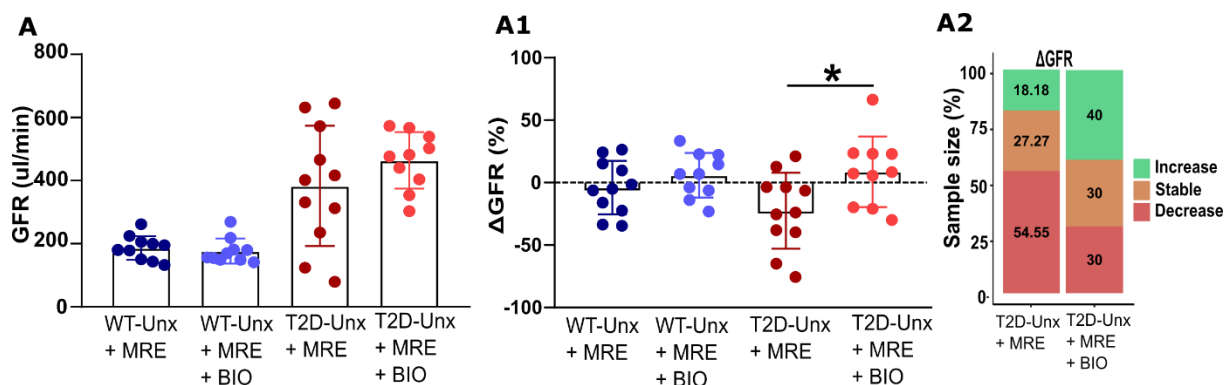


**Figure 28. Impact of combined MRE+BIO treatment on primary outcome.** (A) GFR at the endpoint. (A1)  $\Delta$ GFR. (A2) The mice from each group percentage were indicated in the stacked bar graph. #p-value  $\leq 0.05$  versus WT-Unx group. Abbreviations: GFR, glomerular filtration rate. Statistics were summarized in Table 12.

#### 5.4.2. MRE+BIO treatment reduced glomerulosclerosis in T2D-Unx mice

BIO added no impact to MRE combination therapy on hyperglycemia and body weight (Figure 29A-B) and no further reduction of albuminuria (Fig.29C). Nevertheless, the combination of MRE+BIO treatment improved the proportion of mice, reduced albuminuria relative to MRE therapy alone (Fig.29C). The combination of MRE+BIO treatment did not affect the parameters mentioned above in WT-Unx mice (Fig.29A-C).

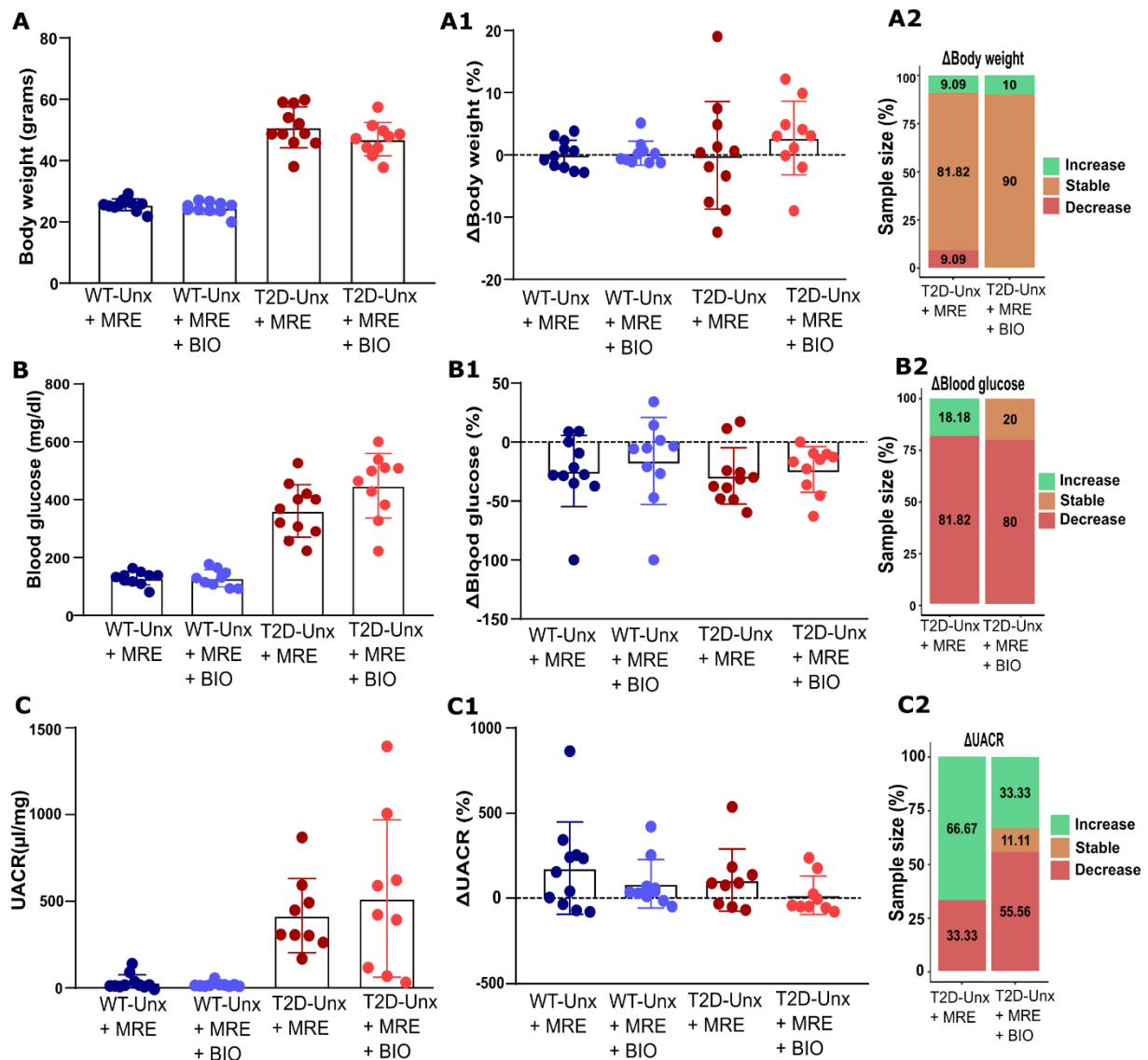


**Figure 29. Impact of combined MRE + BIO treatment on secondary outcomes.** (A) Bodyweight at the endpoint. (A1)  $\Delta$ bodyweight. (A2) The mice from each group percentage were indicated in the stacked bar graph. (B) Blood glucose at the endpoint. (B1)  $\Delta$ blood glucose. (B2) The mice from each group percentage were indicated in the stacked bar graph. (C) UACR levels at the endpoint. (C1)  $\Delta$ UACR. (C2) The mice from each group percentage were indicated in the stacked bar graph. #p-value  $\leq 0.05$  versus the WT-Unx group. Abbreviations: GFR, glomerular filtration rate, UACR, urinary albumin-creatinine ratio. Statistics were summarized in Table 12.

MRE+BIO therapy combination shows a significant reduction in glomerulosclerosis above MRE treatment in juxtamedullary nephrons in Sirius red staining (Fig.30A1) without altering the glomeruli or tubules dimensions (Fig.30A-B). The area of tubular cross-sections is enhanced the structural changes compared with MRE therapy (Fig.30B1).

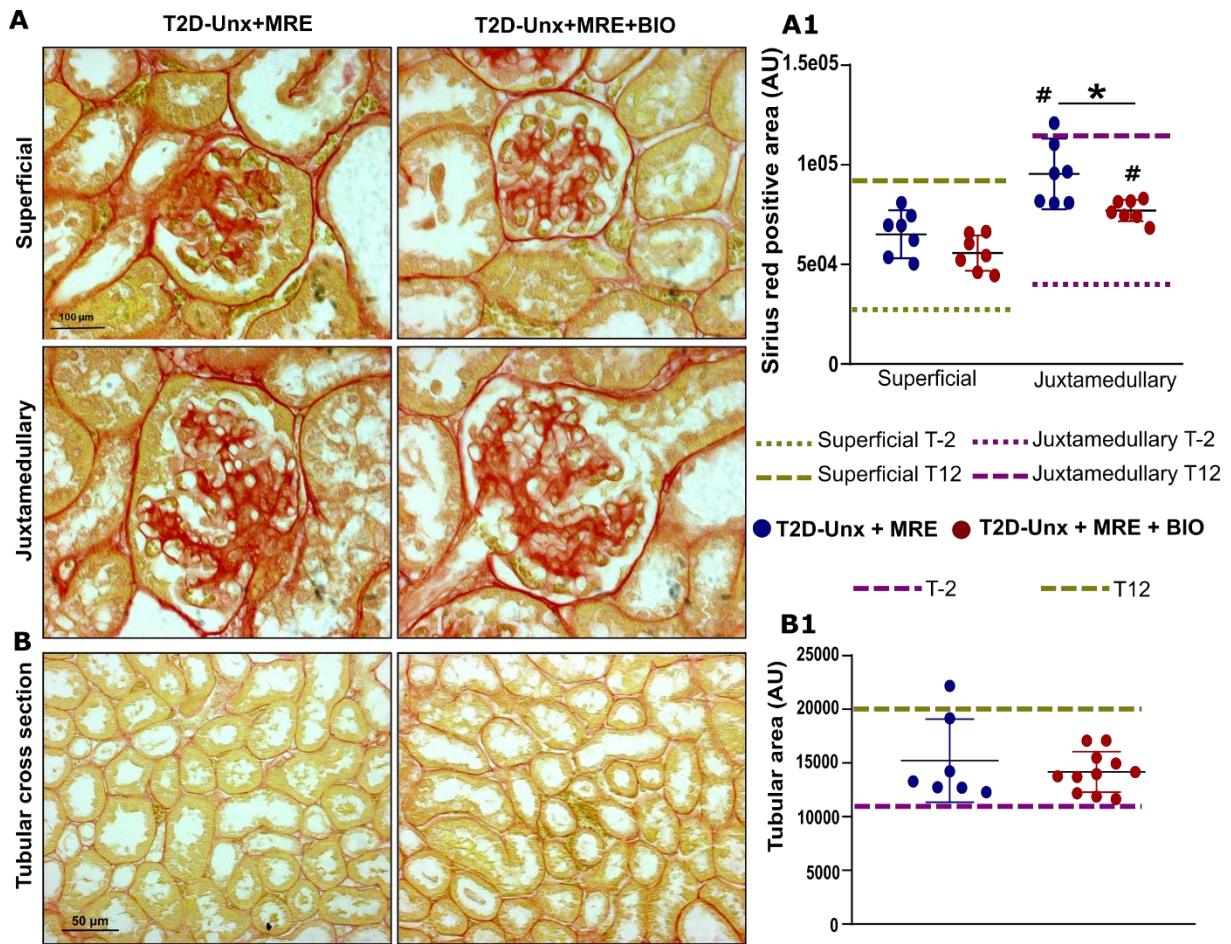


**Figure 30. Impact of MRE + BIO combination treatment on histological outcomes at week 24.** (A) Glomerulosclerosis is accessed as Sirius red positive area (AU) with x40 magnification. (B) Tubular size is quantified in the Sirius red-stained sections with x20 magnification. (D) The podocyte number was quantified in WT-1 sections. In (A1-B1), dotted green lines indicate the baseline from each histological quantification. Dotted green lines indicate the levels before the treatment (week 20). Besides, both types of nephrons were quantified separately, and statistics were summarized in Table 12. \*p-value  $\leq$  0.05, # p-value  $\leq$  0.05 versus superficial nephrons.

In PAS staining sections, I have measured the glomerular tuft area separately in superficial and Juxtamedullary nephrons. The glomerulus' structural changes improved relative to MRE therapy (Fig.31A-A2) and increased the glomerulus' number of open capillaries, leading to a better GFR (Fig.31A2). The MRE+BIO therapy combination also increased podocyte numbers to young T2D mice before uninephrectomy (a week 6). Despite MRE, combination therapy capacity improved podocyte density while densities continued to lower young T2D mice (Fig.31B-B2).

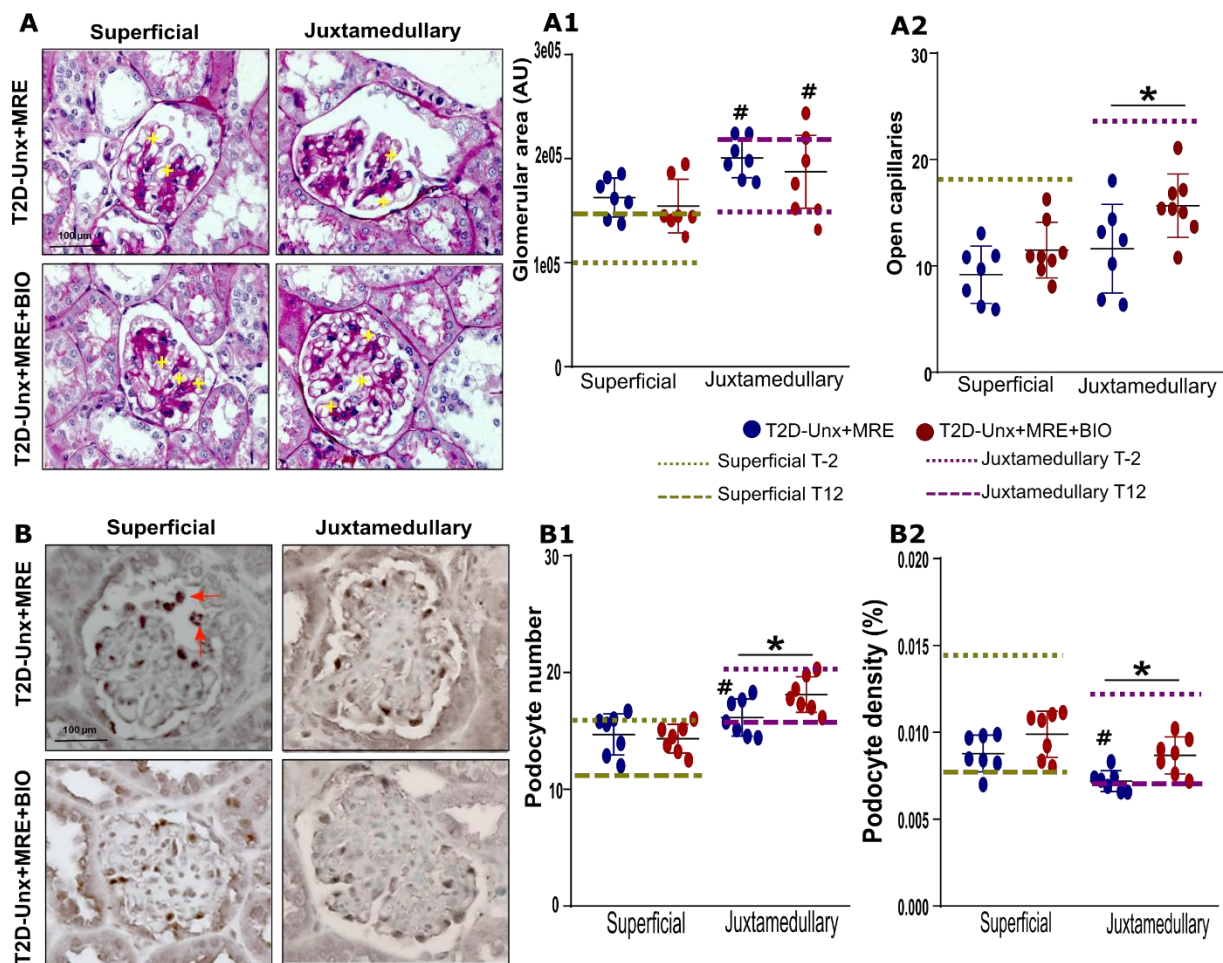


**Figure 31. Impact of combined MRE + BIO treatment on histological outcomes at week 24.** (A) The glomerular area was calculated as the glomerular tuft area (AU) in PAS sections. (B1) Podocyte number, estimated in WT-1 sections. (B2) Podocyte density Both types of nephrons were measured separately, and statistics were summarized in Table 12. Magnification, x40, \*p-value  $\leq 0.05$ , # p-value  $\leq 0.05$  versus superficial nephrons.

Regarding ultrastructural podocyte injury, nephrin protein stained as filtration slit density was determined using STED super-resolution microscopy upon tissue clearing. The combination therapy MRE+BIO, consistent with these findings, increased filtration slit density at the glomerular filtration barrier and almost completely restored the tuft structure. The glomerular filtration barrier was noted from the 3D reconstructions of nephrin protein stained glomeruli (Fig.32B).



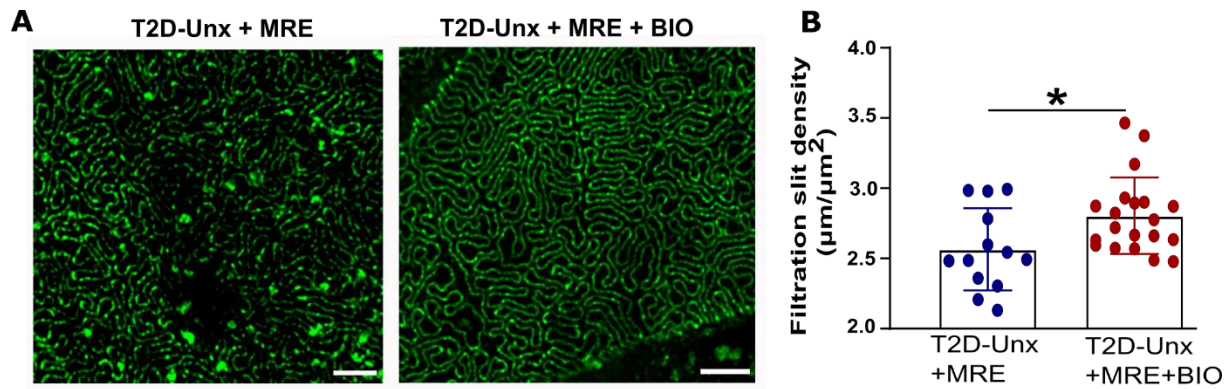


**Figure 32. Filtration slit density.** (A) filtration slit density. The assessment was carried for five randomly picked glomeruli per mouse. Bars = 2μm. Magnification, x100. \*p-value ≤ 0.05. Statistics were summarized in Table 12.

## 5.5. Nephroprotective effects with BIO alone treatment

Finally, I verified the therapeutic effects of BIO vs. a combination of MRE+BIO therapy in T2D-Unx mice.

### 5.5.1. BIO alone treatment had significant protection from GFR decline

To assess the primary outcome, I checked the GFR on these T2D-Unx mice. The Bio-treated mice showed GFR decline, correlated with the MRE+BIO treated group (Fig.33A). The 4-weeks therapy period with BIO significantly reduced ΔGFR (Fig.33A1). It indicates a protective effect on progressive GFR decline in BIO alone treatment.

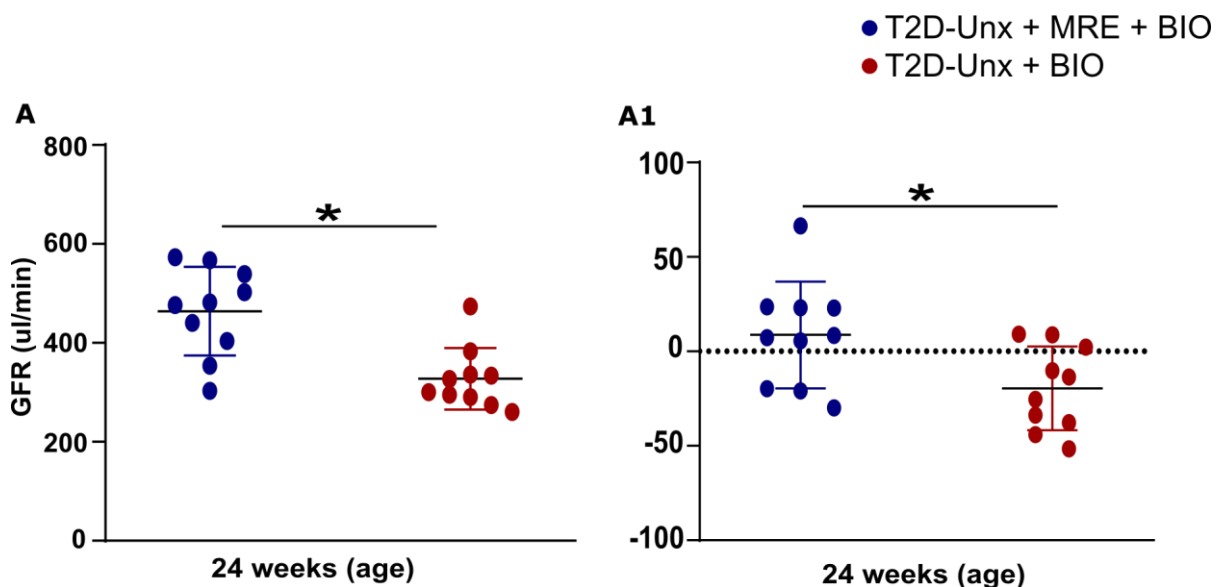


**Figure 33. Impact of combined MRE+BIO treatment on primary outcome.** (A) GFR at the endpoint. (A1) ΔGFR. (A2). #p-value ≤ 0.05. Abbreviations: GFR, glomerular filtration rate. Statistics were summarized in Table 12.

### 5.5.2. In T2D-Unx mice, BIO alone therapy minimized glomerulosclerosis

BIO alone therapy had no effect on hyperglycemia due to lack of MRE therapy but decreased body weight (Fig.34A-B) and did not impact albuminuria (Fig.34C).

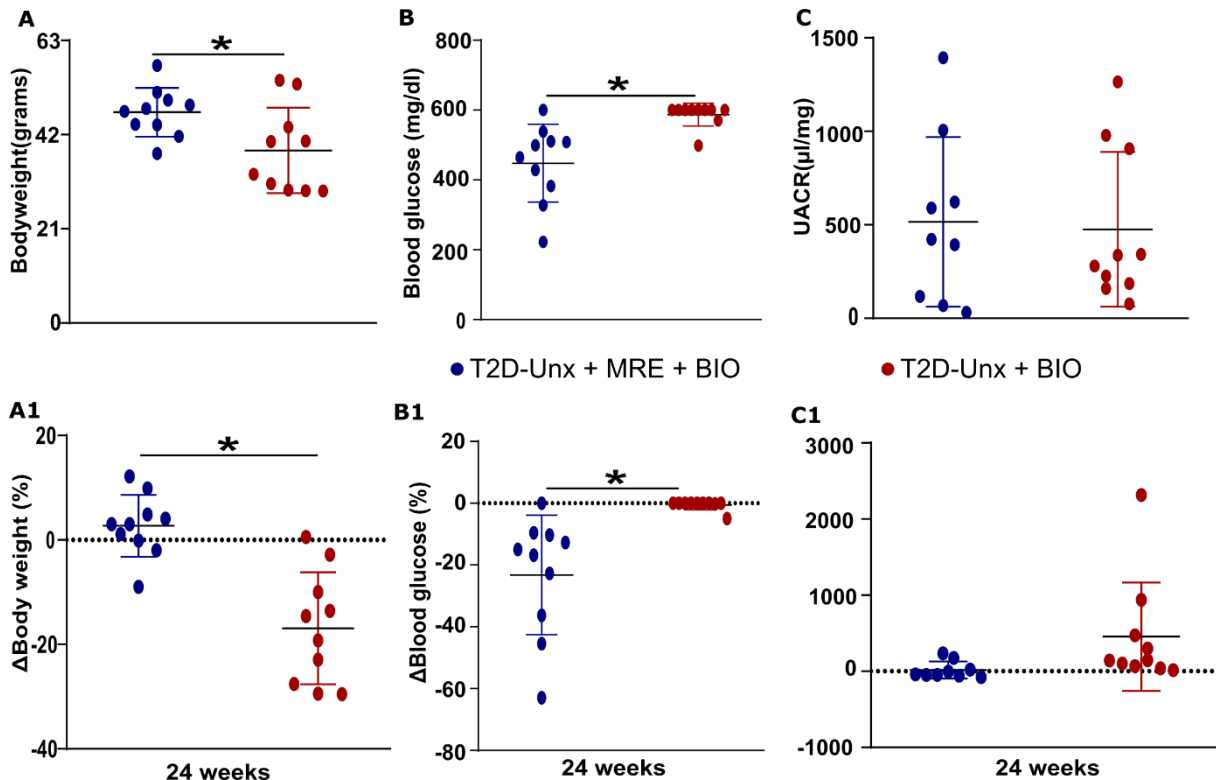


**Figure 34. Impact of BIO treatment on secondary outcomes.** (A) Bodyweight at the endpoint. (A1)  $\Delta$ body weight. (B) Blood glucose levels at the endpoint. (B1)  $\Delta$ blood glucose. (C) UACR levels at the endpoint. (C1)  $\Delta$ UACR. Abbreviations: UACR, urinary albumin-creatinine ratio. Statistical analyses were summarized in Table 14.

Sirius red staining sections measured the glomerular tuft area separately in superficial and Juxtamedullary nephrons. Regarding glomerulosclerosis, the BIO alone therapy showed substantial protection above MRE treatment in both types of nephrons (Fig.35A) and without altering the tubule dimensions (Fig.35B1).

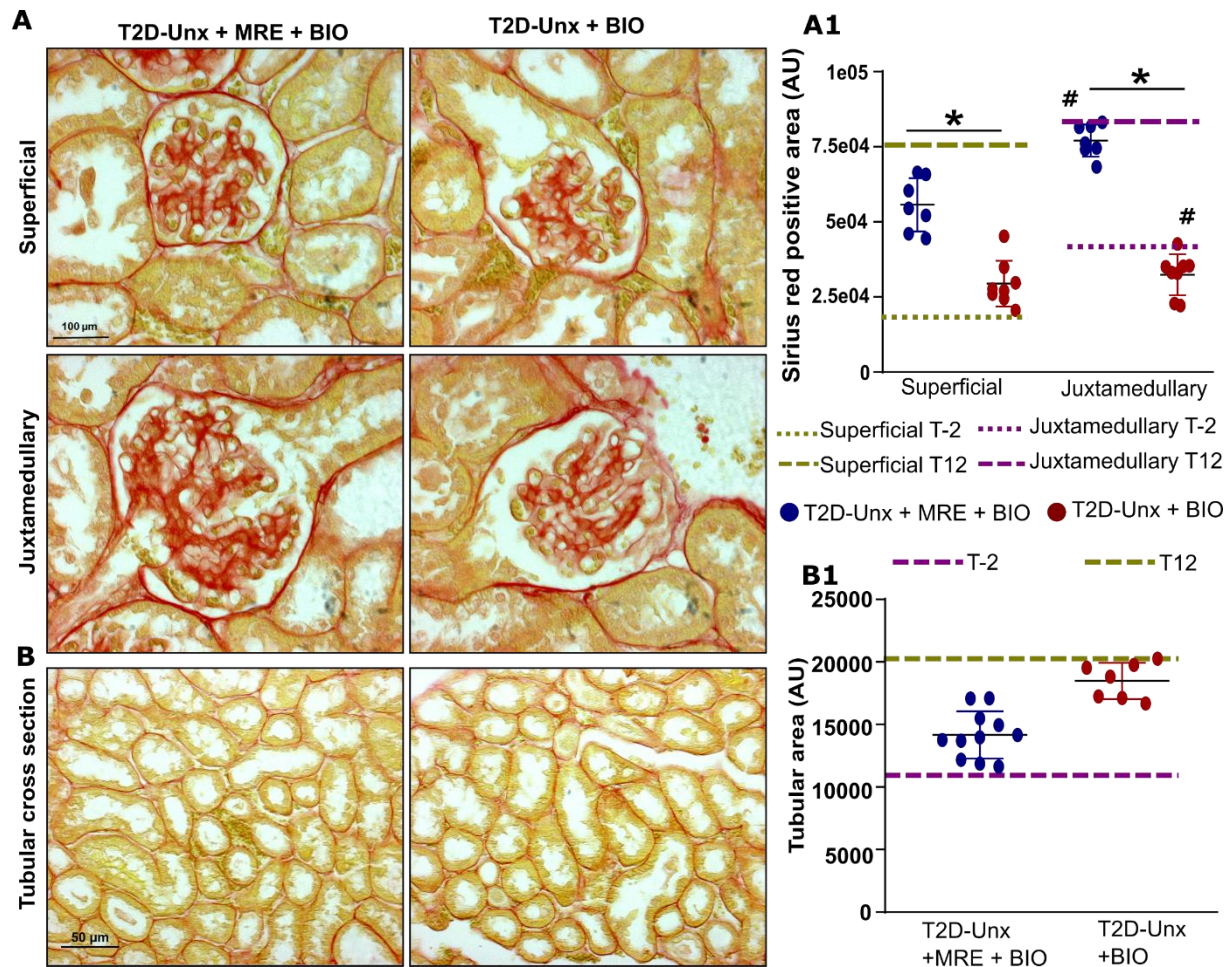


**Figure 35. Impact of BIO treatment on histological outcomes at the endpoint.** (A) Glomerulosclerosis is measured as Sirius Red positive area (AU) with x40 magnification. (B) Tubular size, assessed in Sirius Red stained sections with x20 magnification. In (A-B), dotted yellow lines indicate the baseline (week 6) from each histological assessment. Dotted pink lines indicate the levels before the treatment (week 20). Besides, both types of nephrons were analyzed separately, and statistics were summarized in Table 12. \*p-value  $\leq 0.05$ , # p-value  $\leq 0.05$  versus superficial nephrons.

PAS staining sections measured the glomerular tuft area separately in superficial and Juxtamedullary nephrons, and the BIO alone therapy did not affect the glomerular tuft area (Fig.36A1-A2) and open glomerular capillaries. The BIO alone therapy did not affect the podocyte number (Fig.36B1-B2).

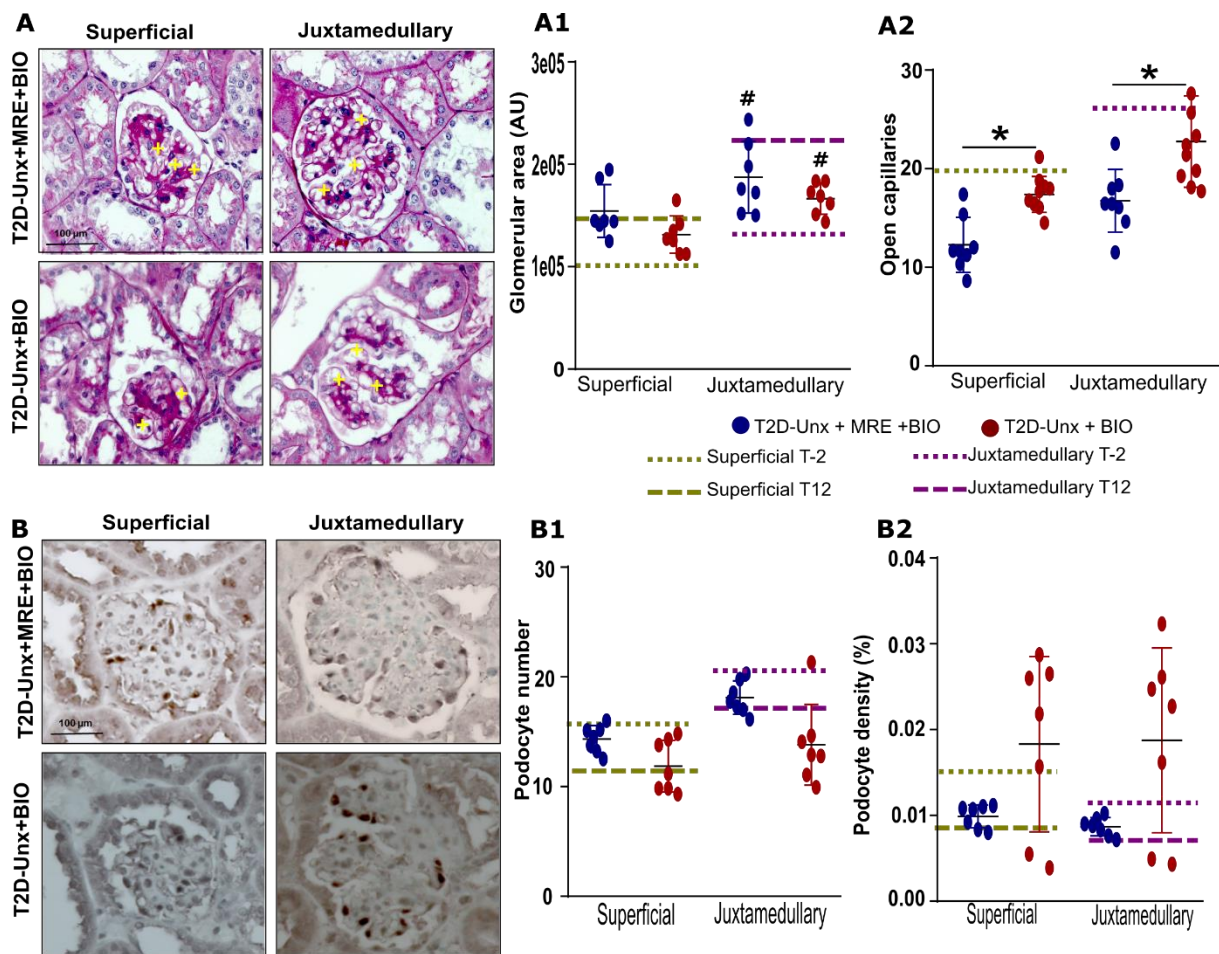


**Figure 36. Effect of BIO therapy on histological outcomes at the endpoint.** (A) The glomerular area was calculated as the glomerular tuft area (AU) in PAS sections. (B1) Podocyte number, estimated in WT-1 sections. (B2) Podocyte density. In (A-B), dotted yellow lines indicate the baseline (week 6) from each histological measurement. Dotted pink lines indicate the levels before the treatment (week 20). Both types of nephrons were measured separately, and statistics were summarized in Table 12. Magnification, x40, \*p-value  $\leq 0.05$ , # p-value  $\leq 0.05$  versus superficial nephrons.

Regarding ultrastructural podocyte injury, nephrin protein stained as filtration slit density was determined using STED super-resolution microscopy upon tissue clearing. BIO alone therapy did not impact filtration slit density at the glomerular filtration barrier relative to combination MRE + BIO therapy (Fig.37A).



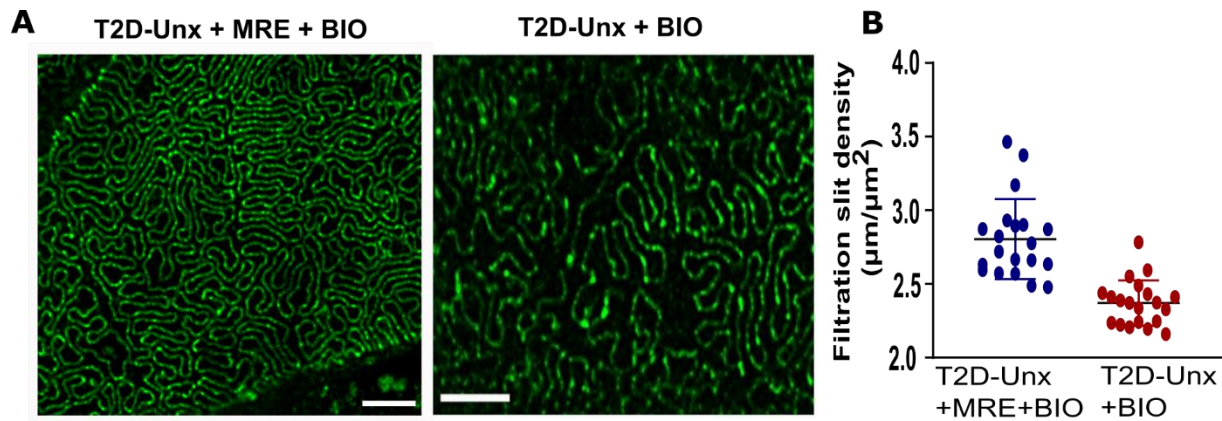


**Figure 37. Filtration slit density.** (A) filtration slit density. The assessment was carried for five randomly picked glomeruli per mouse. Scale bars =  $2\mu\text{m}$  with x100 magnification. Statistical analyses were summarized in Table 14.

### 5.6. Effects of BIO on mouse glomeruli in vitro

BIO specifically affects cultured glomerular cells from the above observation, but we doubted its impact on *in vitro* whole mouse glomeruli. Glomeruli are isolated from high purity mouse kidneys. The isolation procedure by itself combined along with marked low levels of the constitutive mRNA expression of slit diaphragm protein nephrin, the structural alpha-smooth muscle actin protein, and the cell cycle regulator cyclinD1 protein but not in interleukin-6, which is unable to express in glomeruli under normal conditions (Fig.38A-D). Upregulation of IL-6 mRNA levels by glucose exposure, but not in the other transcripts. A substantial expression of nephrin was caused by BIO but did not affect the various mRNAs (Fig.38A-D). Therefore, in non-diabetic and diabetic cases, BIO is a particular nephrin inducer in mouse glomeruli.

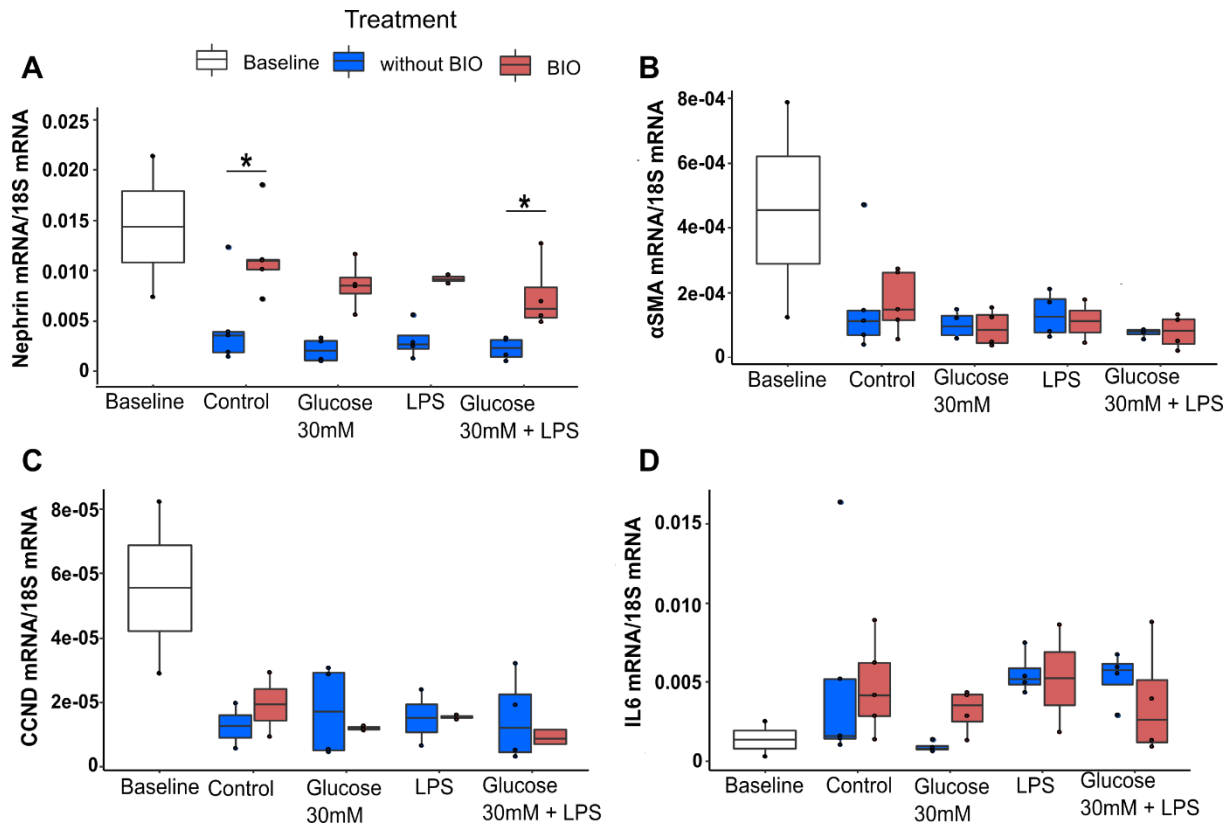


**Figure 38. Impact of BIO treatment on mouse glomeruli *in vitro*.** Gene expression was analyzed by RT-qPCR for (A) nephrin, (B) αSMA, (C) CCND1, and (D) IL6. \* p-value ≤ 0.05. Abbreviations: αSMA, alpha-smooth muscle actin; CCND, cyclin D1; IL6, interleukin 6. Statistical analyses were summarized in Table 14.

## 6. Discussion

We hypothesized that, in addition to MRE treatment in uninephrectomized obese with T2D mice, BIO could minimize CKD progression. Our results verified this hypothesis in terms of glomerulosclerosis conservation, protecting the decline of GFR, and leading to the podocyte injury<sup>101</sup>. It is possible to test new treatments in an experimental setting of T2D along with residual continuous GFR decline against antidiabetic therapy combined with dual inhibition of RAS/SGLT2.

In our study, background treatment contains metformin, ramipril, and empagliflozin. Metformin significantly reduced hyperglycemia by improving glucose and fatty acid metabolism<sup>154,155</sup> reduces the inflammatory response in the pancreas<sup>156</sup> and protects from neuroinflammation<sup>157</sup> and accelerates the wound healing in diabetic mice<sup>158</sup>. RAS inhibitors such as ramipril are improved insulin resistance<sup>159</sup> and protect from kidney injury in diabetic mice<sup>160</sup>. Empagliflozin is a significant increase in glycosuria and has nephron and protective effects by changing mitochondrial dynamics and autophagy in diabetic mice<sup>161–163</sup>. In clinical trials, metformin potentially lowered the hyperglycemia and weight loss in diabetic patients<sup>164</sup>. Further, ramipril-treated patients have strongly prevented the progression of diabetes compared with placebo<sup>84</sup>. SGLT2 inhibitors have been developed as antidiabetic drugs and unexpectedly showed potent effects on CV morbidity, heart failure, and CKD progression in diabetes<sup>92\_93\_94</sup>.

The first objective was to set up a pre-clinical animal model with progressive CKD because animal experiments in this domain resemble the early CKD stage defined by a constant GFR, increased mesangial matrix, and persistent albuminuria equivalent to CKD stage G1A1<sup>165</sup>. In clinical trials, diabetic patients were taking standard-of-care therapy to reduce progressive GFR decline and macroproteinuria<sup>166</sup>. According to this, we performed uninephrectomy on the obese mice to accelerate CKD progression by elevating SNGFR. The important pathomechanism of CKD progression, and later fed a low sodium diet enhance these pathological changes, as previously described<sup>167–169</sup>. The T2D-Unx untreated group (Fig.19) revealed GFR and albuminuria elevated throughout the experiment. Glomerulosclerosis increased and increased kidney hypertrophy and decreased podocyte density (Fig.21) compared with baseline parameters from the immunohistochemistry data. From these observations, our mouse model was equivalent to CKD stage G1A1.

According to the above observations, we had a better pre-clinical animal model with progressive CKD to mimic early phase CKD patients. Furthermore, we implement four weeks of MRE treatment to uninephrectomized obese mice with T2D. This combination is based on the recent findings of many human randomized controlled trials (RCTs) and is expected to represent the standard of care for several RCT in T2D in the future<sup>90,93,170</sup>. Besides, we did not predict an attenuation of decline in the GFR with these four weeks of MRE treatment because these pathological changes needed at least 2–3 years of treatment, e.g., EMPA-REG OUTCOME trials<sup>90</sup>. MRE treated T2D-Unx mice showed a significant reduction of hyperglycemia and weight loss compared with untreated mice. Also, in our model, MRE treatment immediately reduced macroproteinuria and consistent with human RTCs<sup>171</sup>. Proteinuria decline correlated with reducing podocyte loss in cortical and juxtamedullary nephrons in MRE treated T2D-Unx mice, even compared with young obese db/db mice podocyte numbers (fig.22). These findings may involve a possible via *de novo* podocyte production supported by one or many MRE drugs because RAS inhibition can regulate (diabetic) glomerulosclerosis by increasing podocyte regeneration,<sup>139,172–175</sup>. It is attractive to hypothesize that this process promoted the reduction of proteinuria in the MRE treatment group, and we found increased podocyte density and improved filtration slits along the glomerular filtration barrier. Furthermore, MRE treatment reduced glomerular hypertrophy and increased open capillaries for better GFR. Therefore, nephroprotection was demonstrated in T2D-Unx mice after four weeks of MRE treatment. We tested BIO's effects as an add-on to the MRE treatment regimen for four weeks in T2D-Unx mice. Surprisingly, in this progressive glomerulosclerosis model, these four weeks of combination MRE+BIO therapy improved GFR and demonstrated a substantial decrease in glomerulosclerosis, especially juxtamedullary nephrons, compared with MRE treatment alone. Besides, treatment with MRE+BIO greatly decreased hypertrophy and increase podocyte regeneration in juxtamedullary nephrons. We demonstrated that MRE therapy, along with a BIO drug, give an additive effect in T2D-Unx mice from these observations.

Any hypothetical nephroprotective impact of new classes of medications could be virtually overlaid with background treatment. For instance, MRE treatment's direct mechanism of activity and their indirect outcomes might have changed the overall centrality of the pathways focused on by novel medication candidates. To be sure, a few medications demonstrated compelling in rodent studies later indicated nothing or just minor extra impacts when tried in a human RCT<sup>86,176–183</sup>. For instance, regardless of BIO monotherapy's renoprotective effects<sup>175</sup>,

it was indistinct whether BIO could extract a nephroprotective impact beyond the MRE combination therapy. Finally, BIO alone treated T2D-Unx mice affected the kidney compared with BIO add on treatment with MRE. In T2D-Unx mice, the administration of Bio (without MRE therapy) significantly reduced GFR decline and did not affect secondary outcomes due to MRE therapy's absence. However, BIO treatment significantly decreases glomerulosclerosis. The glomerulus showed better 3D reconstructions in BIO alone therapy combination MRE+BIO therapy (Fig.39). Furthermore, glomerular and tubular hypertrophy potentially reduced in MRE+BIO combination therapy treated T2D-Unx mice. Our finding that BIO combination treatment altogether significantly decreased CKD progression in T2D-Unx mice.

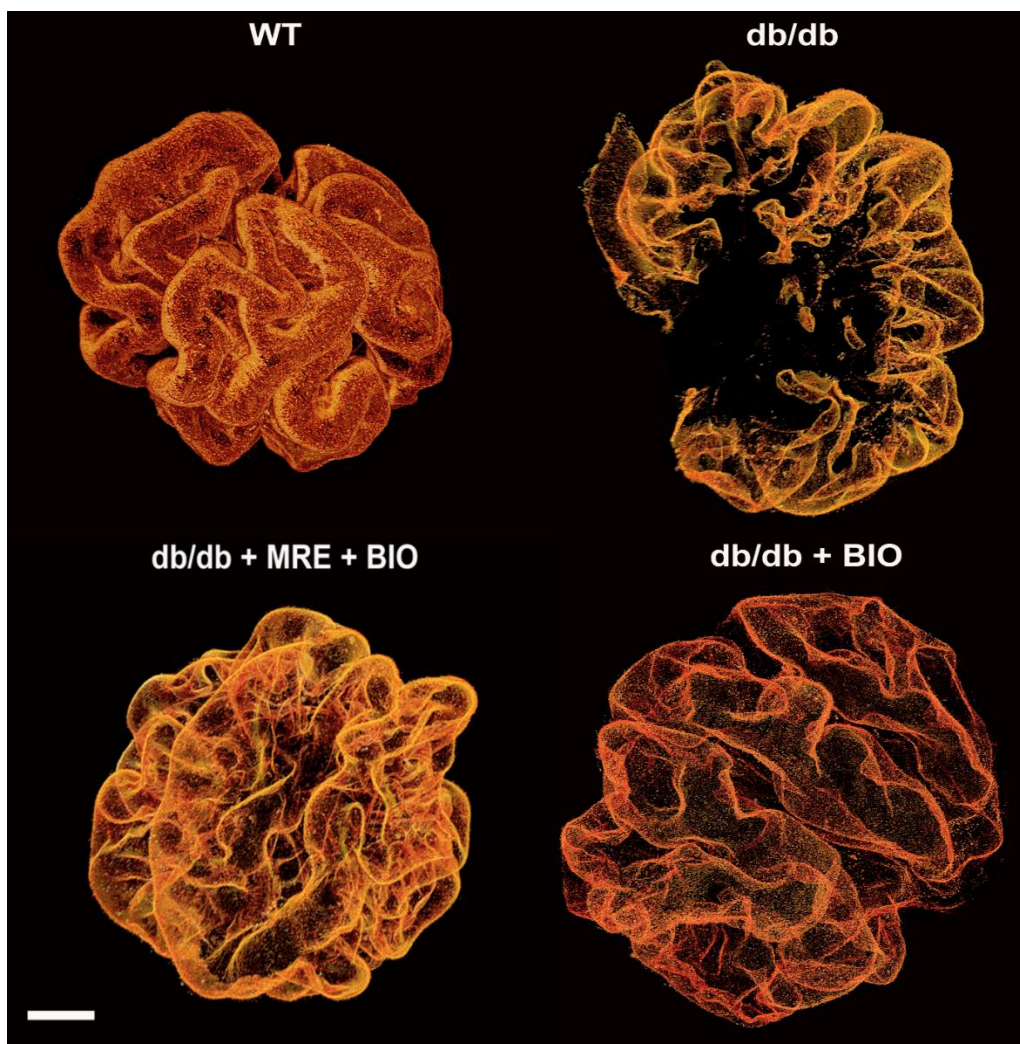


**Figure 39. Nephrin stained 3-dimensional glomeruli upon optical tissue clearing.**

Furthermore, our critical and clinically important endpoint, GFR reduction, beyond MRE treatment is surprising, particularly given the short time frame of treatment. Whether BIO influences, glomerular hemodynamics remains uncertain. BIO tends to support terminal

podocyte regeneration and *de novo* podocyte production from resident kidney progenitors. These pathways facilitate the glomerular filtration barrier integrity and attenuate glomerulosclerosis<sup>127,184–190</sup>. Our observation that the combination therapy of MRE+BIO increased podocyte density and decreased glomerulosclerosis in T2D-Unx mice is consistent with data from Lasagani et al. using the adriamycin nephropathy model.

Combination therapy of MRE+BIO is mostly protected from glomerulosclerosis and podocyte loss in juxtamedullary nephrons rather than cortical nephrons. In one of our previous studies blocking CXCL12 promoted regeneration, especially in cortical nephrons<sup>191</sup>. Disease-specific injury patterns may apply as CKD with diabetes mostly juxtamedullary nephrons undergo injury compared with cortical nephrons<sup>92,193</sup>; thus, BIO may have enhanced podocyte regeneration, particularly in juxtamedullary nephrons. However, in T2D-Unx, SNGFR increased to 50% in superficial and only 25% in the juxtamedullary nephrons<sup>194</sup>.

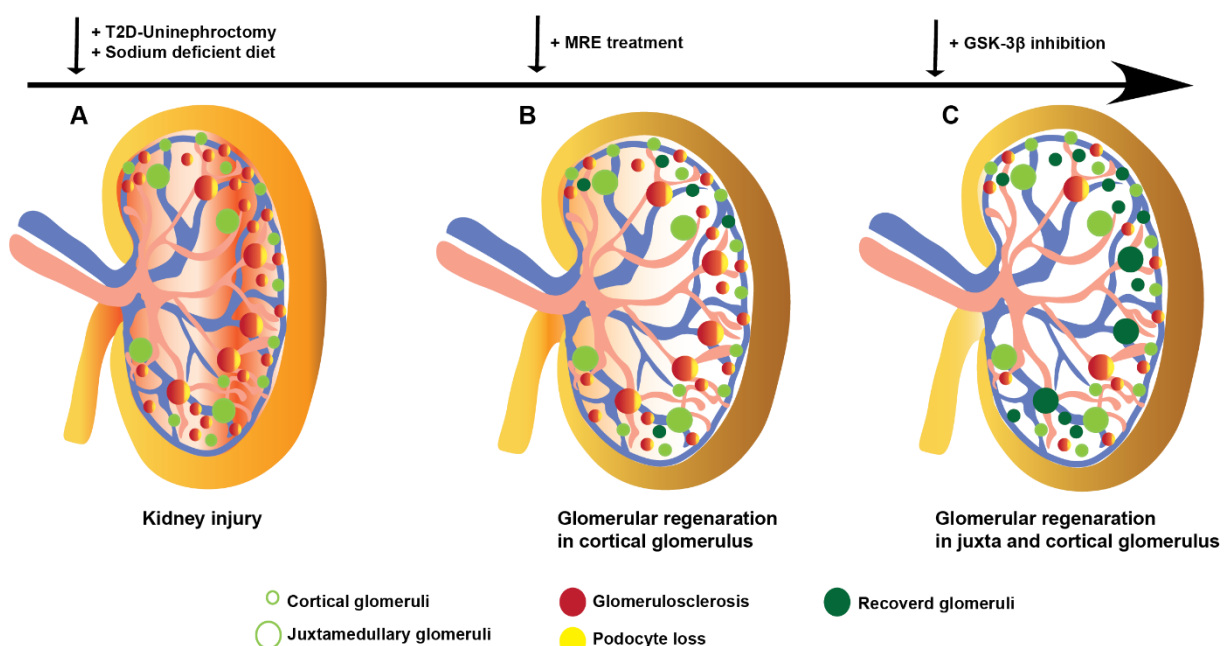


**Figure 40. GSK-3 $\beta$  inhibition reduces the progression of advanced nephropathy in type 2 diabetic mice above treatment with metformin, ramipril, and empagliflozin**

Furthermore, we observed albuminuria reduction in combination therapy with MRE+BIO but not in the BIO alone treatment. This could be due to a low sample size because the data from STED microscopy nephrin staining showed that BIO alone treated T2D-Unx mice increased filtration slit density at the glomerular filtration barrier relatively to untreated T2D-Unx mice. From our observation, BIO, along with MRE therapy, can improve kidney protection and

attune CKD progression in diabetes (Fig. 40). Finally, our safety and well-analysis did not reveal any safety concerns inside and outside the kidney for an add-on BIO therapy.

### **Limitations of the study**

Still, several constraints remain because our study does not imitate sex, age, and other comorbidities of patients contained with diabetic kidney diseases in human RCTs. Although our study model imitates a gradual decline in the GFR, this even occurs in the early stage of increased total GFR, which does not yet mimic an advanced stage of CKD. Subsequently, as opposed to advanced CKD in humans with T2D, interstitial fibrosis was still negligible in our experimental model. Our four weeks of treatment did not reproduce the conservation of GFR with MRE seen following 1–2 years of therapy in human RCTs. Accordingly, our study could detect exclusively immediate treatment impacts. The low-salt diet, particularly regarding ramipril and empagliflozin treatment, could support hypovolemia and high blood pressure in diabetic mice, though high blood pressure predominates in patients with diabetes.

Then again, decreasing salt admission is important for the standard administration of patients with hypertension and proteinuric kidney disease. Our experimental design showed this situation and not one of uncontrolled diabetes or hypertension. Free fluid admission is essential in patients with glucosuria-related osmotic diuresis and conceded to our mice. In T2D-Unx mice treated with MRE, volume problems may have contributed to the relatively high mortality observed in our study and the high-level of variability in the GFR. Also, it was difficult to calculate the number of podocytes on single two-dimensional tissue segments. In any case, according to the tissue section thickness, we tried to update the recently reported technological advancement in podocyte counting and correction factors<sup>195</sup>. Finally, because diabetic mice discharge highly diluted urine, loss of podocyte in the urine was tough to determine, so the entirety of our effort to show urinary podocytes was failed. Nevertheless, in untreated T2D-Unx mice, our careful imaging assessment demonstrated that podocyte detachment from the GBM.

The recent observations from the DAPA-CKD clinical trial overt that the mechanisms-of-action of SGLT2 inhibition is not specific to diabetic nephropathy and that SGLT2 inhibitors are effective in patients with CKD even regardless of diabetes<sup>96</sup>. Accordingly, patients included in diabetic nephropathy trials are diabetic patients with CKD, and the target treatment domain is CKD and not diabetic nephropathy<sup>196</sup>. For patients with CKD and diabetes, the term diabetic

nephropathy should be no longer used unless the CKD's most important diabetes role is confirmed by kidney biopsy. Diabetes is mostly a risk factor for CKD progression because diabetes accelerates the hyperfiltration-related podocyte loss and glomerulosclerosis, but diabetes is frequently not the main cause CKD<sup>196</sup>. As such, diabetes should be treated as one of several risk factors for CKD progression, e.g., with antidiabetic drugs, but particularly targeting “diabetic nephropathy” seems inappropriate. CKD has its shared molecular targets, and SGLT2 is now a treatment target for CKD and no longer only for “diabetic nephropathy.” It will be important to also implement these new insights in medical teaching at the medical schools, medical congresses, and the medical literature to overcome the conceptual hurdle of diabetic nephropathy for CKD's global challenge in obesity-related diabetic patients.

Furthermore, the novel strategies are not enough to delay CKD progression in most cases<sup>88</sup>. For example, SGLT2 inhibitors have shown their strong effects on CV morbidity, heart failure, and CKD progression on the diabetic population but not for long-term results. Canagliflozin maintained stable GFR for up to 12 months. Even in dapagliflozin-treated patients in DAPA-CKD clinical trials, GFR declined with time. So there is space for another novel, innovative treatment beyond the dual inhibition of RAAS/SGLT2. For instance, medications that improve podocyte differentiation from local kidney progenitors also attenuate glomerulosclerosis, nephron loss, and GFR decline<sup>101</sup>.

Therefore, we are considering everything. Our effort to improve drug testing trials for progressive CKD with diabetes integrated a model of GFR decline, group size computation, normal co-medication, randomization to an intervention not set up earlier than the disease, pre-indicated primary and secondary endpoints indistinguishable from those applied in clinical trials, modern morphologic assessment to increase unthinking bits of knowledge, and definite security investigation. In our experimental setting, our medication BIO indicated significant nephroprotective impacts above metformin and dual inhibition of RAS/SGLT2. As the putative mechanism of activity increases in the number of podocytes and glomerular morphology, drugs focusing on these systems could elicit add-on effects in patients with gradual CKD progression with diabetes despite dual RAS/SGLT2 inhibition.



**Table 12. Summary of statistical analysis performed for each figure.**

Figure/Table	Pannel	Normality of variable	Statistic test
Figure 19	A	No	Kruskal Wallis + Dunn's Post Hoc test
	B	No	Kruskal Wallis + Dunn's Post Hoc test
	C	No	Kruskal Wallis + Dunn's Post Hoc test
	D	No	Kruskal Wallis + Dunn's Post Hoc test
Figure 20	A	Yes	Student's t-test
Figure 21	A	No	Kruskal Wallis + Dunn's Post Hoc test
	B	Yes	ANOVA + Tukey's Post Hoc Test
Figure 22	A1	Yes	ANOVA + Tukey's Post Hoc Test
	A2	Yes	ANOVA + Tukey's Post Hoc Test
Figure 23	A	Yes	ANOVA + Tukey's Post Hoc Test
	A1	Yes	Student's t-test
	B	Yes	ANOVA + Tukey's Post Hoc Test
Figure 24	A	No	Kruskal Wallis + Dunn's Post Hoc test
	A1	Yes	ANOVA + Tukey's Post Hoc Test
	B	Yes	ANOVA + Tukey's Post Hoc Test
	B1	Yes	ANOVA + Tukey's Post Hoc Test
	C	No	Kruskal Wallis + Dunn's Post Hoc test
Figure 25	C1	No	Kruskal Wallis + Dunn's Post Hoc test
	A1	Yes	ANOVA + Tukey's Post Hoc Test
	B1	Yes	Student's t-test
Figure 26	A1	Yes	ANOVA + Tukey's Post Hoc Test
	A2	Yes	ANOVA + Tukey's Post Hoc Test
	B1	Yes	ANOVA + Tukey's Post Hoc Test
	B2	Yes	ANOVA + Tukey's Post Hoc Test
Figure 27	D	Yes	ANOVA + Tukey's Post Hoc Test
Figure 28	A	Yes	ANOVA + Tukey's Post Hoc Test
	A1	Yes	ANOVA + Tukey's Post Hoc Test
Figure 29	B	No	Kruskal Wallis + Dunn's Post Hoc test
	B1	Yes	ANOVA + Tukey's Post Hoc Test
	C	Yes	ANOVA + Tukey's Post Hoc Test
	C1	Yes	ANOVA + Tukey's Post Hoc Test
	D	No	Kruskal Wallis + Dunn's Post Hoc test
	D1	No	Kruskal Wallis + Dunn's Post Hoc test
Figure 30	A1	No	Kruskal Wallis + Dunn's Post Hoc test
	B1	No	Wilcoxon test
Figure 31	A1	Yes	ANOVA + Tukey's Post Hoc Test
	A2	Yes	ANOVA + Tukey's Post Hoc Test
	B1	Yes	ANOVA + Tukey's Post Hoc Test
	B2	Yes	ANOVA + Tukey's Post Hoc Test
Figure 32	B	No	Wilcoxon test
Figure 33	A	Yes	Student's t-test

	A1	Yes	Student's t-test
	A	No	Wilcoxon test
Figure 34	A1	Yes	Student's t-test
	B	Yes	Student's t-test
	B1	Yes	Student's t-test
	C	No	Wilcoxon test
	C1	No	Wilcoxon test
Figure 35	A1	No	Wilcoxon test
	B1	No	Wilcoxon test
Figure 36	A1	Yes	Student's t-test
	A2	Yes	Student's t-test
	B1	Yes	Student's t-test
	B2	Yes	Student's t-test
Figure 37	B	No	Wilcoxon test
Figure 38	A	No	Kruskal Wallis + Dunn's Post Hoc test
	B	No	Kruskal Wallis + Dunn's Post Hoc test
	C	No	Kruskal Wallis + Dunn's Post Hoc test
	D	No	Kruskal Wallis + Dunn's Post Hoc test

## 7 Abbreviations

---

Abbreviations	
BIO	6-bromo-indirubin-3'-oxime
CKD	Chronic kidney disease
DKD	Diabetic kidney disease
GFR	Glomerular filtration rate
GBM	Glomerular basement membran
GSK3	Glycogen synthase kinase
KDIGO	Kidney Disease Improving Global Outcomes
MRE	Metformin, ramipril, and empagliflozin
PECs	Parietal epithelial cells
PAS	Periodic acid–Schiff staining
RAS	Renin-angiotensin system
RPCs	Renal progenitor cells
SD	Slit diaphragm
SNGFR	Single nephron GFR
SGLT2	Sodium-glucose transporter-2
SGLT2i	Sodium-glucose cotransporter-2 inhibitor
T2D	Type-2 diabetes
T2D-Unx	Uninephrectomized diabetic mice
T1D	Type-1 diabetes
UACR	Urinary albumin-creatinine ratio
WT1	Williams tumor protein-1
WT-Unx	Uninephrectomized non-diabetic mice

---

## References:

1. Romagnani, P. *et al.* Chronic kidney disease. *Nat. Rev. Dis. Prim.* **3**, (2017).
2. Levey, A. S. & Coresh, J. Chronic kidney disease. *Lancet (London, England)* **379**, 165–180 (2012).
3. Kellum, J. A. & Lameire, N. Diagnosis, evaluation, and management of acute kidney injury: a KDIGO summary (Part 1). *Crit. Care* **17**, 204 (2013).
4. Reiser, J. & Sever, S. Podocyte biology and pathogenesis of kidney disease. *Annu. Rev. Med.* **64**, 357–366 (2013).
5. Kriz, W. & Lemley, K. V. A potential role for mechanical forces in the detachment of podocytes and the progression of CKD. *J. Am. Soc. Nephrol.* **26**, 258–269 (2015).
6. Eckardt, K.-U. *et al.* Evolving importance of kidney disease: from subspecialty to global health burden. *Lancet (London, England)* **382**, 158–169 (2013).
7. Schieppati, A. & Remuzzi, G. Chronic renal diseases as a public health problem: epidemiology, social, and economic implications. *Kidney Int. Suppl.* S7–S10 (2005). doi:10.1111/j.1523-1755.2005.09801.x
8. Levey, A. S. *et al.* The definition, classification, and prognosis of chronic kidney disease: a KDIGO Controversies Conference report. *Kidney international* **80**, 17–28 (2011).
9. Sharma, K. & Ziyadeh, F. N. Renal hypertrophy is associated with upregulation of TGF-beta 1 gene expression in diabetic BB rat and NOD mouse. *Am. J. Physiol.* **267**, F1094-1 (1994).
10. Cho, N. H. *et al.* IDF Diabetes Atlas: Global estimates of diabetes prevalence for 2017 and projections for 2045. *Diabetes Res. Clin. Pract.* **138**, 271–281 (2018).
11. Levey, A. S. *et al.* Nomenclature for kidney function and disease: report of a Kidney Disease: Improving Global Outcomes (KDIGO) Consensus Conference. *Kidney international* **97**, 1117–1129 (2020).
12. Kazi, A. M. & Hashmi, M. F. Glomerulonephritis. in (2020).
13. Jin, C. *et al.* 3D Fast Automatic Segmentation of Kidney Based on Modified AAM and Random Forest. *IEEE Trans. Med. Imaging* **35**, 1395–1407 (2016).
14. Itoh, M. *et al.* The structural and functional organization of the podocyte filtration slits is regulated by Tjp1/ZO-1. *PLoS One* **9**, e106621 (2014).
15. Krause, M., Rak-Raszewska, A., Pietilä, I., Quaggin, S. E. & Vainio, S. Signaling during Kidney Development. *Cells* **4**, 112–132 (2015).
16. Arif, E. & Nihalani, D. Glomerular Filtration Barrier Assembly: An insight. *Postdoc J. a J. Postdr. Res. Postdr. Aff.* **1**, 33–45 (2013).
17. Jourde-Chiche, N. *et al.* Endothelium structure and function in kidney health and disease. *Nat. Rev. Nephrol.* **15**, 87–108 (2019).
18. Miner, J. H. The glomerular basement membrane. *Exp. Cell Res.* **318**, 973–978 (2012).
19. Nagata, M. Podocyte injury and its consequences. *Kidney Int.* **89**, 1221–1230 (2016).
20. Reiser, J. & Altintas, M. M. Podocytes. *F1000Research* **5**, (2016).
21. Powers, A. C. Insulin therapy versus cell-based therapy for type 1 diabetes mellitus: what lies

- ahead? *Nat. Clin. Pract. Endocrinol. Metab.* **4**, 664–665 (2008).
22. Khan, R. M. M. *et al.* From Pre-Diabetes to Diabetes: Diagnosis, Treatments and Translational Research. *Medicina (Kaunas)*. **55**, (2019).
23. Saeedi, P. *et al.* Global and regional diabetes prevalence estimates for 2019 and projections for 2030 and 2045: Results from the International Diabetes Federation Diabetes Atlas, 9(th) edition. *Diabetes Res. Clin. Pract.* **157**, 107843 (2019).
24. Pulgaron, E. R. & Delamater, A. M. Obesity and type 2 diabetes in children: epidemiology and treatment. *Curr. Diab. Rep.* **14**, 508 (2014).
25. Hruby, A. & Hu, F. B. The Epidemiology of Obesity: A Big Picture. *Pharmacoeconomics* **33**, 673–689 (2015).
26. Maric-Bilkan, C. Sex differences in micro- and macro-vascular complications of diabetes mellitus. *Clin. Sci. (Lond)*. **131**, 833–846 (2017).
27. Ogurtsova, K. *et al.* IDF Diabetes Atlas: Global estimates for the prevalence of diabetes for 2015 and 2040. *Diabetes Res. Clin. Pract.* **128**, 40–50 (2017).
28. Akhtar, M., Taha, N. M., Nauman, A., Mujeeb, I. B. & Al-Nabet, A. D. M. H. Diabetic Kidney Disease: Past and Present. *Adv. Anat. Pathol.* **27**, 87–97 (2020).
29. Murea, M., Ma, L. & Freedman, B. I. Genetic and environmental factors associated with type 2 diabetes and diabetic vascular complications. *Rev. Diabet. Stud.* **9**, 6–22 (2012).
30. Marshall, J. A. & Bessesen, D. H. Dietary fat and the development of type 2 diabetes. *Diabetes care* **25**, 620–622 (2002).
31. Diagnosis and classification of diabetes mellitus. *Diabetes Care* **33 Suppl 1**, S62-9 (2010).
32. Alpers, C. E. & Kowalewska, J. Emerging paradigms in the renal pathology of viral diseases. *Clin. J. Am. Soc. Nephrol.* **2 Suppl 1**, S6-12 (2007).
33. Reidy, K., Kang, H. M., Hostetter, T. & Susztak, K. Molecular mechanisms of diabetic kidney disease. *J. Clin. Invest.* **124**, 2333–2340 (2014).
34. Persson, F. & Rossing, P. Diagnosis of diabetic kidney disease: state of the art and future perspective. *Kidney Int. Suppl.* **8**, 2–7 (2018).
35. Tapp, R. J. *et al.* Albuminuria is evident in the early stages of diabetes onset: results from the Australian Diabetes, Obesity, and Lifestyle Study (AusDiab). *Am. J. kidney Dis. Off. J. Natl. Kidney Found.* **44**, 792–798 (2004).
36. Dong, Z. *et al.* Low-pass whole-genome sequencing in clinical cytogenetics: a validated approach. *Genet. Med.* **18**, 940–948 (2016).
37. Kaufman, D. P., Basit, H. & Knoch, S. J. Physiology, Glomerular Filtration Rate (GFR). in (2020).
38. Romagnani, P. *et al.* Chronic kidney disease. *Nature Reviews Disease Primers* **3**, (2017).
39. Denic, A. *et al.* The substantial loss of nephrons in healthy human kidneys with aging. *J. Am. Soc. Nephrol.* **28**, 313–320 (2017).
40. Denic, A. *et al.* Single-nephron glomerular filtration rate in healthy adults. *N. Engl. J. Med.* **376**, 2349–2357 (2017).
41. Hommos, M. S., Glassock, R. J. & Rule, A. D. Structural and functional changes in human kidneys with healthy aging. *Journal of the American Society of Nephrology* **28**, 2838–2844 (2017).

42. Tonneijck, L. *et al.* Glomerular hyperfiltration in diabetes: Mechanisms, clinical significance, and treatment. *Journal of the American Society of Nephrology* **28**, 1023–1039 (2017).
43. Anders, H. J., Huber, T. B., Isermann, B. & Schiffer, M. CKD in diabetes: Diabetic kidney disease versus nondiabetic kidney disease. *Nature Reviews Nephrology* **14**, 361–377 (2018).
44. Guh, J.-Y. Proteinuria versus albuminuria in chronic kidney disease. *Nephrology (Carlton)*. **15 Suppl 2**, 53–56 (2010).
45. Birn, H. & Christensen, E. I. Renal albumin absorption in physiology and pathology. *Kidney Int.* **69**, 440–449 (2006).
46. Gekle, M. Renal tubule albumin transport. *Annu. Rev. Physiol.* **67**, 573–594 (2005).
47. Lambers Heerspink, H. J. & Gansevoort, R. T. Albuminuria Is an Appropriate Therapeutic Target in Patients with CKD: The Pro View. *Clin. J. Am. Soc. Nephrol.* **10**, 1079–1088 (2015).
48. Wang, T. *et al.* Low-Grade Albuminuria Is Associated with Left Ventricular Hypertrophy and Diastolic Dysfunction in Patients with Hypertension. *Kidney Blood Press. Res.* **44**, 590–603 (2019).
49. Berhane, A. M., Weil, E. J., Knowler, W. C., Nelson, R. G. & Hanson, R. L. Albuminuria and estimated glomerular filtration rate as predictors of diabetic end-stage renal disease and death. *Clin. J. Am. Soc. Nephrol.* **6**, 2444–2451 (2011).
50. KDIGO clinical practice guideline for the diagnosis, evaluation, prevention, and treatment of Chronic Kidney Disease-Mineral and Bone Disorder (CKD-MBD). *Kidney Int. Suppl.* S1-130 (2009). doi:10.1038/ki.2009.188
51. Chatzikyrkou, C. *et al.* Predictors for the development of microalbuminuria and interaction with renal function. *J. Hypertens.* **35**, 2501–2509 (2017).
52. Morigi, M. *et al.* Protein overload-induced NF-kappaB activation in proximal tubular cells requires H<sub>2</sub>O<sub>2</sub> through a PKC-dependent pathway. *J. Am. Soc. Nephrol.* **13**, 1179–1189 (2002).
53. Drumm, K., Bauer, B., Freudinger, R. & Gekle, M. Albumin induces NF-kappaB expression in human proximal tubule-derived cells (IHKE-1). *Cell. Physiol. Biochem. Int. J. Exp. Cell. Physiol. Biochem. Pharmacol.* **12**, 187–196 (2002).
54. Lee, E. M., Pollock, C. A., Drumm, K., Barden, J. A. & Poronnik, P. Effects of pathophysiological concentrations of albumin on NHE3 activity and cell proliferation in primary cultures of human proximal tubule cells. *Am. J. Physiol. Renal Physiol.* **285**, F748-57 (2003).
55. Gupta, J. *et al.* Association between albuminuria, kidney function, and inflammatory biomarker profile in CKD in CRIC. *Clin. J. Am. Soc. Nephrol.* **7**, 1938–1946 (2012).
56. Whaley-Connell, A. T. *et al.* Albumin activation of NAD(P)H oxidase activity is mediated via Rac1 in proximal tubule cells. *Am. J. Nephrol.* **27**, 15–23 (2007).
57. Vlachojannis, J. G., Tsakas, S., Petropoulou, C., Goumenos, D. S. & Alexandri, S. Endothelin-1 in the kidney and urine of patients with glomerular disease and proteinuria. *Clin. Nephrol.* **58**, 337–343 (2002).
58. Diwakar, R., Pearson, A. L., Colville-Nash, P., Brunskill, N. J. & Dockrell, M. E. C. The role played by endocytosis in albumin-induced secretion of TGF-beta1 by proximal tubular epithelial cells. *Am. J. Physiol. Renal Physiol.* **292**, F1464-70 (2007).
59. Goumenos, D. S. *et al.* Transforming growth factor-beta(1) in the kidney and urine of patients with glomerular disease and proteinuria. *Nephrol. Dial. Transplant. Off. Publ. Eur. Dial.*

- Transpl. Assoc. - Eur. Ren. Assoc.* **17**, 2145–2152 (2002).
60. Stephan, J.-P. *et al.* Albumin stimulates the accumulation of extracellular matrix in renal tubular epithelial cells. *Am. J. Nephrol.* **24**, 14–19 (2004).
61. Alicic, R. Z., Rooney, M. T. & Tuttle, K. R. Diabetic Kidney Disease: Challenges, Progress, and Possibilities. *Clin. J. Am. Soc. Nephrol.* **12**, 2032–2045 (2017).
62. Ichimura, K. *et al.* Morphological Processes of Foot Process Effacement in Puromycin Aminonucleoside Nephrosis Revealed by FIB/SEM Tomography. *J. Am. Soc. Nephrol.* **30**, 96–108 (2019).
63. Garg, P. A Review of Podocyte Biology. *Am. J. Nephrol.* **47 Suppl 1**, 3–13 (2018).
64. Pavenstädt, H., Kriz, W. & Kretzler, M. Cell biology of the glomerular podocyte. *Physiol. Rev.* **83**, 253–307 (2003).
65. Kriz, W. Glomerular diseases: podocyte hypertrophy mismatch and glomerular disease. *Nature reviews. Nephrology* **8**, 618–619 (2012).
66. Blutke, A., Schneider, M. R., Wolf, E. & Wanke, R. Growth hormone (GH)-transgenic insulin-like growth factor 1 (IGF1)-deficient mice allow dissociation of excess GH and IGF1 effects on glomerular and tubular growth. *Physiol. Rep.* **4**, (2016).
67. Lu, C.-C. *et al.* Role of Podocyte Injury in Glomerulosclerosis. *Adv. Exp. Med. Biol.* **1165**, 195–232 (2019).
68. Vogelmann, S. U., Nelson, W. J., Myers, B. D. & Lemley, K. V. Urinary excretion of viable podocytes in health and renal disease. *Am. J. Physiol. Renal Physiol.* **285**, F40-8 (2003).
69. Bertram, J. F., Soosaipillai, M. C., Ricardo, S. D. & Ryan, G. B. Total numbers of glomeruli and individual glomerular cell types in the normal rat kidney. *Cell Tissue Res.* **270**, 37–45 (1992).
70. Tharaux, P.-L. & Huber, T. B. How Is Proteinuric Diabetic Nephropathy Caused by Disturbed Proteostasis and Autophagy in Podocytes? *Diabetes* **65**, 539–541 (2016).
71. Gödel, M. *et al.* Role of mTOR in podocyte function and diabetic nephropathy in humans and mice. *J. Clin. Invest.* **121**, 2197–2209 (2011).
72. Sweetwyne, M. T. *et al.* Notch1 and Notch2 in Podocytes Play Differential Roles During Diabetic Nephropathy Development. *Diabetes* **64**, 4099–4111 (2015).
73. Lasagni, L., Lazzeri, E., Shankland, S. J., Anders, H.-J. & Romagnani, P. Podocyte mitosis - a catastrophe. *Curr. Mol. Med.* **13**, 13–23 (2013).
74. Hara, M., Oohara, K., Dai, D.-F. & Liapis, H. Mitotic Catastrophe Causes Podocyte Loss in the Urine of Human Diabetics. *Am. J. Pathol.* **189**, 248–257 (2019).
75. Wang, B. *et al.* Effects of RAS inhibitors on diabetic retinopathy: a systematic review and meta-analysis. *lancet. Diabetes Endocrinol.* **3**, 263–274 (2015).
76. Márquez, E., Riera, M., Pascual, J. & Soler, M. J. Renin-angiotensin system within the diabetic podocyte. *Am. J. Physiol. - Ren. Physiol.* **308**, (2015).
77. Roca-Ho, H., Riera, M., Palau, V., Pascual, J. & Soler, M. J. Characterization of ACE and ACE2 expression within different organs of the NOD mouse. *Int. J. Mol. Sci.* **18**, (2017).
78. Crackower, M. A. *et al.* Angiotensin-converting enzyme 2 is an essential regulator of heart function. *Nature* **417**, 822–828 (2002).
79. Soler, M. J., Wysocki, J. & Batlle, D. ACE2 alterations in kidney disease. *Nephrol. Dial.*

- Transplant.* **28**, (2013).
80. Clotet, S., Riera, M., Pascual, J. & Soler, M. J. RAS and sex differences in diabetic nephropathy. *Am. J. Physiol. - Ren. Physiol.* **310**, (2016).
81. Soler, M. J., Lloveras, J. & Batlle, D. Angiotensin converting enzyme 2 and its emerging role in the regulation of the renin angiotensin system. *Med. Clin. (Barc)*. **131**, (2008).
82. Jamerson, K. A., Nesbitt, S. D., Amerena, J. V, Grant, E. & Julius, S. Angiotensin mediates forearm glucose uptake by hemodynamic rather than direct effects. *Hypertens. (Dallas, Tex. 1979)* **27**, 854–858 (1996).
83. Mervaala, E. M. *et al.* Monocyte infiltration and adhesion molecules in a rat model of high human renin hypertension. *Hypertens. (Dallas, Tex. 1979)* **33**, 389–395 (1999).
84. Yusuf, S. *et al.* Ramipril and the development of diabetes. *JAMA* **286**, 1882–1885 (2001).
85. Shahinfar, S., Lyle, P. A., Zhang, Z., Keane, W. F. & Brenner, B. M. Losartan: Lessons learned from the RENAAL study. *Expert Opinion on Pharmacotherapy* **7**, 623–630 (2006).
86. Cao, Z. & Cooper, M. E. Efficacy of renin-angiotensin system (RAS) blockers on cardiovascular and renal outcomes in patients with type 2 diabetes. *Acta Diabetologica* **49**, 243–254 (2012).
87. Vallon, V. The mechanisms and therapeutic potential of SGLT2 inhibitors in diabetes mellitus. *Annu. Rev. Med.* **66**, 255–270 (2015).
88. Anders, H.-J., Davis, J. M. & Thurau, K. Nephron Protection in Diabetic Kidney Disease. *N. Engl. J. Med.* **375**, 2096–2098 (2016).
89. Zinman, B. *et al.* Rationale, design, and baseline characteristics of a randomized, placebo-controlled cardiovascular outcome trial of empagliflozin (EMPA-REG OUTCOME™). *Cardiovasc. Diabetol.* **13**, 102 (2014).
90. Wanner, C. *et al.* Empagliflozin and Progression of Kidney Disease in Type 2 Diabetes. *N. Engl. J. Med.* **375**, 323–334 (2016).
91. Muller, M. E., Pruijm, M., Bonny, O., Burnier, M. & Zanchi, A. Effects of the SGLT-2 Inhibitor Empagliflozin on Renal Tissue Oxygenation in Non-Diabetic Subjects: A Randomized, Double-Blind, Placebo-Controlled Study Protocol. *Adv. Ther.* **35**, 875–885 (2018).
92. Packer, M. *et al.* Cardiovascular and Renal Outcomes with Empagliflozin in Heart Failure. *N. Engl. J. Med.* **383**, 1413–1424 (2020).
93. Perkovic, V. *et al.* Canagliflozin and Renal Outcomes in Type 2 Diabetes and Nephropathy. *N. Engl. J. Med.* **380**, 2295–2306 (2019).
94. Wiviott, S. D. *et al.* Dapagliflozin and Cardiovascular Outcomes in Type 2 Diabetes. *N. Engl. J. Med.* **380**, 347–357 (2019).
95. Martinez, F. A. *et al.* Dapagliflozin in Patients with Heart Failure and Reduced Ejection Fraction. 1–13 (2019). doi:10.1056/NEJMoa1911303
96. Heerspink, H. J. L. *et al.* Dapagliflozin in Patients with Chronic Kidney Disease. *N. Engl. J. Med.* **383**, 1436–1446 (2020).
97. Watts, N. B. *et al.* Effects of canagliflozin on fracture risk in patients with type 2 diabetes mellitus. *J. Clin. Endocrinol. Metab.* **101**, 157–166 (2016).
98. Shubrook, J. H., Bokaie, B. B. & Adkins, S. E. Empagliflozin in the treatment of type 2 diabetes: Evidence to date. *Drug Design, Development and Therapy* **9**, 5793–5803 (2015).



99. Cherney, D. Z. I. *et al.* Renal hemodynamic effect of sodium-glucose cotransporter 2 inhibition in patients with type 1 diabetes mellitus. *Circulation* **129**, 587–597 (2014).
100. Lin, J. S. & Susztak, K. Podocytes: the Weakest Link in Diabetic Kidney Disease? *Curr. Diab. Rep.* **16**, 45 (2016).
101. Motrapu, M. *et al.* Drug Testing for Residual Progression of Diabetic Kidney Disease in Mice Beyond Therapy with Metformin, Ramipril, and Empagliflozin. *J. Am. Soc. Nephrol.* **31**, 1729–1745 (2020).
102. Lasagni, L. *et al.* Podocyte Regeneration Driven by Renal Progenitors Determines Glomerular Disease Remission and Can Be Pharmacologically Enhanced. *Stem Cell Reports* **5**, 248–263 (2015).
103. Kriz, W. Progressive renal failure--inability of podocytes to replicate and the consequences for development of glomerulosclerosis. *Nephrol. Dial. Transplant. Off. Publ. Eur. Dial. Transpl. Assoc. - Eur. Ren. Assoc.* **11**, 1738–1742 (1996).
104. CLasagni, L., Lazzeri, E., Shankland, S. J., Anders, H.-J. & Romagnani, P. c. *Curr. Mol. Med.* **13**, 13–23 (2013).
105. Lasagni, L. & Romagnani, P. Glomerular epithelial stem cells: the good, the bad, and the ugly. *J. Am. Soc. Nephrol.* **21**, 1612–1619 (2010).
106. Romagnani, P. Toward the identification of a 'renopoietic system'? *Stem Cells* **27**, 2247–2253 (2009).
107. Sagrinati, C., Ronconi, E., Lazzeri, E., Lasagni, L. & Romagnani, P. Stem-cell approaches for kidney repair: choosing the right cells. *Trends Mol. Med.* **14**, 277–285 (2008).
108. Zzzzzzzz *et al.* c. *J. Am. Soc. Nephrol.* **18**, 3128–3138 (2007).
109. Angelotti, M. L. *et al.* Characterization of renal progenitors committed toward tubular lineage and their regenerative potential in renal tubular injury. *Stem Cells* **30**, 1714–1725 (2012).
110. Lazzeri, E. *et al.* Regenerative potential of embryonic renal multipotent progenitors in acute renal failure. *J. Am. Soc. Nephrol.* **18**, 3128–3138 (2007).
111. Romagnani, P. & Remuzzi, G. Renal progenitors in non-diabetic and diabetic nephropathies. *Trends Endocrinol. Metab.* **24**, 13–20 (2013).
112. Fogo, A. B. Mechanisms of progression of chronic kidney disease. *Pediatr. Nephrol.* **22**, 2011–2022 (2007).
113. Romagnani, P. & Kalluri, R. Possible mechanisms of kidney repair. *Fibrogenesis Tissue Repair* **2**, 3 (2009).
114. Shankland, S. J., Smeets, B., Pippin, J. W. & Moeller, M. J. The emergence of the glomerular parietal epithelial cell. *Nat. Rev. Nephrol.* **10**, 158–173 (2014).
115. Smeets, B. *et al.* Parietal epithelial cells participate in the formation of sclerotic lesions in focal segmental glomerulosclerosis. *J. Am. Soc. Nephrol.* **22**, 1262–1274 (2011).
116. Smeets, B. *et al.* Renal progenitor cells contribute to hyperplastic lesions of podocytopathies and crescentic glomerulonephritis. *J. Am. Soc. Nephrol.* **20**, 2593–2603 (2009).
117. Chambers, S. M. *et al.* Aging hematopoietic stem cells decline in function and exhibit epigenetic dysregulation. *PLoS Biol.* **5**, e201 (2007).
118. Conboy, I. M. *et al.* Rejuvenation of aged progenitor cells by exposure to a young systemic

- environment. *Nature* **433**, 760–764 (2005).
119. Peired, A. *et al.* Proteinuria impairs podocyte regeneration by sequestering retinoic acid. *J. Am. Soc. Nephrol.* **24**, 1756–1768 (2013).
120. Ryu, M. *et al.* Plasma leakage through glomerular basement membrane ruptures triggers the proliferation of parietal epithelial cells and crescent formation in non-inflammatory glomerular injury. *J. Pathol.* **228**, 482–494 (2012).
121. Guo, D. *et al.* 6-Bromoindirubin-3'-Oxime (6BIO) Suppresses the mTOR Pathway, Promotes Autophagy, and Exerts Anti-aging Effects in Rodent Liver. *Front. Pharmacol.* **10**, 320 (2019).
122. Lasagni, L. *et al.* Podocyte Regeneration Driven by Renal Progenitors Determines Glomerular Disease Remission and Can Be Pharmacologically Enhanced. *Stem cell reports* **5**, 248–263 (2015).
123. Guo, J., Yang, L., Qiao, Y. & Liu, Z. Glycogen synthase kinase-3 $\beta$  is required for epithelial-mesenchymal transition and barrier dysfunction in mouse podocytes under high glucose conditions. *Mol. Med. Rep.* **14**, 4091–4098 (2016).
124. Wan, J. *et al.* GSK-3 $\beta$  inhibitor attenuates urinary albumin excretion in type 2 diabetic db/db mice, and delays epithelial-to-mesenchymal transition in mouse kidneys and podocytes. *Mol. Med. Rep.* **14**, 1771–1784 (2016).
125. Sun, T., Rodriguez, M. & Kim, L. Glycogen synthase kinase 3 in the world of cell migration. *Dev. Growth Differ.* **51**, 735–742 (2009).
126. Wu, X. *et al.* Skin stem cells orchestrate directional migration by regulating microtubule-ACF7 connections through GSK3 $\beta$ . *Cell* **144**, 341–352 (2011).
127. Xu, W., Ge, Y., Liu, Z. & Gong, R. Glycogen synthase kinase 3 $\beta$  orchestrates microtubule remodeling in compensatory glomerular adaptation to podocyte depletion. *J. Biol. Chem.* **290**, 1348–1363 (2015).
128. Nowicki, M. O. *et al.* Lithium inhibits invasion of glioma cells; possible involvement of glycogen synthase kinase-3. *Neuro. Oncol.* **10**, 690–699 (2008).
129. Wang, Z. *et al.* Lithium chloride inhibits vascular smooth muscle cell proliferation and migration and alleviates injury-induced neointimal hyperplasia via induction of PGC-1 $\alpha$ . *PLoS One* **8**, e55471 (2013).
130. Ryu, Y.-K. *et al.* Regulation of glycogen synthase kinase-3 by thymosin beta-4 is associated with gastric cancer cell migration. *Int. J. cancer* **131**, 2067–2077 (2012).
131. Peng, J., Ramesh, G., Sun, L. & Dong, Z. Impaired wound healing in hypoxic renal tubular cells: roles of hypoxia-inducible factor-1 and glycogen synthase kinase 3 $\beta$ / $\beta$ -catenin signaling. *J. Pharmacol. Exp. Ther.* **340**, 176–184 (2012).
132. Wang, Z. *et al.* Redox-sensitive glycogen synthase kinase 3 $\beta$ -directed control of mitochondrial permeability transition: rheostatic regulation of acute kidney injury. *Free Radic. Biol. Med.* **65**, 849–858 (2013).
133. Woodgett, J. R. Physiological roles of glycogen synthase kinase-3: potential as a therapeutic target for diabetes and other disorders. *Curr. Drug Targets. Immune. Endocr. Metabol. Disord.* **3**, 281–290 (2003).
134. MacAulay, K. & Woodgett, J. R. Targeting glycogen synthase kinase-3 (GSK-3) in the treatment of Type 2 diabetes. *Expert Opin. Ther. Targets* **12**, 1265–1274 (2008).
135. Zhang, Z. *et al.* Proteomic analysis of kidney and protective effects of grape seed procyanidin

- B2 in db/db mice indicate MFG-E8 as a key molecule in the development of diabetic nephropathy. *Biochim. Biophys. Acta* **1832**, 805–816 (2013).
136. Pitasi, C. L. *et al.* Implication of glycogen synthase kinase 3 in diabetes-associated islet inflammation. *J. Endocrinol.* **244**, 133–148 (2020).
137. Couser, W. G., Remuzzi, G., Mendis, S. & Tonelli, M. The contribution of chronic kidney disease to the global burden of major noncommunicable diseases. *Kidney Int.* **80**, 1258–1270 (2011).
138. Remuzzi, G., Benigni, A. & Remuzzi, A. Science in medicine Mechanisms of progression and regression of renal lesions of chronic nephropathies and diabetes. **116**, (2006).
139. Gagliardini, E. *et al.* Unlike each drug alone, lisinopril if combined with avosentan promotes regression of renal lesions in experimental diabetes. *Am. J. Physiol. Renal Physiol.* **297**, F1448–56 (2009).
140. Remuzzi, A. *et al.* ACE inhibition reduces glomerulosclerosis and regenerates glomerular tissue in a model of progressive renal disease. *Kidney Int.* **69**, 1124–1130 (2006).
141. Marinides, G. N., Groggel, G. C., Cohen, A. H. & Border, W. A. Enalapril and low protein reverse chronic puromycin aminonucleoside nephropathy. *Kidney Int.* **37**, 749–757 (1990).
142. Ikoma, M., Kawamura, T., Kakinuma, Y., Fogo, A. & Ichikawa, I. Cause of variable therapeutic efficiency of angiotensin converting enzyme inhibitor on glomerular lesions. *Kidney Int.* **40**, 195–202 (1991).
143. Adamczak, M. *et al.* Reversal of glomerulosclerosis after high-dose enalapril treatment in subtotaly nephrectomized rats. *J. Am. Soc. Nephrol.* **14**, 2833–2842 (2003).
144. Ma, L.-J. *et al.* Regression of glomerulosclerosis with high-dose angiotensin inhibition is linked to decreased plasminogen activator inhibitor-1. *J. Am. Soc. Nephrol.* **16**, 966–976 (2005).
145. Aldigier, J. C., Kanjanbuchi, T., Ma, L.-J., Brown, N. J. & Fogo, A. B. Regression of existing glomerulosclerosis by inhibition of aldosterone. *J. Am. Soc. Nephrol.* **16**, 3306–3314 (2005).
146. Ninichuk, V., Kulkarni, O., Clauss, S. & Anders, H.-J. Tubular atrophy, interstitial fibrosis, and inflammation in type 2 diabetic db/db mice. An accelerated model of advanced diabetic nephropathy. *Eur. J. Med. Res.* **12**, 351–355 (2007).
147. Ninichuk, V. *et al.* Late onset of Ccl2 blockade with the Spiegelmer mNOX-E36-3'PEG prevents glomerulosclerosis and improves glomerular filtration rate in db/db mice. *Am. J. Pathol.* **172**, 628–637 (2008).
148. Sayyed, S. G. *et al.* An orally active chemokine receptor CCR2 antagonist prevents glomerulosclerosis and renal failure in type 2 diabetes. *Kidney Int.* **80**, 68–78 (2011).
149. de Zeeuw, D. *et al.* The effect of CCR2 inhibitor CCX140-B on residual albuminuria in patients with type 2 diabetes and nephropathy: a randomised trial. *lancet. Diabetes Endocrinol.* **3**, 687–696 (2015).
150. Vallon, V. *et al.* Salt-sensitivity of proximal reabsorption alters macula densa salt and explains the paradoxical effect of dietary salt on glomerular filtration rate in diabetes mellitus. *J. Am. Soc. Nephrol.* **13**, 1865–1871 (2002).
151. Darisipudi, M. N. *et al.* Dual blockade of the homeostatic chemokine CXCL12 and the proinflammatory chemokine CCL2 has additive protective effects on diabetic kidney disease. *Am. J. Pathol.* **179**, 116–124 (2011).
152. Lei, Y. *et al.* Interleukin-1 $\beta$  Inhibition for Chronic Kidney Disease in Obese Mice With Type 2

- Diabetes. *Front. Immunol.* **10**, 1223 (2019).
153. Schreiber, A. *et al.* Transcutaneous measurement of renal function in conscious mice. *Am. J. Physiol. Renal Physiol.* **303**, F783-8 (2012).
154. Meng, X.-M. *et al.* Metformin improves the glucose and lipid metabolism via influencing the level of serum total bile acids in rats with streptozotocin-induced type 2 diabetes mellitus. *Eur. Rev. Med. Pharmacol. Sci.* **21**, 2232–2237 (2017).
155. Horakova, O. *et al.* Metformin acutely lowers blood glucose levels by inhibition of intestinal glucose transport. *Sci. Rep.* **9**, 6156 (2019).
156. Han, X. *et al.* Metformin ameliorates insulinitis in STZ-induced diabetic mice. *PeerJ* **5**, e3155 (2017).
157. Oliveira, W. H. *et al.* Effects of metformin on inflammation and short-term memory in streptozotocin-induced diabetic mice. *Brain Res.* **1644**, 149–160 (2016).
158. Han, X. *et al.* Metformin accelerates wound healing in type 2 diabetic db/db mice. *Mol. Med. Rep.* **16**, 8691–8698 (2017).
159. Shiuchi, T. *et al.* ACE inhibitor improves insulin resistance in diabetic mouse via bradykinin and NO. *Hypertens. (Dallas, Tex. 1979)* **40**, 329–334 (2002).
160. Tikellis, C. *et al.* ACE2 deficiency modifies renoprotection afforded by ACE inhibition in experimental diabetes. *Diabetes* **57**, 1018–1025 (2008).
161. Kidokoro, K. *et al.* Evaluation of Glomerular Hemodynamic Function by Empagliflozin in Diabetic Mice Using In Vivo Imaging. *Circulation* **140**, 303–315 (2019).
162. Gembardt, F. *et al.* The SGLT2 inhibitor empagliflozin ameliorates early features of diabetic nephropathy in BTBR ob/ob type 2 diabetic mice with and without hypertension. *Am. J. Physiol. Renal Physiol.* **307**, F317-25 (2014).
163. Lee, Y. H. *et al.* Empagliflozin attenuates diabetic tubulopathy by improving mitochondrial fragmentation and autophagy. *Am. J. Physiol. Renal Physiol.* **317**, F767–F780 (2019).
164. Vigneri, R. & Goldfine, I. D. Role of metformin in treatment of diabetes mellitus. *Diabetes Care* **10**, 118–122 (1987).
165. Wei, J. *et al.* New mouse model of chronic kidney disease transitioned from ischemic acute kidney injury. *Am. J. Physiol. Renal Physiol.* **317**, F286–F295 (2019).
166. Anguiano Gómez, L., Lei, Y., Kumar Devarapu, S. & Anders, H.-J. The diabetes pandemic suggests unmet needs for ‘CKD with diabetes’ in addition to ‘diabetic nephropathy’- implications for pre-clinical research and drug testing. *Nephrol. Dial. Transplant. Off. Publ. Eur. Dial. Transpl. Assoc. - Eur. Ren. Assoc.* **33**, 1292–1304 (2018).
167. Vallon, V., Wead, L. M. & Blantz, R. C. Renal hemodynamics and plasma and kidney angiotensin II in established diabetes mellitus in rats: effect of sodium and salt restriction. *J. Am. Soc. Nephrol.* **5**, 1761–1767 (1995).
168. Ekinci, E. I. *et al.* Dietary salt intake and mortality in patients with type 2 diabetes. *Diabetes Care* **34**, 703–709 (2011).
169. Thomas, M. C. *et al.* The association between dietary sodium intake, ESRD, and all-cause mortality in patients with type 1 diabetes. *Diabetes Care* **34**, 861–866 (2011).
170. Neal, B. *et al.* Rationale, design and baseline characteristics of the CANagliflozin cardioVascular Assessment Study-Renal (CANVAS-R): A randomized, placebo-controlled trial.

- Diabetes. Obes. Metab.* **19**, 387–393 (2017).
171. Wanner, C. *et al.* Empagliflozin and Clinical Outcomes in Patients With Type 2 Diabetes Mellitus, Established Cardiovascular Disease, and Chronic Kidney Disease. *Circulation* **137**, 119–129 (2018).
  172. Lichtnekert, J. *et al.* Renin-Angiotensin-Aldosterone System Inhibition Increases Podocyte Derivation from Cells of Renin Lineage. *J. Am. Soc. Nephrol.* **27**, 3611–3627 (2016).
  173. Zhang, J. *et al.* ACE-inhibition increases podocyte number in experimental glomerular disease independent of proliferation. *J. Renin. Angiotensin. Aldosterone. Syst.* **16**, 234–248 (2015).
  174. Macconi, D. *et al.* Podocyte repopulation contributes to regression of glomerular injury induced by ACE inhibition. *Am. J. Pathol.* **174**, 797–807 (2009).
  175. Pichaiwong, W. *et al.* Reversibility of structural and functional damage in a model of advanced diabetic nephropathy. *J. Am. Soc. Nephrol.* **24**, 1088–1102 (2013).
  176. Barnett, A. H. *et al.* Angiotensin-receptor blockade versus converting-enzyme inhibition in type 2 diabetes and nephropathy. *N. Engl. J. Med.* **351**, 1952–1961 (2004).
  177. Haller, H. *et al.* Olmesartan for the delay or prevention of microalbuminuria in type 2 diabetes. *N. Engl. J. Med.* **364**, 907–917 (2011).
  178. Fried, L. F. *et al.* Combined angiotensin inhibition for the treatment of diabetic nephropathy. *N. Engl. J. Med.* **369**, 1892–1903 (2013).
  179. Parving, H.-H. *et al.* Cardiorenal end points in a trial of aliskiren for type 2 diabetes. *N. Engl. J. Med.* **367**, 2204–2213 (2012).
  180. de Zeeuw, D. *et al.* Bardoxolone methyl in type 2 diabetes and stage 4 chronic kidney disease. *N. Engl. J. Med.* **369**, 2492–2503 (2013).
  181. Pergola, P. E. *et al.* Bardoxolone methyl and kidney function in CKD with type 2 diabetes. *N. Engl. J. Med.* **365**, 327–336 (2011).
  182. Mann, J. F. E. *et al.* Avasentan for overt diabetic nephropathy. *J. Am. Soc. Nephrol.* **21**, 527–535 (2010).
  183. Heerspink, H. J. L. *et al.* Atrasentan and renal events in patients with type 2 diabetes and chronic kidney disease (SONAR): a double-blind, randomised, placebo-controlled trial. *Lancet (London, England)* **393**, 1937–1947 (2019).
  184. Paeng, J. *et al.* Enhanced glycogen synthase kinase-3 $\beta$  activity mediates podocyte apoptosis under diabetic conditions. *Apoptosis* **19**, 1678–1690 (2014).
  185. Zhou, S. *et al.* Genetic and Pharmacologic Targeting of Glycogen Synthase Kinase 3 $\beta$  Reinforces the Nrf2 Antioxidant Defense against Podocytopathy. *J. Am. Soc. Nephrol.* **27**, 2289–2308 (2016).
  186. Xu, W., Ge, Y., Liu, Z. & Gong, R. Glycogen synthase kinase 3 $\beta$  dictates podocyte motility and focal adhesion turnover by modulating paxillin activity: implications for the protective effect of low-dose lithium in podocytopathy. *Am. J. Pathol.* **184**, 2742–2756 (2014).
  187. Naves, M. A. *et al.* Podocyte Wnt/ $\beta$ -catenin pathway is activated by integrin-linked kinase in clinical and experimental focal segmental glomerulosclerosis. *J. Nephrol.* **25**, 401–409 (2012).
  188. Lin, C.-L. *et al.* Wnt/ $\beta$ -catenin signaling modulates survival of high glucose-stressed mesangial cells. *J. Am. Soc. Nephrol.* **17**, 2812–2820 (2006).

189. Unnersjö-Jess, D., Scott, L., Blom, H. & Brismar, H. Super-resolution stimulated emission depletion imaging of slit diaphragm proteins in optically cleared kidney tissue. *Kidney Int.* **89**, 243–247 (2016).
190. Siegerist, F. *et al.* Structured illumination microscopy and automatized image processing as a rapid diagnostic tool for podocyte effacement. *Sci. Rep.* **7**, 11473 (2017).
191. Romoli, S. *et al.* CXCL12 blockade preferentially regenerates lost podocytes in cortical nephrons by targeting an intrinsic podocyte-progenitor feedback mechanism. *Kidney Int.* **94**, 1111–1126 (2018).
192. Ohishi, K., Okwueze, M. I., Vari, R. C. & Carmines, P. K. Juxtamedullary microvascular dysfunction during the hyperfiltration stage of diabetes mellitus. *Am. J. Physiol.* **267**, F99–105 (1994).
193. Stanchev, S., Iliev, A., Kotov, G., Malinova, L. & Landzhov, B. A comparative morphometric study of the superficial and juxtamedullary nephrons during the postnatal development in spontaneously hypertensive rats. *Arch. Anat. Physiol.* **3**, 1–4 (2018).
194. Layton, A. T. & Vallon, V. SGLT2 inhibition in a kidney with reduced nephron number: modeling and analysis of solute transport and metabolism. *Am. J. Physiol. Renal Physiol.* **314**, F969–F984 (2018).
195. Venkatareddy, M. *et al.* Estimating podocyte number and density using a single histologic section. *J. Am. Soc. Nephrol.* **25**, 1118–1129 (2014).
196. Anders, H.-J. CKD in diabetes: diabetic kidney disease versus nondiabetic kidney disease. *Nat. Rev. Nephrol.* doi:10.1038/s41581-018-0001-y

## Declaration

Here I am declared that all of the present work embodied in this thesis was carried out by myself from 10/2017 until 10/2021 under Prof. Dr. Hans Joachim Anders, Nephrologisches Zentrum, Medizinische Klinik und Poliklinik IV, LMU Klinikum. This work has not been submitted to any other university or institute for any degree or diploma.

Part of the work was done by others, as mentioned below:

1. Ms.Irene Mesas, Graduate FöFoLe fellow, University of Munich, Germany.

She has performed *in-vitro* studies to find out the effect of BIO on Glomeruli. The data is presented in the results section 5.6 of this thesis.

2. Prof. Paola Romagnani, University of Florence, Italy.

She has quantified filtration slit density as a marker of podocyte tertiary foot process coverage. The data is presented in the results part, figures 25,30, and 35 of this thesis.

Date: .....

Signature: .....

Place: Munich, Germany

(Manga Motrapu)

## Acknowledgment

Many have helped, as well as inspired during this doctoral study. I might want to pass on my gratitude to all those people.

Firstly, I would like to thank *God Almighty* for inspiring, guiding, and accompanying me through ups and downs. Without his blessing, I could not have reached this far in my career.

I take this opportunity to thank my mentor & guide, *Prof. Hans-Joachim Anders*. He patiently provided the vision, encouragement, and counsel necessary to proceed throughout the doctoral program. I would like to thank *Prof. Paola Romagnani*, University of Florence, Italy, for sharing her knowledge and co-operation to complete this thesis.

My sincere thanks to my co-worker Lidia helped me in many aspects and taught me lab methods, critical thinking, troubleshooting, and team spirit. To Dan and Jana, and Anna, many thanks for the preparation of histological sections. Thank you for your love and support. I would thank all my colleagues Yutian, Shishi, Julian, Steffie, Bobos, and others. Thank you for giving me long life memories, friendship, international dinners, and unconditional support. You guys made my journey in Anders and Vielhauer's laboratory full of unforgettable memories.

There are no words to express my feeling, love, and affectionate gratitude to my family for their faith, love, inspiration, selfless sacrifices, and constant encouragement throughout my life. What is more, to wrap things up, I need to thank my friend and partner, Rajkishor. Thanks for continuous support and dedication, for making me happy and laugh, for comforting me in all moments, and for your love and affection.

I am grateful to everybody who has been part of my life and helped in some way or other, but if I failed to mention his or her names, thank you all.

I must express my tearful acknowledgment to the animals, which have been sacrificed for human beings' betterment.

Date: .....

Place: Munich, Germany

Signature: .....

(Manga Motrapu)





Dean's Office  
Faculty of Medicine



## Affidavit

**Motrapu Manga**

Surname, first name

**Munich**

Street

**Germany**

Zip code, town, Country

I hereby declare, that the submitted thesis entitle

Targeting the residual progression of chronic kidney disease with  
type-2 diabetes beyond the renoprotective effects of a metformin-  
ramipril-empagliflozin combination

is my own work. I have only used the sources indicated and have not made unauthorised  
use of services of a third party. Where the work of others has been quoted or reproduced,  
the source is always given.

I further declare that the submitted thesis or parts thereof have not been presented as part  
of an examination degree to any other university.

**Munich, 30.07.2021**

Place, date

**Manga Motrapu**

Signature doctoral candidate